UNIVERSITY OF CALIFORNIA, SAN DIEGO

Macroscopic implications from phase space dynamics of tokamak turbulence: relaxation, transport, and flow generation

A dissertation submitted in partial satisfaction of the
requirements for the degree
Doctor of Philosophy

in

Physics

by

Yusuke Kosuga

Committee in charge:

Professor Patrick H Diamond, Chair
Professor Herbert Levine
Professor Thomas M O'Neil
Professor George R Tynan
Professor William Young

2012

The dissertation of Yusuke Kosuga is approved, and it is acceptable in quality and form for publication on microfilm and electronically:

_____

_____

_____

_____

_____
Chair

University of California, San Diego

2012

TABLE OF CONTENTS

LIST OF FIGURES

LIST OF TABLES

ACKNOWLEDGEMENTS

I have been supported by uncountable people to complete my study in US. I really, really could have not been able to come to this point without helps from the valuable people surrounding me. First of all, I would like to thank my advisor Pat Diamond, or 'Neko sensei,' for supporting a 'mouse' from a far east country. Education and training that he provided me have been very exciting and challenging (and tough at the same time, that I have spent all of my ability and energy at 120 % to digest them!!!). I would have not been able to come to this level without the training! Now I am about to take a one step further toward being 'Kosuga sensei', while surely there are still many challenges awaiting before becoming a real sensei. The interaction with him will surely have deep impacts for further developments, both personally and academically in the rest of my life.

Through my life at a graduate school, I have been also much benefitted and encouraged from other scientists (sensei); Fukuyama sensei, Kimitaka sensei, Sanae sensei, Yagi sensei, T.S. Hahm, John Rice, Nic Brummell, David Hughes, Ozcur Gurcan, Chris McDevitt, Guilhem Dif-Pradalier, Lu Wang, Maxime Lesur. Discussions on research subjects, as well as continuous encouragements, are appreciated VERY MUCH!

I also should thank my office mates, Chris Lee, Lei Zhao, Pei-Chun Hsu, Zhibin Guo. I was really happy to share a time through our developing stage together. I also thank the secretary of our group, Stephanie Conover, for her help on administrative issues. I also would like to thank Jang Hoon Seo and Eisung Yoon, for helping me to survive in Korea.

My thanks also go to my classmates; Aaron Day, Diana Jeong, Colin Crystal, Alex Rodin, Chris Palmer, Ben Heldt, John Dwyer. The time and alcohol that we spent together were very valuable experience for me. I also owe them to practice my English! Though I was not quite sure if my English was improving or their understanding on my broken English was improving.

My family has also been a source of motivation for me. As the oldest son in the family from Japan, I am supposed to give them back or even support them at this point, though I never did. I hope they get encouraged in any way from that I

keep challenging toward a higher level. I was about to stop it at one time during the study here; I owe my brother for fixing it to bring me back to a route for the challenge.

Finally, I thank my wife, Mami, for her valuable and indispensable support and understanding. I really could have not been able to be at this point without her.

Chapter 2 is a reprint of material appearing in Y. Kosuga, P. H. Diamond and O.D. Gurcan, Phys Plasmas, **17**, 102313 (2010). The dissertation author was the primary investigator and author of this article.

Chapter 3 is a reprint of material in submission to Phys Plasmas, Y. Kosuga and P. H. Diamond, (2012). The dissertation author was the primary investigator and author of this article.

Chapter 4 is a reprint of material appearing in Y. Kosuga and P. H. Diamond, Phys Plasmas, **18**, 122305 (2011). The dissertation author was the primary investigator and author of this article.

VITA

2007	B.E. Nuclear Engineering, Kyoto University, Kyoto, Japan
2007-2008	Teaching Assistant, University of California, San Diego
2008-2012	Graduate Student Researcher, University of California, San Diego
2009	M.Sc. Physics, University of California, San Diego
2010	C.Phil. Physics, University of California, San Diego
2012	Ph.D. Physics, University of California, San Diego

PUBLICATIONS

P.H. Diamond, O.D. Gurcan, T.S. Hahm, K. Miki, Y. Kosuga and X. Garbet, "Momentum Theorems and Structure of Atmospheric Jets and Zonal Flows in Plasmas," Plasma Phys. Control. Fusion **50**, 124018 (2008)

Y. Kosuga and P.H. Diamond, "Collisionless Dynamical Friction and Relaxation in a Simple Model of Drift Wave-Zonal Flow Turbulence," Plasma Fusion Res. **5**, S2051 (2010)

Y. Kosuga, P.H. Diamond and O.D. Gurcan, "On the Efficiency of Intrinsic Rotation Generation in Tokamaks," Phys. Plasmas **17**, 102313 (2010)

J. Rice, J. Hughes, Z. Yan, M. Xu, G.R. Tynan, P.H. Diamond, Y. Kosuga, T.S. Hahm, O.D. Gurcan, C. Holland, R. McDermott, C.J. McDevitt, S.H. Muller and Y. Podpaly, "Progress Towards a Physics Based Phenomenology of Intrinsic Rotation in H-mode and I-mode," *Proceedings of the 23rd IAEA Fusion Energy Conference, Daejeon, Korea* (IAEA Vienna, 2010), IAEA-CN-165/EXC/3-3

J.E. Rice, J.W. Hughes, P.H. Diamond, Y. Kosuga, Y.A. Podpaly, M.L. Reinke, M.J. Greenwald, O.D. Gurcan, T.S. Hahm, A.E. Hubbard, E.S. Marmar, C.J. McDevitt, and D.G. Whyte, "Edge Temperature Gradient as Intrinsic Rotation Drive in Alcator *C*-Mod Tokamak Plasmas," Phys. Rev. Lett. **106**, 215001 (2011)

Y. Kosuga and P.H. Diamond, "On relaxation and transport in gyrokinetic drift wave turbulence with zonal flow", Phys. Plasmas **18**, 122305 (2011)

Y. Kosuga and P.H. Diamond, "Drift hole structure and dynamics with turbulence driven flows", submitted to Phys. Plasmas (2012)

FIELDS OF STUDY

Major Field: Physics

Studies in Theoretical Mechanics
Professor D. Dubin

Studies in Mathematical Physics
Professor M. Fogler

Studies in Quantum Mechanics
Professor G. Fuller and Professor L. J. Sham

Studies in Advanced Classical Electrodynamics
Professor T. M. O'Neil

Studies in Equilibrium and Non-equilibrium Statistical Mechanics
Professor R. Pathria and Professor T. Hwa

Studies in Quantum Field Theory
Professor E. Jenkins

Studies in Renormalization Group Theory
Professor T. Hwa

Studies in Plasma Physics and Nonlinear Plasma Theory
Professor P. H. Diamond

ABSTRACT OF THE DISSERTATION

Macroscopic implications from phase space dynamics of tokamak turbulence: relaxation, transport, and flow generation

by

Yusuke Kosuga

Doctor of Philosophy in Physics

University of California, San Diego, 2012

Professor Patrick H Diamond, Chair

Aspects of the macroscopic phenomenology of tokamak plasmas - relaxation, transport, and flow generation - are analyzed in the context of phase space dynamics. Particular problems of interest are: i) fluctuation entropy evolution with turbulence driven flows and its application to flow generation by heat flux driven turbulence, and ii) dynamical coupling between phase space structures and zonal flows and its implication for macroscopic relaxation and transport.

In chapter 2, intrinsic toroidal rotation drive by heat flux driven turbulence in tokamak is analyzed based on phase space dynamics. In particular, the dynamics of fluctuation entropy with turbulence driven flows is formulated. The entropy budget is utilized to quantify tokamaks as a heat engine system, where heat flux is

converted to macroscopic flows. Efficiency of the flow generation process is defined as the ratio of entropy destruction via flow generation to entropy production via heat input. Comparison of the results to experimental scalings is discussed as well.

In chapter 3, dynamics of a single phase space structure (drift hole) is discussed for a strongly magnetized 3D plasma. The drift hole is shown to be dynamically coupled to zonal flows by polarization charge scattering. The coupled dynamics of the drift hole and zonal flow is formulated based on momentum budget. As an application, a bound on the self-bound drift hole potential amplitude is derived. The results show that zonal flow damping appears as a controlling parameter.

In chapter 4, dynamics of both a single structure and multi-structures in phase space are discussed for a relevant system, i.e. trapped ion driven ion temperature gradient turbulence. The structures are dynamically coupled to zonal flows, since they must scatter polarization charge to satisfy the quasi-neutrality. The coupled evolution of the structures and flows is formulated as a momentum theorem. An implication for transport process is discussed as well. The transport flux is prescribed by dynamical friction exerted by structures on flows. The dynamical friction exerted by zonal flow is a novel effect and reduces transport by algebraically competing against other fluxes, such as a quasilinear diffusive flux.

Chapter 1

Introduction

Magnetic confinement fusion[7, 8] ultimately aims to produce energy by confining hot plasmas via a magnetic field and by enabling ion nuclei therein to fuse with each other. In the magnetic confinement, hot plasmas are confined in a device of a torus shape, which is called a tokamak(Fig.1.1). In tokamak confinement, a strong magnetic field along the torus prohibits cross field motion of plasmas, and hence confines plasmas. By retaining plasmas sufficiently hot ($\sim$ 10keV$\sim$ $100,000,000$ degree celsius!), we expect ion nuclei to fuse each other, and then to release their mass energy.

From an early stage of fusion research, anomalous transport[9] has been a major issue. Here, transport is said to be 'anomalous' since the observed level of transport cannot be explained by a transport prediction based on collisional processes[9]. Indeed, the observed transport level is 1-2 order of magnitude larger than the collisional transport prediction. Such anomalous transport is attributed to turbulence[10], which is driven by inhomogeneity in plasmas, a necessary consequence of 'confinement.' (hot in the core and cool at the edge.) Indeed, the turbulence and turbulent transport in fusion plasmas are ubiquitous and thus it even seems that the anomalous transport is a usual state of tokamak plasmas.

Turbulence in magnetically confined plasmas can be characterized by its tendency to support numerous collective oscillations and instabilities[10]. This idea is well laid out by Kadomtsev[10] as " *when applying the term "turbulence" to a plasma, it is used in a broader sense than in conventional hydrodynamics.*

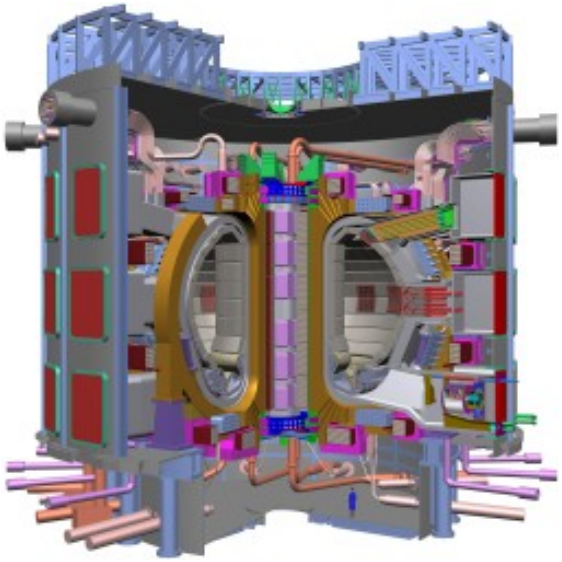

Figure 1.1: A tokamak device for the magnetic confinement.[1] The tokamak is one of the major magnetic confinement devices, and is chosen as a design for the International Thermonuclear Experimental Reactor (ITER).

If hydrodynamic turbulence represents a system made up of a large number of mutually interacting eddies, then in a plasma we have together with the eddies (or instead of them), also the possible excitation of a great variety of oscillations." A typical example of such turbulence is drift wave turbulence, where the turbulence is an ensemble of weakly interacting collective oscillations or waves. Indeed, drift wave turbulence is a standard paradigm for the cause of the anomalous transport in magnetic fusion, partly because drift wave turbulence can give rise to observed anomalous transport levels[11, 12].

While the tendency to support collective oscillations is one of the characteristics of turbulence in magnetically confined plasmas, here we add that turbulence in fusion plasmas is also characterized by its tendency to support *macroscopic flows* and *structures*[13]. Macroscopic flows in turbulent systems are commonly observed. Examples include shear flows in fluid turbulence[14], stellar rotation in convective turbulence[15], planetary flows in atmospheric turbulence[16], etc. In the tokamak context, such flows in turbulence are observed as zonal flows[17] in drift wave turbulence. Flows in tokamak turbulence are an important element,

since such flows can shear apart eddies and reduce transport to the collisional level[18]. Moreover, flows in tokamak turbulence can be driven by turbulence itself via the Reynolds force, and the flows in turn feedback to the turbulence via shearing. Such coupling requires self-consistent treatment of the dynamics of the flows and turbulence, whose understanding is essential for the predictive modeling of tokamak turbulence and associated transport.

As with turbulence driven flows, structures often accompany turbulence. Here, by structures we refer to components of turbulence which cannot be described as collective oscillations or flows, and which have a tendency to persist for a certain lifetime. Examples of such structures in turbulence include coherent vortices, eddies, etc. Note that by definition coherent vortices have a very long life time while eddies have a short life time, albeit finite. What we refer to by 'structure' may be further clarified in the context of Jupiter. Namely, Jupiter has spectrum of fluctuations, including Rossby waves, zonal flows, as well as coherent vortices (long lived 'eyes') and turbulent eddies (vortices which break apart, say, in one turn-over time). In the collisionless tokamak context, such structures including coherent vortices and turbulent eddies can form in *phase space*. This is one of the distinguishing characteristics of plasma turbulence. Being collisionless, plasma turbulence involves resonant interactions between waves and particles. When the resonance is strong, it leads to a trapping of particles in a potential trough, and to the formation of phase space structures. Such phase space structures are observed (numerically) as BGK vortices in phase space[19], phase space density holes[20] (variant of the BGK solutions), phase space density granulations[21], etc. As explained later, such phase space structures also contribute to a relaxation process by exerting dynamical friction[22], whose effects cannot be captured by a conventional quasilinear analysis.

This thesis places special emphasis on turbulence driven flows and structures (especially phase space structures) in tokamak plasma turbulence. In particular, we discuss i) an 'engine' picture of flow generation in heat driven tokamak turbulence and ii) turbulent transport with phase space structures. Here we start from brief discussions of each topic (the engine picture in section 1.1 and the phase

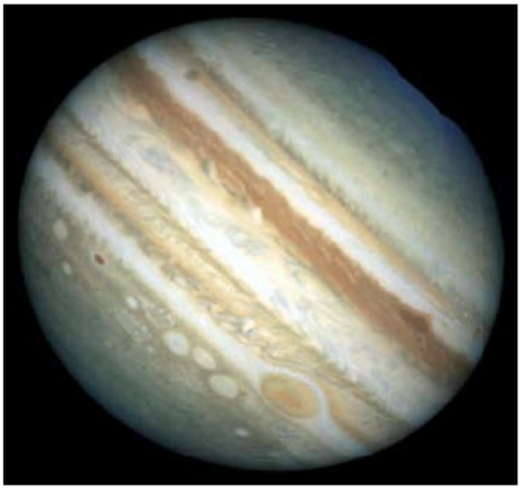

Figure 1.2: Jupiter[2]

space structures in section 1.2.). While the two phenomenologies look quite different, both problems are conveniently formulated based on phase space dynamics. A brief discussion on the common theme of the phenomenologies based on the phase space dynamics is given in section 1.3.

1.1 Intrinsic toroidal generation by drift wave turbulence: an engine paradigm for toroidal rotation generation

Toroidal rotation in tokamak plasmas plays an important role in tokamak confinement by stabilizing harmful magnetohydrodynamic (MHD) instabilities (such as Resistive Wall Mode) and by controlling transport processes. While toroidal rotation is primarily driven by an external torque exerted via Neutral Beam Injection (NBI), the NBI acceleration may be less efficient for future larger devices due to their larger inertia and shallow beam penetration depth. Instead, in future tokamaks, it is argued that we can exploit the property that *plasmas tend to self-accelerate via a heat flux.*

The spontaneous spin-up of toroidal plasmas, so called intrinsic rotation[23,

3], is observed by heating plasmas at rest, while there is no obvious momentum input. The phenomena is robust and observed in a wide variety of toroidal machines including tokamaks as well as stellarators. Empirical scalings (Figs.1.3 and 1.4.) for the resultant velocity are obtained experimentally[23, 3, 4]. The scalings are obtained for toroidal velocity that results across transition from low confinement to improved confinement. The scalings are summarized as [23, 3, 4]

$$\Delta v_\phi(0) \propto \frac{\Delta W_p}{I_p} \text{ or } \nabla T \tag{1.1}$$

Here, ΔW_p is the increment in the energy stored in the plasmas, I_p is the plasma current, and ∇T is the temperature gradient at the plasma edge in the improved confinement[24]. The experimental scalings indicate that the resultant toroidal velocity is proportional to the energy stored in plasmas or the local temperature gradient at the plasma edge in the improved confinement. Since the plasma stored energy or the temperature gradient is ultimately set by heat input, it seems that we can view intrinsic toroidal rotation generation as a result of *a heat engine process*[25, 26], where heat is converted to flows under the action of turbulence.

Such flow generation in heat driven turbulence is not limited only to tokamaks. Rotation of planets' atmosphere or stars can be also viewed as a consequence of heat conversion processes. Indeed, super-rotation of Venus's atmosphere may likely be an example of a heat flux converted flow. In Venus, heat input from the Sun drives convective turbulence in the atmosphere, and the heat flux driven turbulence accelerates Venus's atmosphere to rotate faster than Venus itself. In the Sun, heat is generated from the fusion reaction at the core, and conducted by convective turbulence. The convective turbulence produces differential rotation of the sun, which can be viewed as another example of engine process.

In chapter 2, we discuss the engine picture of tokamak toroidal rotation generation. The aim of the discussion is to derive a simple scaling relation between heat input and resultant flow speed, in an attempt to understand the origin of empirical trends of toroidal rotation observed in tokamak experiments. In particular, we *quantify* tokamak plasmas as an engine system by calculating its entropy budget based on microscopic phase space dynamics. The entropy budget is further utilized

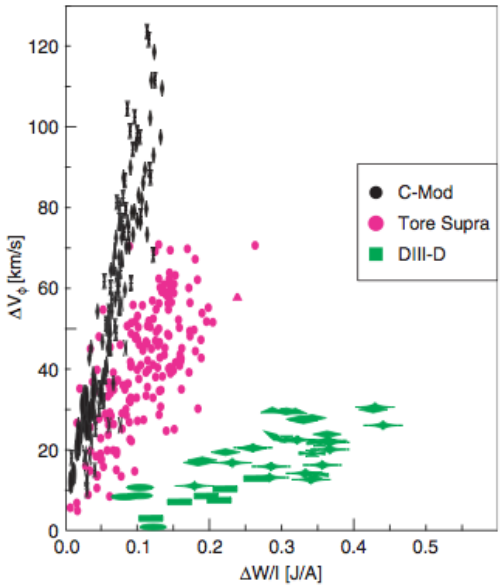

Figure 1.3: The toroidal velocity increment across the L-H transition[3]. The velocity increment is proportional to the increment of the energy stored in the plasmas W_p and is inversely proportional to the plasma current I_p.

to define flow generation efficiency. The flow generation efficiency is defined as a ratio between the entropy production via heat input and the entropy destruction via flow generation. The result agrees well with experimental observations, both qualitatively and quantitatively.

1.2 Turbulent relaxation and transport with phase space structures: whether quasilinear theory wither?

Mean field modeling of turbulent transport, which attempts to represent transport flux in terms of mean field quantities and transport coefficients, is an important issue for many applications, including magnetic fusion energy. An oft-used example of the mean field theory is quasilinear theory[27, 28, 10], which assumes turbulence as an ensemble of weakly interacting waves[27, 28, 10]. The

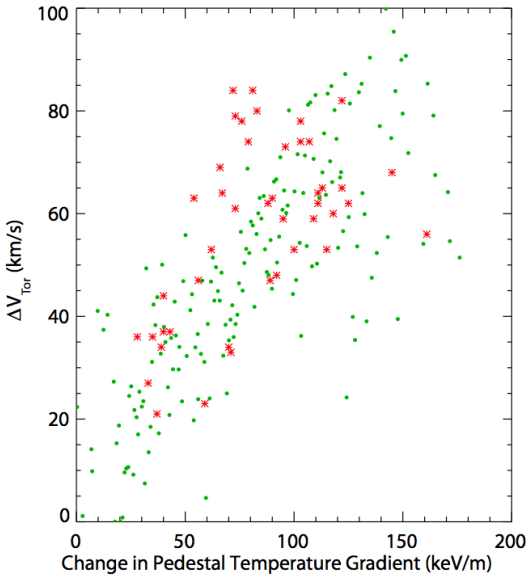

Figure 1.4: The local scaling of the toroidal velocity increment from L- to I-mode[4]. The velocity increment is proportional to the local temperature gradient ∇T. A similar scaling is obtained for H-mode[4].

quasilinear theory has been successfully applied to numerous problems, including residual stress modeling[29] in tokamak physics. However, while the quasilinear theory is an extremely useful concept, and while its prediction often agrees with experimental observations in fusion plasmas, the quasilinear theory *alone* cannot be a complete description of turbulent transport. A shortcoming of the quasilinear theory is particularly apparent when strong wave-particle resonance occurs, which leads to the formation of phase space structures[19, 20, 30]. As discussed in the following, the effect of such structures enters transport flux as dynamical friction[22], whose effect *cannot* be captured by the quasilinear analysis.

In the presence of strong wave-particle resonance, structures in phase space can form. Simply put, this is a consequence of trapping of particles in a potential trough, since the trapped particles in turn provide a self-potential to trap themselves, leading to self-sustained structures[19, 21, 20]. An example of such phase space structure is a BGK vortex[19], as shown in Fig.1.5. The BGK vortex has a long life time and can be viewed as a coherent vortex in phase space. Other

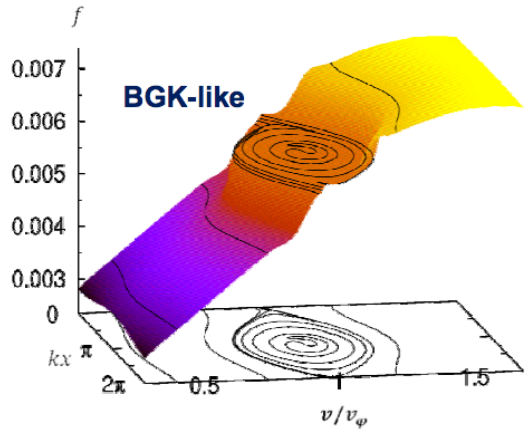

Figure 1.5: A coherent vortex in phase space[5]

examples of such coherent structures in phase space include phase space density holes[20], clump-hole pairs in the Berk-Breizman model[31], etc. While coherent structures have a long life time, there are another type of phase space structures with a shorter life time (albeit finite). Such phase space structures break apart while they are circulating in phase space, since trapped particles are detrapped by turbulent scattering caused by other structures. Such phase space structures may be viewed as analogous to cascading eddies in fluid turbulence, which break apart in one turn over time. An example of such phase space structure (or eddies in phase space) is phase space density granulation[21].

In any case, particle trapping leads to the formation of phase space structures. Once formed, the phase space structures can impact relaxation and transport by exerting dynamical friction on each other[22]. Here, the idea is that we view the phase space structures as macro-particles, consisting of correlated trapped particles. By looking at the phase space structures as a macro-particle, we can see that these macro-particles can exert dynamical friction with each other, since these macro-particles emit potential wakes. This is very much like the wake drag effect on an object in water, which feels a drag by emitting radiating water waves (Fig.1.6). Such effect enters the transport flux as dynamical friction, which leads to a total

Figure 1.6: Structures and wakes[6]

flux (for a simple 1D Vlasov plasma)

$$J(v) = -D\frac{\partial\langle f\rangle}{\partial v} + F\langle f\rangle \tag{1.2}$$

where D is the quasi-linear like diffusion and F is dynamical friction. In the presence of phase space structures, then, transport flux is not the simple quasilinear diffusion, but becomes a Lenard-Balescu type, with both the diffusive term and dynamical friction. Of course, the effect of phase space structures as dynamical friction cannot be captured by the conventional quasilinear analysis.

While the idea of transport with phase space structures has been noted from time to time in the fusion community[32, 33, 34], the role of turbulence driven zonal flows in turbulent relaxation with phase space structures has not been addressed before. Zonal flow coupling in phase space turbulence in magnetized plasmas is quite likely, since structures must scatter polarization charges to satisfy the overall quasineutrality condition, which leads to non-zero zonal flow coupling via the Taylor identity[35] $\langle\tilde{v}_r\nabla_\perp^2\tilde{\phi}\rangle = \partial_r\langle\tilde{v}_r\tilde{v}_\theta\rangle$. The zonal flow coupling is a relevant issue, since zonal flows can enter as a critical element to determine dynamical evolution of turbulence with phase space structures. Since turbulence determines the transport level, such zonal flow effects in turbulence with phase space structures surely leave a footprint in transport process.

Such turbulent relaxation and transport with phase space structures and turbulence driven zonal flows are discussed in chapter 3 and chapter 4.

1.3 A unifying concept: phase space density correlation and its relatives

While the two phenomenologies discussed above seem quite different, both problems are conveniently formulated based on phase space density correlation δf^2 evolution. As shown below, δf^2 is analogous to potential enstrophy in a quasi-geostrophic system. As such, the phase space density correlation is called as 'phasetrophy'[30]. Phasetrophy is further related to fluctuation entropy[36], as well as the fluctuation pseudomomentum of phase space structures[37, 38]. Leaving the detailed discussion to the later chapters, here we briefly discuss the utility and the physical interpretation of δf^2 in a simplified system.

In general, dynamics of magnetized plasmas is described by the Vlasov equation for a distribution function f (or phase space density) and by the Maxwell equations for an electric and a magnetic field. While the Vlasov-Maxwell systems may be exact, it is still far too complicated for any practical use. In fusion plasmas, however, we can simplify the set of equations by exploiting the fact that plasmas are strongly magnetized. The strong magnetic field makes the cyclotron frequency of charged particles the fastest times scale in dynamics. By integrating out the fastest time scale associated with the charged particle gyration, we can reduce the full Vlasov-Maxwell equations to gyrokinetic(GK) Vlasov-Maxwell equations, which describe dynamics with the reduced degrees of freedom. The GK equations are one of the standard tools for the analysis of tokamak turbulence and transport. For detailed discussion and derivation, see the literature[39, 40]. We add that the GK equations are further reduced if there is another fast motion, such as the bouncing motion of particles trapped in a magnetic mirror. The integration over the fast bounce motion gives a bounce kinetic equation, which is useful to analyze trapped particle driven turbulence in tokamaks. The bounce kinetic equation is used in chapter 4 to analyze trapped ion driven ion temperature gradient turbulence.

Here, as an example of GK dynamics, we consider a simplified GK model which consists of drift kinetic equations for both ions and electrons ($\sigma = i, e$) and

Table 1.1: Comparison of the QG system and the GK system

	QG system	GK system
Dynamical variable	PV, $q(x,t)$	distribution function, $f(x,v,t)$
Potential Vorticity Relation	PV, $q = \nabla^2\phi + F(\phi, n)$	GK Poisson, Pol Charge $\int d^3v f + \rho_s^2\nabla^2\phi = g(\phi, n_e, ...)$
Time evolution	$\frac{dq}{dt} = \partial_t q + \{q, \phi\} = 0$	$\frac{df}{dt} = \partial_t f + \{f, H\} = 0$
Linear waves	Rossby waves $\omega_k = -\frac{\beta k_x}{k_\perp^2}$	Drift waves $\omega_k = \frac{\omega_{*e}}{1 + k_\perp^2\rho_s^2}$

the GK Poisson equation:

$$\partial_t f_\sigma + v_\parallel \nabla_\parallel f_\sigma + \mathbf{v}_{E\times B}\cdot\nabla f_\sigma + \frac{e_\sigma}{m_\sigma} E_\parallel \frac{\partial f_\sigma}{\partial v_\parallel} = 0 \tag{1.3}$$

$$-\rho_s^2\nabla_\perp^2\frac{e\phi}{T_e} = \int dv_\parallel f_i - \int dv_\parallel f_e \tag{1.4}$$

Here, the equations are simplified in that the finite Larmor radius effect - a product of gyrokinetic analysis - is only kept in the gyrokinetic Poisson equation and neglected in ion phase space density evolution (in full gyrokinetics the finite Larmor radius effect enters the equation for f_i as the Bessel function $J_0(k_\perp\rho_i)$).

We note that the dynamics described by the simplified model is similar to potential vorticity (PV) dynamics in quasi-geostrophic (QG) systems (Table.1.1). In the simplified GK model, phase space density f is conserved along a trajectory produced by Hamiltonian. This is analogous to the conservation of PV q in the QG systems. Furthermore, a physical content of the conserved quantities, f and q, is quite analogous to each other, since both consist of the vorticity part and the other part (planetary part for the QG system, mean distribution function $\langle f\rangle$ for the GK system). As shown below, the simplified system support drift waves. This is analogous to Rossby waves in the QG system.

Linear dynamics of the simplified model is described by linear eigenmodes,

whose dispersion relation is obtained as follows. In the simplified model, fluctuating phase space density is calculated as

$$\delta f_{\sigma k} = \frac{i}{\omega - k_\parallel v_\parallel} i(\hat{\omega}_{*\sigma}(v_\parallel) - k_\parallel v_\parallel)\frac{e_\sigma \tilde{\phi}_k}{T_\sigma}\langle f_\sigma \rangle \tag{1.5}$$

Here $\hat{\omega}_{*\sigma}(v_\parallel) \equiv (cT_\sigma)/(Be_\sigma)\partial_x \langle f_\sigma \rangle / \langle f_\sigma \rangle = \omega_{*\sigma}\{1 + \eta_\sigma(v_\parallel^2/v_{th\sigma}^2 - 1)/2\}$ and $\langle f_\sigma \rangle$ is assumed to be the local Maxwellian. Assuming $k_\parallel v_{thi} < \omega < k_\parallel v_{the}$, the fluctuation density is given as

$$\frac{\delta n_{ik}}{n_0} = \int dv_\parallel \delta f_{ik} = \frac{\omega_{*e}}{\omega}\frac{|e|\tilde{\phi}_k}{T_e} + \frac{k_\parallel^2 c_s^2}{\omega^2}\left(1 - \frac{\omega_{*i}(1+\eta_i)}{\omega}\right)\frac{|e|\tilde{\phi}_k}{T_e} \tag{1.6}$$

$$\frac{\delta n_{ek}}{n_0} = \int dv_\parallel \delta f_{ek} = \frac{|e|\tilde{\phi}_k}{T_e} \tag{1.7}$$

Substituting the fluctuation densities for the GK Poisson equation gives the dispersion relation

$$1 + k_\perp^2 \rho_s^2 - \frac{\omega_{*e}}{\omega} - \frac{k_\parallel^2 c_s^2}{\omega^2}\left(1 - \frac{\omega_{*i}(1+\eta_i)}{\omega}\right) = 0 \tag{1.8}$$

The eigenmodes consist of two branches, namely electron drift waves and ion temperature gradient (ITG) modes (in particular the negative compressibility driven ITG). When the acoustic coupling is small, the dispersion relation gives the electron drift wave solution:

$$\omega = \frac{\omega_{*e}}{1 + k_\perp^2 \rho_s^2} = \frac{k_y v_{*e}}{1 + k_\perp^2 \rho_s^2} \tag{1.9}$$

The electron drift waves are analogous to Rossby waves, as the dispersion relation of the electron drift waves is similar to that of the Rossby waves:

$$\omega = -\frac{k_x \beta}{k_\perp^2} \tag{1.10}$$

The dispersion relation gives an ITG solution when the density profile is relatively flat (η_i large) and the perpendicular wave number is relatively small, compared to the inverse of the ion sound Larmor radius. In this case, the dispersion

relation simplifies to

$$\omega^2 = k_\parallel^2 c_s^2 \left(1 - \frac{\omega_{*i}\eta_i}{\omega}\right) \tag{1.11}$$

This is the negative compressibility driven ITG. The effect of the negative compressibility may be better understood by comparing the dispersion relation to Jean's instability of a self-gravitating matter:

$$\omega^2 = k^2 v_{th}^2 \left(1 - \frac{4\pi\rho_m G}{k^2}\right) \tag{1.12}$$

Jean's instability describes a collapse of a self-gravitating gas. As can be explicitly seen in the competition in the parenthesis, the collapse is possible when the attractive gravitational force can overcome the stabilizing effect from acoustic waves. Back to ITG, we can see that the instability is possible when the ion acoustic coupling is dominated by the negative compressibility by η_i. Note that the negative compressibility is possible only when a mode is propagating in the ion diamagnetic direction, $\omega_{*i}/\omega > 0$. Now, when the negative compressibility dominates, the dispersion relation is obtained as

$$\omega = (k_\parallel^2 c_s^2 |\omega_{*i}|\eta_i)^{1/3} \left(1, -\frac{1}{2} \pm i\frac{\sqrt{3}}{2}\right) \tag{1.13}$$

which contains the unstable branch with $\gamma_k > 0$.

The role of δf^2 in the simplified model merits some discussion. Here, for simplicity, we assume electrons are responding adiabatically and calculate δf_i^2. The δf_i^2 balance is then calculated to be ($\langle ... \rangle$ is the spatial average in y and z)

$$\partial_t \langle \delta f_i^2 \rangle + \partial_x \langle \tilde{v}_x \delta f_i^2 \rangle + \frac{|e|}{m_i} \frac{\partial}{\partial v_\parallel} \langle \tilde{E}_\parallel \delta f_i^2 \rangle = -2\langle \tilde{v}_x \delta f_i \rangle \langle f_i \rangle' - 2\frac{|e|}{m_i} \langle \tilde{E}_\parallel \delta f_i \rangle \frac{\partial \langle f_i \rangle}{\partial v_\parallel} \tag{1.14}$$

The righthand side takes the conventional form of fluctuation production, namely the form of the fluxes times the gradients. The lefthand side consists of 'spreading' of phase space turbulence δf_i^2 in both configuration and velocity spaces. The δf_i^2 balance can be converted to forms with more clear physical meaning, namely that of fluctuation entropy ($\int dv_\parallel \langle \delta f_i^2 \rangle / \langle f_i \rangle$) balance or fluctuation pseudomomentum

($\int dv_\parallel \langle \delta f_i^2 \rangle / \langle f_i \rangle'$) balance.

The δf^2 balance is related to fluctuation entropy balance:

$$\partial_t \int dv_\parallel \frac{\langle \delta f_i^2 \rangle}{\langle f_i \rangle} + \partial_x \left\langle \tilde{v}_x \int dv_\parallel \frac{\delta f_i^2}{\langle f_i \rangle} \right\rangle = \mathcal{P} \tag{1.15}$$

Here we assumed that fluctuations vary rapidly compared to mean quantities ($\alpha = x, t$),

$$\partial_\alpha \delta f_i / \delta f_i > \partial_\alpha \langle f_i \rangle / \langle f_i \rangle,$$

and $\mathcal{P}$ is defined as

$$\mathcal{P} \equiv -2 \int dv_\parallel \langle \tilde{v}_x \delta f_i \rangle \frac{\langle f_i \rangle'}{\langle f_i \rangle} - 2 \frac{|e|}{m_i} \int dv_\parallel \langle \tilde{E}_\parallel \delta f_i \rangle \frac{1}{\langle f_i \rangle} \frac{\partial \langle f_i \rangle}{\partial v_\parallel} \tag{1.16}$$

$\mathcal{P}$ describes the local production of entropy by turbulent relaxation. The quasilinear calculation yields

$$\mathcal{P} = \frac{2 D_{QL}^{xx}}{L_n^2} + \frac{D_{QL}^{xx}}{L_T^2} \tag{1.17}$$

Here $D_{QL} \equiv \sum_k c_s^2 \mathrm{Re}(i/\omega_k)(k_\theta \rho_s)^2 |e\phi_k / T_e|^2$ is the quasilinear spatial diffusion coefficient, $L_n^{-1} \equiv \partial_x \ln \langle n \rangle$ and $L_{T_i}^{-1} \equiv \partial_x \ln \langle T_i \rangle$. The production term is clearly related to the entropy production, as it can be written as

$$\mathcal{P} = -\frac{2}{\langle n \rangle^2} \left(-D_{QL}^{xx} \frac{\partial \langle n \rangle}{\partial x} \right) \frac{\partial \langle n \rangle}{\partial x} - \frac{1}{\langle T_i \rangle^2} \left(-D_{QL}^{xx} \frac{\partial \langle T_i \rangle}{\partial x} \right) \frac{\partial \langle T_i \rangle}{\partial x} \tag{1.18}$$

Written in this form, the production term has the conventional form of the entropy production, namely the form of the flux times the gradient. In chapter 2 the entropy balance is extended to include turbulent driven flows and utilized to describe a tokamak as a heat engine.

The δf_i^2 balance also gives fluctuation pseudomomentum balance:

$$\begin{aligned} &\partial_t \int dv_\parallel \frac{\langle \delta f_i^2 \rangle}{\langle f_i \rangle'} + \partial_x \left\langle \tilde{v}_x \int dv_\parallel \frac{\delta f_i^2}{\langle f_i \rangle'} \right\rangle \\ &= -2 \int dv_\parallel \langle \tilde{v}_x \delta f_i \rangle - 2 \int dv_\parallel \frac{|e|}{m_i} \langle \tilde{E}_\parallel \delta f_i \rangle \frac{\partial \langle f_i \rangle / \partial v_\parallel}{\partial \langle f_i \rangle / \partial x} \end{aligned} \tag{1.19}$$

Here, $\int dv_\parallel \langle \delta f_i^2 \rangle / \langle f_i \rangle'$ gives the negative of drift wave momentum density, as

$$\int dv_\parallel \frac{\langle \delta f_i^2 \rangle}{\langle f_i \rangle'} = \sum_k L_n \frac{\omega_{*e}^2}{\omega^2} \left| \frac{e\phi_k}{T_e} \right|^2 = -\rho_s c_s \sum_k k_y \frac{\mathcal{E}_k}{\omega_k} \tag{1.20}$$

Here $\omega = \omega_k = \omega_{*e}/(1 + k_\perp^2 \rho_s^2)$ and $\mathcal{E}_k = (1+\rho_s^2 k_\perp^2)|e\phi_k/T_e|^2$ is the energy density of drift waves. Since $\mathcal{E}_k/\omega_k$ is the action density of drift waves, $(\mathcal{E}_k/\omega_k)k_y$ is the drift wave momentum density in y direction. Hence $\int dv_\parallel \langle \delta f_i^2 \rangle / \langle f_i \rangle'$ is related to fluctuation momentum. Indeed, $\int dv_\parallel \langle \delta f_i^2 \rangle / \langle f_i \rangle'$ balance describes momentum budget between turbulence and flows. The flow coupling is contained in the righthand side, as

$$\int dv_\parallel \langle \tilde{v}_x \delta f_i \rangle = -\frac{\rho_s^2 |e|}{T_e} \langle \tilde{v}_x \nabla_\perp^2 \tilde{\phi} \rangle = -\frac{1}{\omega_{ci}} \partial_x \langle \tilde{v}_x \tilde{v_y} \rangle \tag{1.21}$$

Here, the GK Poisson equation was used in the first line and the Taylor identity was used in the second line. Since the Reynolds forcing describes turbulent drive of zonal flow $\langle v_y \rangle$, the $\int dv_\parallel \langle \delta f_i^2 \rangle / \langle f_i \rangle'$ balance describes momentum budget between turbulence and flows. More explicitly, by employing a simplified model for turbulence driven zonal flow $\partial_t \langle v_y \rangle = -\partial_x \langle \tilde{v}_x \tilde{v}_y \rangle - \nu_c \langle v_y \rangle$, we have a coupled evolution equation for phase space density perturbations and zonal flow as:

$$\begin{aligned} &\partial_t \left(\frac{\langle v_y \rangle}{\omega_{ci}} + \int dv_\parallel \frac{\langle \delta f_i^2 \rangle}{2\langle f_i \rangle'} \right) = -\langle \tilde{v}_x \delta n_e \rangle \\ &- \int dv_\parallel \frac{|e|}{m_i} \langle \tilde{E}_\parallel \delta f_i \rangle \frac{\partial \langle f_i \rangle / \partial v_\parallel}{\partial \langle f_i \rangle / \partial x} - \partial_x \left\langle \tilde{v}_x \int dv_\parallel \frac{\delta f_i^2}{2\langle f_i \rangle'} \right\rangle - \frac{\nu_c}{\omega_{ci}} \langle v_y \rangle \end{aligned} \tag{1.22}$$

This is a momentum theorem for the simplified model for drift wave turbulence and zonal flows.

While we assumed that fluctuations are supported by waves to connect kinetic pseudomomentum to wave momentum, the psuedomomentum is a more generalized concept than wave momentum. Indeed, as shown later, the kinetic pseudomomentum enters momentum budget between phase space structures and zonal flows. Utilities and implications of the momentum budget between phase space structures and zonal flows are treated in chapter 3 and chapter 4.

1.4 Organization of the thesis

In the remainder of the thesis, turbulence driven flows and phase space structures in tokamak turbulence are characterized based on phase space density correlation evolution. In chapter 2, intrinsic toroidal rotation is treated as an example of turbulence driven flows, and the flow engine calculation is presented. There, a special emphasis is made to quantify the tokamak as a heat engine, where heat is converted to toroidal flows. Specifically, an efficiency of the flow generation process is defined and calculated. Comparison to experimental scalings is discussed as well. Chapter 3 and chapter 4 discuss relaxation and transport by phase space structures. In chapter 3, it is argued that in a generic drift wave system the drift hole is formed and cause subcritical instability. Coupling to zonal flows is emphasized throughout. Specifically, roles of zonal flows in determining drift hole structure and in describing drift hole dynamics are discussed. In chapter 4, hole and granulation in trapped ion induced ion temperature gradient driven turbulence are discussed. We show that zonal flows reduce transport by exerting dynamical friction, which algebraically competes against other transport fluxes, such as a quasilinear diffusive flux.

Chapter 2

Efficiency of Intrinsic Rotation Generation in Tokamaks

2.1 Introduction

Turbulence driven mesoscale and mean flows in fusion plasmas, such as $E \times B$ shear flows (zonal flow, ZF)[17] and intrinsic rotation in toroidal direction[41, 23], play an important role in achieving better confinement and improving stability. The reduction of turbulent transport by radially sheared $E \times B$ flow[18, 33] is a widely accepted concept in the fusion community. The reduction of transport by sheared toroidal rotation[18] is also argued, based on the idea that the radial force balance relates the toroidal rotation to the radial electric field E_r, which is responsible for the transport reduction. The stabilization of resistive wall modes by toroidal rotation[42] is discussed as a means to achieve and sustain a high β discharge. The need for intrinsic flow in the transport reduction and the stabilization will surely increase for the future larger machines since it becomes harder to drive the plasma rotation by external means (NBI) due to shallow beam penetration and large plasma inertia.

One of the main issues in intrinsic flow physics is to explain its generation processes. The system is characterized by *no* external momentum input, while energy is injected into a system using methods such as radio-frequency heating.

To explain the generation of flows, the concept of a wave driven *residual stress* was developed and extensive experimental[41, 43, 44] and theoretical[45, 46] research on this topic is ongoing. The residual stress is a component of momentum flux which is not proportional to either flow or flow shear, as

$$\langle \tilde{V}_r \tilde{V}_\parallel \rangle = -\chi_\phi \langle V_\parallel \rangle' + U_r \langle V_\parallel \rangle + \Pi_{r\parallel}^{res} \tag{2.1}$$

The first term is diffusive part, the second term is pinch[47, 48, 49], and the last term is the residual stress. Intrinsic torque in toroidal plasmas, which is related to the residual stress via $\eta = -\nabla \cdot \Pi_{r\parallel}^{res}$, was observed for a plasma with no flow and unbalanced NBI injection (1 co + 2 counter)[43]. For a cylindrical plasma, the residual stress was determined by measuring the total flux $\langle \tilde{V}_r \tilde{V}_\theta \rangle$ and the diffusive part $-\chi_\theta \langle V_\theta \rangle'$ separately[44]. Note the direction of intrinsic flow is azimuthal in the case of a cylindrically symmetric plasma. The residual contribution was determined by calculating the difference of the two (i.e. the total flux and the diffusive flux), since there was no radial convection, i.e. no pinch effect, in the experiment. Symmetry breaking mechanisms were identified and shown to induce a non-zero Reynolds stress $\langle \tilde{V}_r \tilde{V}_\parallel \rangle \propto \langle k_\parallel k_\theta \rangle$ which includes the residual stress[46]. The momentum conservation theorem was formulated for wave-particle interaction and the resultant momentum flux, which includes the diffusive flux, the pinch, and the wave-driven residual stress, was calculated[45].

In the framework of residual stress, the generation process of flows can be understood as a conversion of thermal energy, which is injected into a system by heating, into kinetic energy of macroscopic flow by drift wave turbulence excited by ∇T, ∇n, etc (Fig. 2.1). From this picture, one may conceptually view the plasma as a type of an *engine*, where energy input drives turbulence, which leads to ∇T relaxation but also to the generation of flow. See Table 2.1 for a comparison between a 'car' and intrinsic rotation.

The idea of attributing flow generation to heat was mentioned by Carnot[25] to explain the general circulation of the Earth's atmosphere. The concept of an engine may be applied to the problem of the solar differential rotation as well. In the case of solar differential rotation, energy is generated by fusion at the core

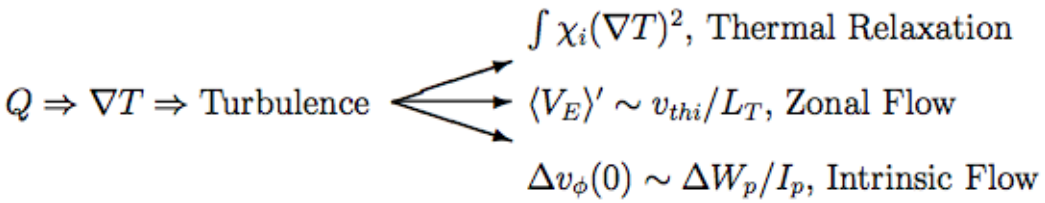

Figure 2.1: Energy input Q sets temperature profile ∇T which generates turbulence in a system. The turbulence leads to both relaxation and generation of flow

Table 2.1: Car and Intrinsic flow

	Car	Intrinsic Rotation
Fuel	Gas	Heating $\Rightarrow \nabla T$
Conversion	Burn	∇T driven DW Turbulence
Work	Cylinder/Cam	Residual Stress direction - symmetry breaking
Result	Wheel Rotation	Flow

of the sun (an example of fusion which actually works, albeit one using inertial confinement), leading to excitation of turbulence at the convective zone and generation of the solar differential rotation profile. See Table 2.2 for a comparison. In the fusion community, some attempts to characterize flow generation in plasmas as the result of the action of a *thermodynamic* engine have been discussed[50, 51]. In those, flow generation is treated as analogous to *the work* (power, more precisely) which can be extracted from the exchange of heat between hot and cold part of plasmas, i.e. the heat flux driven by ∇T. However, these discussions have not given a systematic calculation for the *figure of merit* of the engine.

In this paper, using the physical picture of plasma flow generation as an engine and a simple kinetic model with drift kinetic ions and adiabatic electrons, we formulate an explicit expression for the criterion for engine *efficiency* by comparing *rates of entropy production/destruction* due to thermal relaxation/flow generation. Flow generation reduces entropy since it leads to large scale order in the system. We formulate the entropy budget for the turbulent relaxation process by calculating the time evolution of the mean field entropy[52]. The mean field entropy is the

Table 2.2: Comparison of differential rotation in the sun and intrinsic rotation in tokamak

	Sun	Tokamak
Heat Source	fusion reaction at the core	Heat deposition
Turbulence Source	∇T	∇T
Threshold	Schwarzschild Criteria $\frac{1}{T}\left\|\frac{dT}{dz}\right\| > (\gamma-1)\frac{1}{\rho}\left\|\frac{d\rho}{dz}\right\|$	ITG $R/L_T > R/L_{T,c}$
Turbulence	Convective Turbulence	ITG Turbulence
Symmetry Breaking	Rotation, β Stratification	velocity shear, $\langle V_E\rangle'$ Intensity gradient, $I(x)$, ...
Resultant Flow	Polar Differential Rotation $v_\phi(\theta)$	Intrinsic Rotation $v_\parallel(r)$
B.C.	?	SOL, Edge, ...

part of entropy defined using only the mean field distribution function as $S_0 \equiv -\int d\Gamma \langle f\rangle \ln\langle f\rangle$, which evolves due to the action of turbulence. Note that S_0 is defined in terms of coarse grained fields. We show that thermal relaxation creates entropy, while intrinsic flow generation decreases the entropy of the system, consistent with the physical picture of flow as an ordered state. We also show that the destruction of entropy due to zonal flow is larger in magnitude than that due to intrinsic toroidal rotation by order of $O(k_\parallel/k_\perp)$, where k is a representative wave number of the drift waves. Given the disparity in their magnitude, we discuss the nature of the stationary state achieved by order-by-order balance in the entropy budget. We show that the lowest order balance, i.e. the balance between the entropy production rate due to the thermal relaxation and the entropy destruction rate due to the zonal flow generation, recovers the conventional stationary state, where turbulence is suppressed by zonal flow shearing. After discussing the class of possible stationary states, we define and calculate the efficiency of plasma flow drive using the entropy production rate and destruction rate. More precisely, an *upper* bound on the efficiency is calculated, since only the dominant contribution to the entropy production rate is retained. The scaling of intrinsic toroidal rotation generation is derived by using the entropy destruction rate due wave driven residual stress and shown to be proportional to $\rho_*^2(L_s^2/L_T^2)$. We emphasize these results are

obtained for, and apply only to, a standard, generic model of drift wave turbulence.

The reminder of the paper is organized as follows. In Sec. II, the entropy budget for turbulent relaxation with flow generation, is formulated. Using the expression for the entropy budget, we discuss the possible stationary state with coupling to flows. In Sec. III, we define and calculate the efficiency of the plasma flow drive, by using the entropy production rate derived in Sec. II. In Sec. IV, we present discussion and conclusions.

2.2 Entropy Budget

In this section, we formulate the entropy budget for the processes of turbulent relaxation and flow generation for a simple model of drift-ITG mode turbulence. In this derivation, we assume simple drift kinetic ions and adiabatic electrons. Given the basic structure of entropy budget, we discuss the possible stationary states with and without flow generation. We derive a coupled set of equations for turbulent fluctuations, δf^2 and shear flow evolution, which are analogous to the conventional predator-prey model for drift wave-zonal flow turbulence system, but are formulated at the level of phase space dynamics. The role of intrinsic toroidal rotation generation in stationary state is discussed as well.

2.2.1 Formulation

In kinetic theory, entropy is given as $S \equiv -\int d^3x d^3v f \ln f$ where f is the distribution function of a system. Here f is normalized to $\int d^3v f = n$. For a general case, f evolves in time according to the Boltzmann equation $df/dt = C(f)$ where $C(f)$ is a collision operator. For this system – which is open – one can calculate the evolution of entropy as ($d\Gamma \equiv d^3x d^3v$)

$$\partial_t S = -\int d\Gamma C(f) \ln f + \int d^3v \int d\mathbf{A} \cdot (\mathbf{v} f \ln f) \tag{2.2}$$

where $\int d\mathbf{A}$ denotes the integral over the surface area. From this relation, one can see that the net entropy of a system changes in two ways, i.e. by collisional

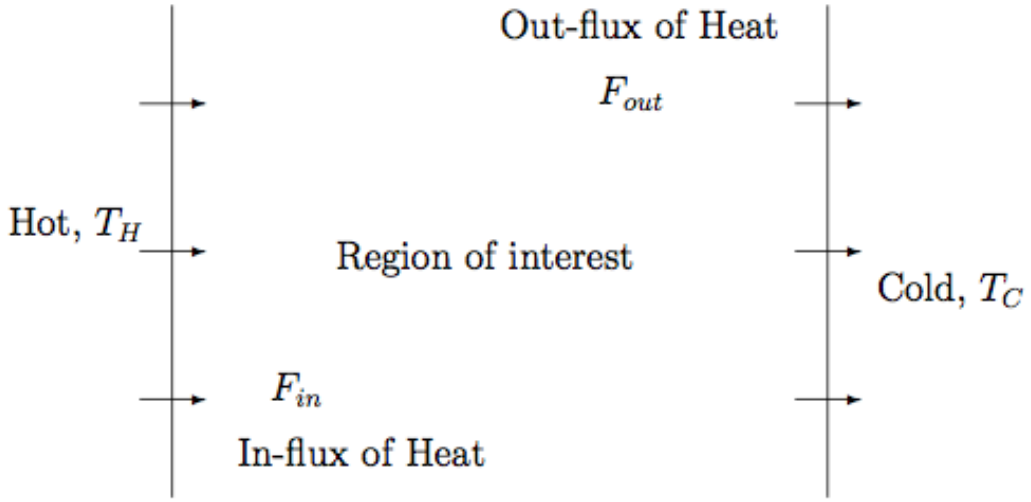

Figure 2.2: Heat flux through boundary. The region of interest is surrounded by hot and cold region with the temperature T_H and T_C.

entropy production (positive by H-theorem) and by a boundary flux term, which arises as a consequence of outflow of particles, heat, turbulence intensity, etc. In the following analysis the boundary term is dropped by assuming a boundary condition such as $f \propto n \to 0$ or $v_n \to 0$ where v_n is the velocity component normal to the boundary. *Before preceding, we offer the observation that the boundary term may play an important role in the entropy budget.* For example, the role of the boundary term for thermodynamic systems is described by Ozawa *et.al.*[26] as follows. For a system as shown in Fig. 2.2, the region of interest exchanges heat across the boundary between hot and cold regions. The entropy production associated with the heat exchange through the boundaries is $-F_{in}/T_H$ and F_{out}/T_C respectively, where $F_{in} > 0$ is the inflow of heat, $F_{out} > 0$ is the outflow of heat, T_H is the temperature of hot region, T_C is the temperature of cold region. Since for a stationary state, the influx and outflux are equal, the total effect of the boundary term on the net entropy balance is

$$-\frac{F_{in}}{T_H} + \frac{F_{out}}{T_C} = F\frac{T_H - T_C}{T_C T_H} > 0 \tag{2.3}$$

which shows a net contribution to the entropy budget from the boundary terms. Such an effect can be important in tokamak plasmas when one considers an annular region with steep temperature gradient, which suggests a significant difference in temperature across boundary. Here we consider a simplified case with no entropy outflow, so net volume integrated production and dissipation must cancel. As a consequence then, this theory is probably more directly relevant to δf particle simulations – which impose the boundary condition $\nabla\phi = 0$ and so preclude any out flux of entropy – than to actual tokamak plasmas. Indeed, since trends in the evolution of intrinsic rotation appear closely linked to the L-H transition, we note that the drop in the cross-boundary flux $\langle\tilde{v}_r\delta f^2\rangle/\langle f\rangle$ (which necessarily occurs at the transition) will impact the global entropy budget, and thus should be considered in models of intrinsic rotation evolution.

Since we are interested in turbulent relaxation, we focus on the generation of the "mean field" entropy[52], $S_0 \equiv -\int d\Gamma\langle f\rangle \ln\langle f\rangle$, where $\langle f\rangle$ is a coarse grained mean distribution fucntion. By decomposing $f = \langle f\rangle + \delta f$, one can approximate the coarse grained entropy as

$$\begin{aligned}\langle S\rangle &= -\int d\Gamma\langle(\langle f\rangle + \delta f)\ln(\langle f\rangle + \delta f)\rangle \\ &\cong -\int d\Gamma\langle f\rangle\ln\langle f\rangle - \int d\Gamma\frac{\langle\delta f^2\rangle}{\langle f\rangle} \\ &\equiv S_0 + S_2\end{aligned}$$

where $S_2 \equiv -\int d\Gamma\langle\delta f^2\rangle/\langle f\rangle$ is entropy of fluctuations. Using the decomposition of entropy and a linearized collision operator, i.e. $C(f) = C(\langle f\rangle) + C(\delta f) \cong C(\delta f)$, with $\langle f\rangle$ thus driven to a local Maxwellian, Eq. (2.2) can be rewritten in terms of S_0 as

$$\begin{aligned}\partial_t S_0 =& -\partial_t S_2 - \int d\Gamma\frac{\langle\delta f C(\delta f)\rangle}{\langle f\rangle} \\ =&\partial_t\int d\Gamma\frac{\langle\delta f^2\rangle}{\langle f\rangle} - \int d\Gamma\frac{\langle\delta f C(\delta f)\rangle}{\langle f\rangle}\end{aligned} \tag{2.4}$$

which relates the evolution of the mean field entropy to the evolution of and col-

lisional dissipation of δf^2. Note the last term, collisional dissipation, is positive definite, as a consequence of the H-theorem.

To calculate δf^2 generation, we employ a simple drift kinetic equation for ions

$$\partial_t f + v_\parallel \nabla_\parallel f + \frac{c}{B}\hat{\mathbf{z}} \times \nabla\tilde{\phi} \cdot \nabla f + \frac{|e|}{m_i}\tilde{E}_\parallel \frac{\partial f}{\partial v_\parallel} = C(f) \tag{2.5}$$

and assume adiabatic response for electrons

$$\frac{\delta n_e}{n_0} = \frac{|e|\tilde{\phi}}{T_e} \tag{2.6}$$

Thus we are interested in ITG turbulence as a specific model of drift wave turbulence. For δf^2 balance, we have

$$\begin{aligned} &\partial_t \left\langle \frac{\delta f^2}{2\langle f\rangle} \right\rangle + \frac{1}{r}\partial_r \left(r \left\langle \tilde{V}_r \frac{\delta f^2}{2\langle f\rangle} \right\rangle \right) - \frac{\langle \delta f C(\delta f)\rangle}{\langle f\rangle} \\ =& -\langle \tilde{v}_r \delta f\rangle \frac{\langle f\rangle'}{\langle f\rangle} - \frac{|e|}{m_i}\langle \tilde{E}_\parallel \delta f\rangle \frac{1}{\langle f\rangle}\frac{\partial \langle f\rangle}{\partial v_\parallel} \end{aligned} \tag{2.7}$$

where a scale separation between mean and fluctuation, i.e. $\partial_t \delta f \gg \partial_t \langle f\rangle$ and $\nabla \delta f \gg \nabla \langle f\rangle$ was assumed. Since we are interested in the evolution of

$$\int d\Gamma \langle \delta f^2\rangle / \langle f\rangle$$

(see Eq. (2.4)), we need to integrate Eq. (2.7) over phase space. Taking the phase space integral, one obtains

$$\partial_t \int d\Gamma \frac{\langle \delta f^2\rangle}{2\langle f\rangle} = \int d^3x (\mathcal{P} - \mathcal{D}) \tag{2.8}$$

where

$$\mathcal{P} \equiv \int d^3v \left(-\langle \tilde{v}_r \delta f\rangle \frac{\langle f\rangle'}{\langle f\rangle} - \frac{|e|}{m_i}\langle \tilde{E}_\parallel \delta f\rangle \frac{1}{\langle f\rangle}\frac{\partial \langle f\rangle}{\partial v_\parallel} \right) \tag{2.9a}$$

$$\mathcal{D} = -\int d^3v \frac{\langle \delta f C(\delta f)\rangle}{\langle f\rangle} \tag{2.9b}$$

Here $\mathcal{P}$ is the δf^2 production rate due to the free energy in configuration space (i.e. $\sim \partial\langle f\rangle/\partial r$) and velocity space (i.e. $\sim \partial\langle f\rangle/\partial v_\parallel$). $\mathcal{D}$ is the collisional dissipation.

To calculate $\mathcal{P}$, we assume $\langle f\rangle$ as a local Maxwellian with a mean shear flow, $\langle V_\perp\rangle(r)$ and $\langle V_\parallel\rangle(r)$. With quasi-neutrality $\tilde{n}_e = \tilde{n}_i$, one obtains

$$\begin{aligned}\mathcal{P} = &-\frac{n}{T_i L_T} Q^i_{turb} - \frac{n}{v^2_{thi}}\langle V_\perp\rangle'\langle \tilde{V}_r\tilde{V}_\perp\rangle \\ &- \frac{n}{v^2_{thi}}\langle V_\parallel\rangle'\langle \tilde{V}_r\tilde{V}_\parallel\rangle + \frac{1}{T_i}\langle \tilde{J}^i_\parallel \tilde{E}_\parallel\rangle \end{aligned} \tag{2.10}$$

where $v_{thi} \equiv \sqrt{(T_i/m_i)}$, $L_T^{-1} \equiv (dT_i/dr)/T_i$, $Q^i_{turb} \equiv n^{-1}\int d^3v E\langle \tilde{V}_r\delta f\rangle = \langle \tilde{V}_r\tilde{T}_i\rangle$, $\langle \tilde{V}_r\tilde{\mathbf{V}}\rangle \equiv n^{-1}\int d^3v(\mathbf{v}-\langle\mathbf{V}\rangle)\langle \tilde{V}_r\delta f\rangle$ and $\langle \tilde{J}^i_\parallel\tilde{E}_\parallel\rangle = |e|\int d^3v(v_\parallel - \langle V_\parallel\rangle)\langle \delta f\tilde{E}_\parallel\rangle$. Note the mean *ion* velocity was replaced by the mean *plasma* velocity, due to the large ion inertia. The first three terms are related to the spatial inhomogeneity of a local Maxwellian and have the standard form of the entropy production rate $\mathcal{J}_k\mathcal{X}_k$, where $\mathcal{J}_k = \{Q^i_{turb},\ \langle \tilde{V}_r\tilde{V}_\perp\rangle,\ \langle \tilde{V}_r\tilde{V}_\parallel\rangle\}$ is the flux vector and $\mathcal{X}_k = \{-\langle T\rangle',\ -\langle V_\perp\rangle',\ -\langle V_\parallel\rangle'\}$ is the thermodynamic force. In the following, we further simplify the entropy production rate by employing a simple model to calculate the turbulent flux as $\mathcal{J}_k = \mathcal{J}_k[\mathcal{X}_l]$ and discuss their consequences. The last term in Eq. (2.10) comes from the velocity space dependence in the distribution function and represents the effect of resonant heating. Using Poynting's theorem[53], one can write the heating term as

$$\begin{aligned}&\int d^3x\langle \tilde{J}^i_\parallel\tilde{E}_\parallel\rangle \\ &= \int d^3x(-\partial_t W - \nabla\cdot\mathbf{S}_w - \langle\tilde{\mathbf{J}}_\perp\cdot\tilde{\mathbf{E}}_\perp\rangle)\end{aligned} \tag{2.11}$$

Here W is wave energy density and $\mathbf{S}_w$ is flux of wave energy density. For a stationary state, the first term in the right hand side is zero, $\partial_t W = 0$. The second term also vanishes due to the boundary conditions, $\int d^3x\nabla\cdot\mathbf{S}_w = \int d\mathbf{A}\cdot\mathbf{S}_w|_{boundary} \to 0$. In other words we assumed there are no outgoing waves, again as enforced in simulations. The third term is also zero, $\langle\tilde{\mathbf{J}}_\perp\cdot\tilde{\mathbf{E}}_\perp\rangle = 0$, since $\mathbf{J}_\perp \propto \mathbf{E}\times\mathbf{B}$ at the lowest order. Thus the heating term is dropped in the following discussion.

To further simplify the entropy production rate term in Eq. (2.10), we employ a simple model for flux terms here. The first term in Eq. (2.10) is related

to the thermal relaxation. For simple ITG turbulence, we have a simple flux-gradient relation $Q^i_{turb} = -\chi_i \nabla T$, where the thermal conductivity χ_i is

$$\chi_i \sim \sum_k \tau_k^{DW} |\tilde{v}_r|_k^2 \Theta(R/L_T - R/L_{T,c}) \tag{2.12}$$

Here τ_k^{DW} is the correlation time for ITG drift wave turbulence and Θ is the step function, which accounts for the threshold condition. Using the flux-gradient relation, it follows that the production rate due to thermal relaxation is positive definite, i.e.

$$-\frac{n}{T_i L_T} Q^i_{turb} = n\chi_i \left(\frac{\nabla T}{T}\right)^2 > 0 \tag{2.13}$$

Thus turbulent thermal relaxation produces entropy. The second and the third term in Eq. (2.10) are the momentum flux in the perpendicular and parallel direction, which contain information concerning flow generation. For the perpendicular flow, for simplicity we consider only $E \times B$ shear flow or zonal flow, $\langle V_\perp \rangle' = \langle V_E \rangle'$. The momentum flux in the perpendicular direction can be calculated using the wave kinetic equation as $\langle \tilde{V}_r \tilde{V}_\theta \rangle = K \langle V_E \rangle'$ (See appendix B for the derivation) where

$$K \equiv \sum_k c_s^2 \tau_{ZF} \frac{\rho_s^2 k_\theta^2}{(1 + k_\perp^2 \rho_s^2)^2} \left(-k_r \frac{\partial \langle \eta_k \rangle}{\partial k_r}\right) \tag{2.14}$$

$$\eta_k \equiv (1 + k_\perp^2 \rho_s^2)^2 \left|\frac{e\phi_k}{T_e}\right|^2 \tag{2.15}$$

Here τ_{ZF} is the correlation time of the zonal flow, η_k is the fluctuation potential enstrophy and K is related to the nonlinear growth rate of zonal flow as $\gamma_{ZF} = q_r^2 K$ with q_r as the radial wave number of the zonal flow. Making *the assumption* that the zonal flow grows ($\gamma_{ZF} > 0 \Leftrightarrow K > 0 \Leftrightarrow -k_r \partial \langle \eta_k \rangle / \partial k_r$, a standard criteria for the zonal flow growth[17]), one can show that the entropy production rate due to zonal flow growth is negative definite, i.e.

$$-\frac{n}{v_{thi}^2} \langle V_\perp \rangle' \langle \tilde{V}_r \tilde{V}_\perp \rangle = -nK \left(\frac{\langle V_E \rangle'}{v_{thi}}\right)^2 < 0 \tag{2.16}$$

Hence, the generation of zonal flow leads to a *destruction* of entropy. This is physically plausible and can be easily understood, since zonal flow shears oppose relaxation of ∇T by reducing transport, and hence acts *against* entropy production. Put differently, one can regard zonal flow as a large scale coherent structure, and the generation of a coherent structure may be viewed as restoring "order" to the system, thus decreasing the entropy of that system. Note that the entropy destruction occurs only in the sense that it opposes entropy production due to other relaxation processes, i.e. thermal relaxation, here. The overall entropy production rate, i.e. the sum of those due to thermal relaxation and zonal flow generation, cannot be negative. The parallel momentum flux can be decomposed as[29]

$$\langle \tilde{V}_r \tilde{V}_\parallel \rangle = -\chi_\phi \langle V_\parallel \rangle' + U \langle V_\parallel \rangle + \Pi_{r\parallel}^{res} \tag{2.17}$$

The first term is turbulent diffusion of parallel momentum, the second term shows the effect of the pinch and the third term is residual stress, which leads to generation of intrinsic toroidal rotation. The pinch term is taken to be zero for simplicity hereafter, since it only re-distributes momentum by radial convection. For a stationary state, there is no torque input, so we must have

$$\langle \tilde{V}_r \tilde{V}_\parallel \rangle = -\chi_\phi \langle V_\parallel \rangle' + \Pi_{r\parallel}^{res} = 0 \tag{2.18}$$

to get a non-trivial toroidal flow profile, $\langle V_\parallel \rangle' = \Pi_{r\parallel}^{res} / \chi_\phi$. From this consideration, we see that the *total* entropy production rate due to parallel momentum flux, $\propto \langle V_\parallel \rangle' \langle \tilde{V}_r \tilde{V}_\parallel \rangle$, is *zero* for a stationary state of intrinsic toroidal rotation. However, it consists of *two* competing parts, i.e. the terms due to the diffusive and residual parts of the momentum flux, respectively. The diffusive part gives rise to viscous *heating* and the resultant entropy production rate is shown to be *positive definite*, i.e.

$$-\frac{n}{v_{thi}} \langle V_\parallel \rangle' \langle \tilde{V}_r \tilde{V}_\parallel \rangle |_{diff} = n \chi_\phi \left(\frac{\langle V_\parallel \rangle'}{v_{thi}} \right)^2 > 0 \tag{2.19}$$

The residual part in the parallel momentum flux leads to the *generation of intrinsic toroidal rotation* and the resultant entropy production rate is shown to be *negative*

definite, i.e.

$$\begin{aligned} &- \frac{n}{v_{thi}^2}\langle V_\parallel\rangle'\langle\tilde{V}_r\tilde{V}_\parallel\rangle|_{res} \\ =&- \frac{n}{v_{thi}^2}\langle V_\parallel\rangle'\Pi_{r\parallel}^{res} = -\frac{n}{\chi_\phi v_{thi}^2}\Pi_{r\parallel}^{res2} < 0 \end{aligned} \tag{2.20}$$

where the stationary condition for the parallel momentum flux $\langle V_\parallel\rangle' = \Pi_{r\parallel}^{res}/\chi_\phi$ was used.

After the simplification above, we have

$$\begin{aligned} \mathcal{P} =& n\chi_i\left(\frac{\nabla T}{T}\right)^2 - nK\left(\frac{\langle V_E\rangle'}{v_{thi}}\right)^2 \\ &+ n\chi_\phi\left(\frac{\langle V_\parallel\rangle'}{v_{thi}}\right)^2 - n\frac{\Pi_{r\parallel}^{res2}}{v_{thi}^2\chi_\phi} \end{aligned} \tag{2.21}$$

The first term is due thermal relaxation and is positive definite. The second term is related to the zonal flow generation and is negative definite, given that the zonal flow grows. The third term is due to viscous heating and is positive definite. The fourth term comes from the generation of intrinsic toroidal rotation and is negative definite.

2.2.2 Flow generation and stationary state

Since we are interested in the calculation of the efficiency of an engine for a *stationary* state, it would be important to clarify the criteria for stationarity and the physical picture of the system we are concerned with. Here we discuss the class of states which is defined by requiring δf^2 to be stationary. First we discuss the stationary state when the flow generation is *weak*. Then we consider the case with generation of flow.

When the generation of the flow is weak and the instability source is the temperature gradient, the production rate becomes

$$\mathcal{P} \cong n\chi_i\left(\frac{\nabla T}{T}\right)^2 > 0 \tag{2.22}$$

Table 2.3: Comparison of δf^2 stationary state

	$\mathcal{P} = \mathcal{D}$	$\mathcal{P} = 0$
Flow generation	Not necessarily	Yes
δf^2 production	∇T relaxation	∇T relaxation
δf^2 destruction	Collisional dissipation (small scale)	Flow generation (meso scale)

which is positive definite as long as a supercritical temperature gradient is maintained. To achieve stationarity, we must balance production with dissipation, i.e. $\mathcal{P} = \mathcal{D}$. Note that this is a global balance in phase space. One may understand this balance as a cascade of 'phasetrophy' δf^2 in phase space[30, 54], where δf^2 is produced by inhomogeneity in $\langle f \rangle(x)$ at some scale in phase space, transferred to smaller scale by nonlinear interaction and eventually dissipated by collision.

However, by allowing the generation of flow, one can access different type of stationary states, since entropy *destruction* occurs due to flow generation, as we saw in the last section. With the generation of flow, one can achieve stationary state with $\mathcal{P} \cong 0$. See Table 2.3 for the comparison.

Since $\langle \tilde{V}_r \tilde{V}_\perp \rangle \propto k_\theta k_\perp$, $\langle \tilde{V}_r \tilde{V}_\parallel \rangle \propto k_\theta k_\parallel$ and $k_\perp > k_\parallel$ for typical drift wave turbulence, the entropy destruction rate due to zonal flow generation is virtually *always* larger than that due to intrinsic toroidal rotation generation. Alternatively put, since self-generated flows are ultimately driven by wave momentum (i.e. momentum conservation laws relates flow momentum plus turbulence pseudomomentum to sources, sinks etc), and since $p_\theta = k_\theta N$ while $p_\parallel = k_\parallel N$, poloidal wave momentum naturally exceeds parallel wave momentum. In turn then, absent damping, poloidal and zonal flows naturally can be expected to exceed intrinsic toroidal flows. Hence, the $\mathcal{P} \cong 0$ state can be calculated order by order. To the lowest order in $O(k_\parallel / k_\perp)$,

$$\mathcal{P} \cong n\chi_i \left(\frac{\nabla T}{T} \right)^2 - nK \left(\frac{\langle V_E \rangle'}{v_{thi}} \right)^2 + O(k_\parallel / k_\perp)$$

Note that $K > 0$ for zonal flow growth. A non-trivial stationary state is evident

with $\mathcal{P} \cong 0$, i.e. when:

$$\langle V_E \rangle'^2 = \frac{\chi_i}{K} \frac{v_{thi}^2}{L_T^2} \tag{2.23}$$

Note that χ_i and K approximately cancel, i.e. $\chi_i/K \sim 1$, since $\chi_i \cong \sum_k |\tilde{v}_r|_k^2 \tau_k^{DW}$, $K \cong \sum_k |\tilde{v}_r|_k^2 \tau_k^{ZF}$ and $\tau_{ZF} \sim \tau_{DW}$ for a simple model. Here $\tau_k^{ZF} \sim 1/\nu_{eff}$, $\tau_k^{DW} \sim 1/\Delta\omega_k$ where ν_{eff} is the 'Krook' operator for wave-wave scattering process[30], $\Delta\omega_k$ is the decorrelation rate. Thus the stationary flow shear is tied directly to the ∇T force by:

$$\langle V_E \rangle'^2 \cong \frac{v_{thi}^2}{L_T^2} \Theta(L_T^{-1} - L_{T,c}^{-1}) = v_{thi}^2 \left(\frac{\nabla T}{T} \right)^2 \Theta(L_T^{-1} - L_{T,c}^{-1}) \tag{2.24}$$

where the step function $\Theta(L_T^{-1} - L_{T,c}^{-1})$ accounts for the threshold behavior, originating from the turbulent thermal conductivity χ_i. Note that the profile of zonal flow is relatively smooth. In other words the zonal flow treated here is a large scale flow, at the limit of long wave length.

It is interesting to see how δf^2 evolves in time with the dominant terms in the production rate, i.e. that of ∇T relaxation and zonal flow generation:

$$\partial_t \int d\Gamma \frac{\langle \delta f^2 \rangle}{2\langle f \rangle} = \int d^3x \left(n\chi_i \left(\frac{\nabla T}{T} \right)^2 - nK \left(\frac{\langle V_E \rangle'}{v_{thi}} \right)^2 \right) \tag{2.25}$$

Adding the equation for flow shear amplification by Reynolds stress, we have

$$\partial_t \int d\Gamma \frac{\langle \delta f^2 \rangle}{2\langle f \rangle} = \int d^3x \left(n\chi_i \left(\frac{\nabla T}{T} \right)^2 - nK \left(\frac{\langle V_E \rangle'}{v_{thi}} \right)^2 \right) \tag{2.26a}$$

$$\partial_t \frac{\langle V_E \rangle'^2}{2} = K \bar{q_r^2} \langle V_E \rangle'^2 - \nu_{col} \langle V_E \rangle'^2 \tag{2.26b}$$

where $\bar{q_r^2} \equiv \sum_q q_r^2 \langle V_E \rangle_q'^2 / \langle V_E \rangle'^2$ is the spectral average of the radial wave number of the zonal flow, q_r. Note that Eqs. (2.26a) and (2.26b) have the same structure as the familiar predator-prey model for the DW-ZF turbulence system[17, 55]. For comparison, recall the standard predator-prey form:

$$\partial_t \varepsilon = \gamma_L \varepsilon - \alpha V'^2 \varepsilon - \Delta\omega(\varepsilon)\varepsilon \tag{2.27a}$$

$$\partial_t V'^2 = \alpha V'^2 \varepsilon - \nu_{col} V'^2 \tag{2.27b}$$

where ε is the turbulence intensity, V'^2 is flow shear, γ_L is linear growth rate of a mode, α represents a coupling between flow and fluctuations, $\Delta\omega$ is a decorrelation rate, ν_{col} is a collisional drag on flow. By comparing the two set of equations, not surprisingly, we see that the fluctuation entropy or δf^2 plays the same role of the fluctuation intensity ε. In the terminology of the predator-prey system, δf^2 or fluctuation entropy is the 'prey' and the zonal flow shear is the 'predator.' The 'prey' grows with the relaxation process, $n\chi_i(\nabla T/T)^2$, and decreases with the generation of the 'predator,' $n\langle V_E\rangle'^2 K/v_{thi}^2$. The 'predator' increases by consuming the 'prey' (i.e. flow generated by fluctuations), $K\bar{q_r^2}\langle V_E\rangle'^2$, and eventually dissipated by small, but finite, collisional damping, $\nu_{col}\langle V_E\rangle'^2$. The steady state occurs when entropy generation and destruction balance each other. The stationary state is thus

$$\langle V_E\rangle'^2 = \frac{\chi_i}{K}\frac{v_{thi}^2}{L_T^2} \tag{2.28a}$$

$$K(|\hat{\phi}|^2) = \frac{\nu_{col}}{\bar{q_r^2}} \tag{2.28b}$$

which has the same structure as a stationary solution for the familiar predator-prey system, namely:

$$V'^2 = \frac{1}{\alpha}(\gamma_L - \Delta\omega(\varepsilon)) \tag{2.29a}$$

$$\varepsilon = \frac{\nu_{col}}{\alpha} \tag{2.29b}$$

The stationary level of the flow has similar structure in both systems, through the χ_i/L_T^2 and $\gamma_L - \Delta\omega$ dependence. Both systems show threshold behavior, $\chi_i \propto \Theta(L_{T,c}/L_T - 1)$ and $\gamma_L - \Delta\omega$. The flow level increases as drive of instability is strengthened, as manifested in $1/L_T$ and γ_L. This reflects the fact that the dynamical system naturally couples ∇T free energy to the flow. The stationary level of turbulence, $K \sim \chi_i$ in the model and ε in the standard predator-prey, is tied to the collisionality in flow, $\chi_i \sim K = \nu_{col}/\bar{q_r^2}$ and $\varepsilon = \nu_{col}/\alpha$, which is consistent with gyrokinetic simulations[56].

The role of generation of intrinsic *toroidal* rotation in stationary state can be seen by going to the higher order $O(k_\parallel/k_\perp)$ balance in the production rate term.

After the cancellation at the lowest order terms, the production rate becomes

$$\mathcal{P} = n\frac{\chi_\phi}{v_{thi}^2}\langle V_\parallel\rangle'^2 - n\frac{\Pi_{r\parallel}^{res2}}{v_{thi}^2\chi_\phi} \tag{2.30}$$

which consists of the production due to turbulent viscous heating and the destruction due to toroidal flow generation. The two terms cancel for a stationary state of intrinsic toroidal rotation, since

$$\langle \tilde{V}_r\tilde{V}_\parallel\rangle = -\chi_\phi\langle V_\parallel\rangle' + \Pi_{r\parallel}^{res} = 0 \tag{2.31}$$

Hence the *total* entropy production rate by the parallel momentum flux vanishes in a stationary state, i.e. the entropy production by intrinsic toroidal flow is balanced by the entropy destruction by intrinsic toroidal flow generation, to order $O(k_\parallel/k_\perp)$.

To summarize, we considered the two classes of stationary state: $\mathcal{P}$=$\mathcal{D}$ and $\mathcal{P} \cong 0$. The former is the stationary state with the balance between production (positive definite) and total dissipation, without the coupling to the flow generation. One may understand this process as the cascade of the 'phasetrophy'. The latter is achieved by including the effect of flow generation. The $\mathcal{P} = 0$ state is achieved order by order since the entropy destruction rate due to zonal flow and intrinsic toroidal rotation differ by $O(k_\parallel/k_\perp)$. The dominant balance occurs between ∇T relaxation and zonal flow generation. The effect of intrinsic toroidal rotation generation appears in the next order in $O(k_\parallel/k_\perp)$ and vanishes for a stationary state. Given all the terms calculated above, the total production rate becomes

$$\begin{aligned}\mathcal{P} =& n\chi_i\left(\frac{\nabla T}{T}\right)^2 - nK\left(\frac{\langle V_E\rangle'}{v_{thi}}\right)^2 \\ &+ n\chi_\phi\left(\frac{\langle V_\parallel\rangle'}{v_{thi}}\right)^2 - n\frac{\Pi_{r\parallel}^{res2}}{v_{thi}^2\chi_\phi}\end{aligned} \tag{2.32}$$

The first two terms balance at the lowest order and the next two terms balance at the next order. In the next section, we calculate the efficiency of flow generation for the stationary state with flow, i.e. the $\mathcal{P} = 0$ state.

2.3 Efficiency of Intrinsic Flow Drive

Having established the entropy budget for the flow generation and relaxation process, we are ready to calculate the efficiency of flow generation. In this section, we present a definition and calculation for the plasma flow generation efficiency. First, we define the efficiency using the entropy budget in the last section. After defining the efficiency, we give the actual calculation of its value and *scaling*, both for zonal flow and intrinsic toroidal rotation.

2.3.1 Definition of Efficiency

With the flow generation terms in the production rate, we have

$$\partial_t S_0 = \int d^3x \left(n\chi_i \left(\frac{\nabla T}{T} \right)^2 - nK \frac{\langle V_E \rangle'^2}{v_{thi}^2} + n\chi_\phi \frac{\langle V_\parallel \rangle'^2}{v_{thi}^2} - n \frac{\Pi_{r\parallel}^{res\,2}}{v_{thi}^2 \chi_\phi} \right) \tag{2.33}$$

We calculate the efficiency of flow generation for stationary state with $\mathcal{P} = 0$ where the balance is achieved order by order as explained in the last section. Using the expression for the entropy production rate, we define the efficiency of plasma flow generation as follows:

$$e \equiv \frac{|\int d^3x \mathcal{P}_{flow}|}{\int d^3x \mathcal{P}_{net}} \tag{2.34}$$

i.e. the ratio between the magnitude of the entropy destruction rate due to flow generation and the total entropy production rate due to relaxation. Note that the efficiency here is defined using the entropy production *rate* and destruction *rate* ($\propto \dot{Q}$ where Q is heat, not heat *flux*), while usually the efficiency of a *thermodynamic engine* is defined in terms of *heat and work* ($\propto Q$). In other words, the former is defined using ratios of *power*, while the latter is defined using ratios of *energy*. As for the entropy destruction mechanism, we can consider two cases, i.e. zonal flow generation $\mathcal{P}_{flow} = -(nK\langle V_E \rangle'^2)/v_{thi}^2$ and intrinsic toroidal flow generation

$\mathcal{P}_{flow} = -n(\Pi_{r\|}^{res})^2/\chi_\phi$. As for the net production rate, we have

$$\mathcal{P}_{net} = n\chi_i \left(\frac{\nabla T}{T}\right)^2 + n\chi_\phi \left(\frac{\langle V_\| \rangle'}{v_{thi}}\right)^2 \tag{2.35}$$

The first term is related to ∇T relaxation due to turbulence. The second term is related to the turbulent viscous heating. The second term is smaller than the first term by order of $(\langle V_\| \rangle / v_{thi})^2$, where $(\langle V_\| \rangle / v_{thi})^2 \equiv M_{th}^2 \sim 0.01$, typically. This follows, in part, from:

$$\begin{aligned} n\chi_\phi \left(\frac{\langle V_\| \rangle'}{v_{thi}}\right)^2 &\sim n\chi_\phi \left(\frac{\langle V_\| \rangle'}{\langle V_\| \rangle}\right)^2 \frac{\langle V_\| \rangle^2}{v_{thi}^2} \\ &\sim n\chi_i \left(\frac{\nabla T}{T}\right)^2 \frac{\langle V_\| \rangle^2}{v_{thi}^2} \end{aligned}$$

with $Pr \equiv \chi_\phi/\chi_i \sim 1$ and $\nabla T/T \sim \langle V_\| \rangle'/\langle V_\| \rangle$. Hereafter, we only keep the dominant contribution to the net entropy balance, i.e. $P_{net} \cong \chi_i(\nabla T/T)^2$. Since we drop the positive definite term (the turbulent viscous heating) in the denominator in Eq. (2.34), we calculate an *upper bound* for the efficiency.

2.3.2 Efficiency of zonal flow generation

As the first case, we consider the efficiency of zonal flow generation, although the outcome is trivial as shown below. Using the definition given above, we obtain, as an upper bound,

$$e_{ZF} \lesssim \frac{\int d^3x (nK\langle V_E \rangle'^2)/v_{thi}^2}{\int d^3x (n\chi_i)/L_T^2}. \tag{2.36}$$

Since we are interested in the efficiency at a stationary state, we substitute Eq. (2.23) for the value of $\langle V_E \rangle'$. With the substitution, one obtains

$$e_{ZF} \lesssim 1 \tag{2.37}$$

This is the result we should expect given the *assumption* we made, i.e. we considered flow shear dominated state for δf^2 balance

$$\partial_t \int d\Gamma \frac{\langle \delta f^2 \rangle}{\langle f \rangle} = \int d^3x \left(n \frac{\chi_i}{L_T^2} - \frac{n \langle V_E \rangle'^2}{v_{thi}^2} K \right) = 0 \tag{2.38}$$

and defined the efficiency to be the ratio of the two terms in the right hand side. Hence

$$e_{ZF} \lesssim 1 \tag{2.39}$$

is just the restatement of the fact that we have a stationary state by balancing the entropy production rate due to thermal relaxation and the dominant entropy destruction rate due to zonal flow growth.

2.3.3 Efficiency of intrinsic toroidal flow generation

The efficiency of zonal flow production was calculated using dominant terms in the production rate, Eq. (2.32). By going to next order in $O(k_\parallel/k_\perp)$, we can calculate the efficiency of intrinsic toroidal rotation generation. In this picture, generation of intrinsic toroidal rotation is considered to be a two step process (Fig. 2.3): Firstly, a stationary state is achieved by a balance between dominant terms in the entropy production rate, i.e. temperature relaxation and zonal flow generation. This is the state given by the stationary solution of Eq.(2.26a) and Eq.(2.26b) with $e_{ZF} \sim 1$. As a secondary process, this preexisting stationary turbulent plasma and shear flow give rise to the wave driven residual stress, which generates an intrinsic toroidal torque. Thus, the efficiency of intrinsic toroidal flow in this process is, from the definition,

$$e_{IR} \cong \frac{\int d^3x n (\Pi_{r\parallel}^{res})^2 / (v_{thi}^2 \chi_\phi)}{\int d^3x n \chi_i (\nabla T/T)^2} \tag{2.40}$$

We can easily estimate the order of magnitude for e_{IR}. Using the stationary condition for intrinsic flow $\Pi_{r\parallel}^{res} = \chi_\phi \langle V_\parallel \rangle'$ and assuming $\langle V_\parallel \rangle' / \langle V_\parallel \rangle \sim \sigma \nabla T/T$ (where σ is a $O(1)$ constant factor), we can obtain (here $M_i \equiv \langle V_\parallel \rangle / v_{thi}$ is toroidal

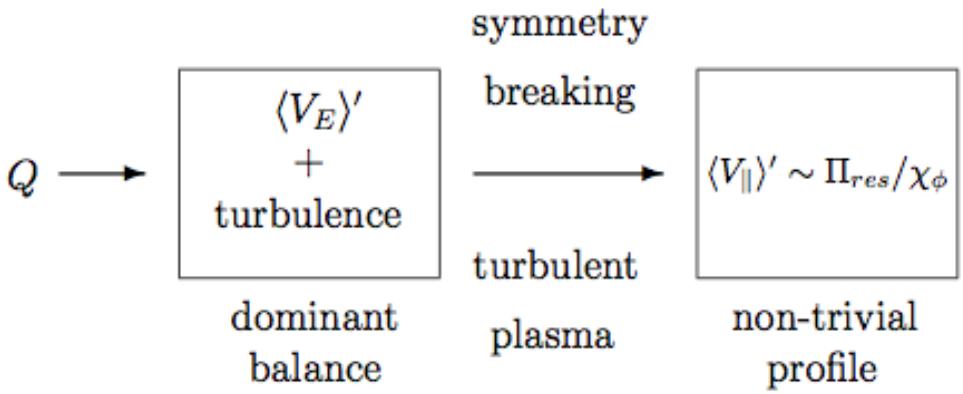

Figure 2.3: Turbulent plasma and flow generation

Mach number)

$$e_{IR} = \frac{\int d^3x n \chi_\phi \langle V_\parallel \rangle'^2 / v_{thi}^2}{\int d^3x n \chi_i (\nabla T/T)^2} \sim \sigma^2 M_i^2 \tag{2.41}$$

For a typical value of $M_i \sim 0.1$ and $\sigma \sim 1$, we have $e_{IR} \sim 0.01$ which states that intrinsic toroidal rotation generation has low efficiency. This is also consistent with the assumption that intrinsic toroidal rotation contribution to entropy generation is smaller than that from zonal flow. Both are a straightforward consequence of the ordering $k_\parallel < k_\perp$. Note that more careful consideration must be given to cases with reversed shear.

In order to explicitly *calculate* the scaling form of e_{IR}, one needs the modeling of residual stress. In doing so, we consider a simple $\langle V_E \rangle'$ driven case, since $\langle V_E \rangle'$ is already given as a consequence of lowest order balance in δf^2 stationarity. In this case, a shift in the spectral envelope, which is required for non-zero Reynolds stress $\langle k_\parallel k_\theta \rangle \propto \langle x \rangle$, originates from the radial electric field shear or $\langle V_E \rangle'$ as[46]

$$\left\langle \frac{k_\parallel}{k_\theta} \right\rangle = -\rho_* \frac{L_s}{2c_s} \langle V_E \rangle' \tag{2.42}$$

for simple drift wave turbulence. Here $\rho_* \equiv \rho_s/a$, ρ_s is ion sound Larmor radius, $L_s^{-1} = \hat{s}/(qR)$ is a shear length, a is the minor radius. This can be further

calculated by using the stationary value for the $E \times B$ flow, Eq. (2.24):

$$\left\langle \frac{k_\parallel}{k_\theta} \right\rangle = \mp \rho_* \frac{L_s}{2c_s} \sqrt{\frac{\chi_i}{K}} \frac{v_{thi}}{L_T} = \mp \frac{\rho_*}{2\tau} \sqrt{\frac{\chi_i}{K}} \frac{L_s}{L_T} \tag{2.43}$$

where $\tau \equiv T_e/T_i$. The sign is ultimately determined by the sign of $E \times B$ shear; however, in the following discussion we only need the squared value of $\langle k_\parallel/k_\theta \rangle$, so the sign is not important. Given the symmetry breaking by $E \times B$ shear, one can calculate the residual stress driven by the wave momentum flux as[45]

$$\Pi_{r\parallel}^{res} = K \langle V_E \rangle' \left\langle \frac{k_\parallel}{k_\theta} \right\rangle \tag{2.44}$$

$$= -\rho_* \frac{L_s}{2c_s} K \langle V_E \rangle'^2 \tag{2.45}$$

$$= -\rho_* \frac{L_s}{2c_s} \chi_i \left(\frac{\nabla T}{T} \right)^2 v_{thi}^2 \tag{2.46}$$

Here we assumed the $E \times B$ flow shear symmetry breaking in the second equality and δf^2 stationarity in the third equality. Note that the residual stress scales directly as the temperature gradient, ∇T. This is due to the fact that to estimate $\langle V_E \rangle'$, we used δf^2 stationarity instead of radial force balance, which would relate $\langle V_E \rangle'$ to the pressure gradient ∇P, rather than ∇T. Use of δf^2 stationarity is more consistent, with both the model under study and with assumptions made in the theory. A recent simulation result by Wang, et.al.[57] exhibits a similar behavior, albeit the scaling is between intrinsic *torque* ($\propto \nabla \cdot \Pi_{r\parallel}^{res}$) and ion temperature gradient. Wang has also noted that intrinsic torque scales with ∇T_e for CTEM turbulence.[58]

One of the consequences of the residual stress modeling here, although somewhat outside of the scope of the paper, is that one can calculate a non-trivial stationary profile of intrinsic toroidal flow as

$$\langle V_\parallel \rangle' = \frac{\Pi_{r\parallel}^{res}}{\chi_\phi} = -\frac{1}{2} \rho_* \frac{\chi_i}{\chi_\phi} \frac{L_s}{c_s} \left(\frac{\nabla T}{T} \right)^2 v_{thi}^2 \tag{2.47}$$

This simple relation directly relates the intrinsic toroidal flow shear to the temperature gradient – which is consistent with recent experiments on LHD[59] and

Alcator C-Mod – and the magnetic shear. Note that the intrinsic toroidal flow shear depends strongly on temperature gradient as $\langle V_\parallel \rangle' \propto (\nabla T)^2$, while zonal flow shear is directly proportional to temperature gradient, $\langle V_E \rangle' \propto \nabla T$. This is because in this model, $E \times B$ shear flow plays a dual role in intrinsic toroidal flow shear; i.e. $E \times B$ shear flow breaks symmetry ($\langle k_\parallel k_\theta \rangle \propto \langle V_E \rangle'$) and gives rise to the flux of wave momentum ($\Pi_{r\parallel}^{res} \propto \langle V_E \rangle'$).[30] Hence $\langle V_\parallel \rangle' \propto \langle V_E \rangle'^2$, which gives the $(\nabla T)^2$ dependence. Note also the explicit ρ_* dependence, which originates from the symmetry breaking. One can also calculate the flow velocity $\langle V_\parallel \rangle$ by integrating once to show:

$$\frac{\langle V_\parallel \rangle}{v_{thi}} \cong \frac{1}{2} \rho_* \frac{\chi_i}{\chi_\phi} \frac{L_s}{L_T} \sqrt{\frac{T_i}{T_e}} \tag{2.48}$$

Here we used $(T'/T)' = -(T'/T)^2 + T''/T \cong -(T'/T)^2$. The scaling derived here can be compared to Rice scaling[23] $\Delta v_\phi(0) \sim \Delta W_p / I_p$, which shows similar behavior; ∇T is large when confinement is good, such as the H-mode, which tracks the ΔW_p behavior. Current scaling can enter through the geometry of the B field, $L_s \propto q/\hat{s}$, which suggests the scaling, $q \propto B_\theta \sim I_p^{-1}$. Note that the scaling calculated here shows the direct dependence on ∇T rather than ∇P, since $\langle \delta f^2 \rangle$ stationarity is used to calculate $\langle V_E \rangle'$ and $\langle \delta f^2 \rangle$ evolves via ITG turbulence. Note also that the expression for the flow contains the information regarding directionality. However, the sign of the flow direction is strongly model dependent.[46] Moreover, this is a consequence of residual stress modeling and is not directly related to the efficiency calculation, which is the main focus of the paper. Indeed, note $e \sim \Pi_{r\parallel}^{res\,2}$, so e is independent of the sign of $\Pi_{r\parallel}^{res}$. Hence here we do not pursue a detailed discussion regarding the relation between flow direction and entropy, but rather leave this to a future publication. We also note that a similar scaling $\Delta v_\phi \sim \nabla \langle T \rangle / B_\theta$ was proposed on the basis of the modeling of off-diagonal components in momentum flux.[60, 61] That work was concerned with the velocity increment for the change of NBI direction and included the explicit momentum source (NBI torque) in the analysis.

The efficiency can be calculated by using the value for $\Pi_{r\parallel}^{res}$:

$$e_{IR} = \frac{\int d^3x n \frac{\chi_i}{\chi_\phi} \chi_i (\nabla T/T)^2 \frac{L_s^2}{L_T^2} \frac{\rho_*^2}{4} \frac{v_{thi}^2}{c_s^2}}{\int d^3x n \chi_i (\nabla T/T)^2} \sim \rho_*^2 \frac{q^2}{\hat{s}^2} \frac{R^2}{{L_T}^2} \tag{2.49}$$

where we assumed that $\chi_i \sim \chi_\phi$, $T_e \sim T_i$, $\hat{s} \neq 0$. The efficiency depends on: i) machine size, ρ_*, which implies the efficiency will decrease for larger machines. Note that the ρ_* scaling appears, even *after* calcualting the ratio of turbulence driven quantities, i.e. it is not a trivial consequence of $|e|\tilde{\phi}/T_e \sim \rho_*$ scaling. In fact, the ρ_* scaling originates from ρ_* dependence in the symmetry breaking correlator, $\langle k_\parallel k_\theta \rangle \propto \langle x \rangle \propto \rho_*$. We speculate the ρ_* dependence is thus inherent to any residual stress modeling based on $k_\parallel$ symmetry breaking of drift wave turbulence. ii) geometry of the B field, $q/\hat{s}$. In a simple geometry with $\hat{s} = const \sim O(1)$, the efficiency varies as $q \propto B_\theta \sim I_p^{-1}$, which shows an *unfavorable* current scaling, as in the Rice scaling[23] $\Delta v_\phi(0) \sim \Delta W_p/I_p$. Note this is a $q(r)$ scaling, not an I_p scaling. and iii) temperature gradient, R/L_T, which originates from both symmetry breaking and wave momentum flux driven by $V_E' \propto \nabla T$. Plasmas with a steep gradient, i.e. such as H-mode plasmas, are more effective and efficient for driving intrinsic toroidal rotation. The dependence on ∇T can be linked to the ΔW_p dependence in the Rice scaling. Here, the efficiency scaling of intrinsic rotation drive is directly tied to ∇T rather than ∇P. This is a consequence of the fact that the model in this paper is derived for ITG turbulence. The resultant $E \times B$ flow is also driven by ITG turbulence, so it is no surprise that we have $\langle V_E \rangle' \propto \nabla T$. Note that the scaling was evaluated in local form in the last expression. This is a reasonable approximation when a system has a well-defined gradient region, such as for a peaked profile or a transport barrier, for example. Of course the case with reversed shear internal transport barrier is of great interest; however, this is beyond the scope of the paper, which assumes normal shear with $\hat{s} \sim O(1)$.

2.4 conclusion

In this paper, by analogy between plasma flow generation and an engine, we introduced the concept of flow generation efficiency by calculating the ratio of the entropy destruction rate due to turbulent flow generation to the entropy production rate due to thermal relaxation. The principal results are:

1. The entropy production rate was calculated and shown to be

$$\begin{aligned}\mathcal{P} =& n\chi_i \left(\frac{\nabla T}{T}\right)^2 - nK\left(\frac{\langle V_E\rangle'}{v_{thi}}\right)^2 \\ &+ n\chi_\phi \left(\frac{\langle V_\parallel\rangle'}{v_{thi}}\right)^2 - n\frac{\Pi_{r\parallel}^{res\,2}}{v_{thi}^2\chi_\phi}\end{aligned}$$

   Thermal relaxation and viscous heating produce entropy. Flow generation, driving both zonal flow and intrinsic toroidal rotation, leads to the destruction of entropy. The first two terms is larger than the last two terms by the order of $O(k_\parallel/k_\perp)$. The production rate due thermal relaxation (the first term) and viscous heating (the third term) differs in magnitude by $M_i^2 \equiv (\langle V_\parallel\rangle/v_{thi})^2 \sim 0.01$ for a typical value of $M_i \sim 0.1$, since $\chi_i \sim \chi_\phi$, $(\langle V_\parallel\rangle'/v_{thi}) \sim M_i(\langle V_\parallel\rangle'/\langle V_\parallel\rangle)$, $(\nabla T/T) \sim \sigma(\langle V_\parallel\rangle'/\langle V_\parallel\rangle)$ and $\sigma \sim 1$.

2. Coupled equations for phase space density fluctuation intensity δf^2 and zonal flow were formulated based on entropy budget and wave kinetic analysis. They have a similar structure to the familiar predator-prey model

$$\begin{aligned}&\partial_t \int d\Gamma \frac{\langle \delta f^2\rangle}{2\langle f\rangle} \\ &= \int d^3x \left(n\chi_i \left(\frac{\nabla T}{T}\right)^2 - nK\left(\frac{\langle V_E\rangle'}{v_{thi}}\right)^2\right)\end{aligned}$$

$$\partial_t \frac{\langle V_E\rangle'^2}{2} = K\bar{q_r^2}\langle V_E\rangle'^2 - \nu_{col}\langle V_E\rangle'^2$$

   where δf^2 plays the role of the prey population density.

3. The stationary levels of zonal flow and intrinsic toroidal rotation were cal-

culated for the state achieved by imposing $\mathcal{P} = 0$ order by order. They are

$$\langle V_E \rangle'^2 = \frac{\chi_i}{K} \frac{v_{thi}^2}{L_T^2}$$
$$\langle V_\parallel \rangle' = -\frac{1}{2} \rho_* \frac{\chi_i}{\chi_\phi} \frac{L_s}{c_s} \left(\frac{\nabla T}{T} \right)^2 v_{thi}^2$$
$$\frac{\langle V_\parallel \rangle}{v_{thi}} \cong \frac{1}{2} \rho_* \frac{\chi_i}{\chi_\phi} \frac{L_s}{L_T} \sqrt{\frac{T_i}{T_e}}$$

The first relation is obtained from lowest order balance in the entropy production rate. The $E \times B$ shear is tied to the ∇T thermodynamic force directly, since at saturation entropy destruction due zonal flow balances entropy production due thermal relaxation. The second relation is calculated from the next order balance in the entropy production rate and the third relation is obtained by integrating the second relation. The intrinsic toroidal flow shows a similar scaling to the Rice scaling $\Delta v_\phi(0) \sim \Delta W_p / I_p$, i.e. $L_T^{-1} \sim \nabla T$ corresponds to ΔW_p and $L_s \propto q \sim B_\theta$ for fixed magnetic shear corresponds to I_p^{-1}. Explicit ρ_* scaling originates from the symmetry breaking mechanism invoked in the model.

4. The efficiency of flow generation is defined as the ratio of entropy destruction rate due to flow generation to entropy production rate due to thermal relaxation. The actual value for the efficiency was calculated for intrinsic toroidal rotation and shown to be $e_{IR} \sim M_i^2 \sim 0.01 - 0.1$ for a value of $M_i \sim 0.1 - 0.3$. This indicates that the drive of toroidal rotation is inherently one of a process of modest efficiency. This finding follows from $k_\parallel < k_\perp$.

5. The scaling of the intrinsic toroidal flow generation efficiency was derived as

$$e_{IR} = \rho_*^2 \frac{q^2}{\hat{s}^2} \frac{R^2}{L_T^2}$$

The efficiency of intrinsic toroidal flow generation scale as machine size ρ_*, geometry of the B field $q/\hat{s}$ and temperature profile R/L_T. Related to 3.) above, the efficiency exhibits a similar scaling behavior to the Rice scaling,

except for the appearance of explicit ρ_* scaling. Note that the efficiency scaling suggests a possible origin of the unfavorable current scaling through the safety factor[62], q.

As a caveat, the model cannot capture the phenomenology of flow direction dependence on plasma current direction. In particular, the model cannot describe the reversal of flow direction in TCV[63], since this reversal is likely related to the conversion of drift modes between ion and electron branches. However, model presented here includes only ITG turbulence. A recent simulation by W. X. Wang also showed that the residual stress scaling is strongly dependent upon the kind of driving turbulence, i.e. the residual stress scale with ∇T_i for ITG turbulence and with ∇P_e for CTEM turbulence[58], which is likely to give a different efficiency scaling for CTEM turbulence. To capture the flow reversal physics and clarify the mode dependence of the efficiency scaling, one would need a further extension of the theory to include the dynamics of non-adiabatic electrons and their role in the entropy budget. The boundary term is dropped throughout the analysis as well. These may also have an impact on the entropy budget. Note that in H-mode, turbulence is unlikely and fluctuation flux, a cause of the boundary terms, is quenched. Note also that the calculation implemented here is a reasonably faithful model of the computer simulation studies by W. X. Wang[57]. In that δf PIC simulation using GTS, $\nabla\phi = 0$ is imposed at the boundaries, thus guaranteeing no entropy outflow. Interestingly, that simulation observed symmetry breaking by zonal flow shear $\langle V_E\rangle'$ and a level of intrinsic toroidal rotation $\langle V_\phi\rangle \sim \nabla T$, as calculated here. This suggests that it would be interesting for the simulation to examine the ρ_* and I_p scaling of the intrinsic rotation, as well as to directly calculate the efficiency and compare with theoretical predictions. The role of the boundary term will pursued in the future publication.

2.A Appendix: Linear mode

In this section, we review basic properties of drift waves (DW) which we need in the calculation of shift in the mode.

First we start with DW without symmetry breaking. Susceptibility for DW ($\tilde{n}/n = \chi(|e|\tilde{\phi}/T_e)$) is given by

$$\chi = \frac{\omega_{*e}}{\omega} + \frac{k_\parallel^2 c_s^2}{\omega^2} - 1 - k_\perp^2 \rho_s^2 \tag{2.51}$$

In sheared magnetic field, susceptibility takes a operator form

$$\hat{\chi} = \frac{\omega_{*e}}{\omega} + \frac{k_y^2 c_s^2 x^2}{\omega^2 L_s^2} - 1 - k_y^2 \rho_s^2 + \rho_s^2 \partial_x^2 \tag{2.52}$$

Solving the eigenvalue problem $\hat{\chi}\hat{\phi} = 0$, one obtains

$$\omega = \frac{\omega_{*e}}{1 + k_y^2 \rho_s^2} - i\frac{|L_n|}{|L_s|} \tag{2.53}$$

$$\phi \propto \exp(-i\frac{\mu}{2}x^2) \text{ with } \mu \equiv \frac{L_n}{\rho_s^2 L_s} \tag{2.54}$$

With $E \times B$ shear flow as a symmetry breaker,

$$\hat{\chi} \cong \frac{\omega_{*e}}{\omega}(1 - \frac{k_y \langle V_E \rangle' x}{\omega}) + \frac{k_y^2 c_s^2 x^2}{\omega^2 L_s^2} - 1 - k_y^2 \rho_s^2 + \rho_s^2 \partial_x^2 \tag{2.55}$$

and the mode will be shifted around a rational surface by

$$x_0 = -\rho_* \frac{L_s^2}{2c_s} \langle V_E \rangle' \tag{2.56}$$

$$\phi \propto \exp(-i\frac{\mu}{2}(x + x_0)^2) \tag{2.57}$$

Then the spectral average of $k_\parallel$ is obtained as

$$\left\langle \frac{k_\parallel}{k_\theta} \right\rangle = \left\langle \frac{x_0}{L_s} \right\rangle = -\rho_* \frac{L_s}{2c_s} \langle V_E \rangle' \tag{2.58}$$

2.B Appendix: Wave Kinetic Analysis of flow generation

In this section, we derive the radial momentum flux of $E \times B$ shear flow, the growth rate of the mean $E \times B$ flow and the radial momentum flux of IR, based on wave kinetic equations.

We start with wave kinetic equation

$$\begin{aligned} &\partial_t N_k + \frac{\partial \omega_k}{\partial \mathbf{k}} \cdot \frac{\partial N_k}{\partial \mathbf{x}} - \frac{\partial \omega_k}{\partial \mathbf{x}} \cdot \frac{\partial N_k}{\partial \mathbf{k}} \\ =& -2\frac{\mathrm{Im}\epsilon}{\partial \epsilon/\partial \omega} N_k + C_w(N_k) \end{aligned} \tag{2.59}$$

Here $N_k = (\partial\epsilon/\partial\omega)(|E_k|^2/8\pi)$ is wave action density and we allowed wave-wave scattering in the right hand side. At the simplest level one can employ Krook type operator $C_w(N_k) = -\nu_{eff}\delta N_k$. In the following calculation we assume strong 'collisionality' between waves, i.e. ν_{eff}^{-1} is assumed to be the fastest timescale[17]. Note the dielectric function ϵ is related to the susceptibility in the last section as $\epsilon = 1 - \chi/(k^2\lambda_{De}^2)$. For example, wave action density for EDW is

$$N_k = -\frac{\partial \chi}{\partial \omega}\frac{|E_k|^2}{8\pi k^2 \lambda_{De}^2} = \frac{nT_e}{2\omega_{*e}}(1 + k_\perp^2\rho_s^2)^2 \left|\frac{e\phi_k}{T_e}\right|^2 \tag{2.60}$$

Inhomogeneity in medium, such as intensity gradient and $E \times B$ shear flow, builds up inhomogeneity in wave population density. For the general derivation and discussion, see [17]. For the purpose of this paper, it is sufficient to consider a pure $\langle V_E \rangle'(x)$ driven case. For this case, one can solve wave kinetic equation to obtain

$$\delta N_k(x) = \frac{1}{\nu_{eff}} k_\theta \delta \langle V_E \rangle'(x) \frac{\partial \langle N_k \rangle}{\partial k_r} \tag{2.61}$$

With this, one can calculate the Reynolds Stress to drive ZF and the residual stress for IR.

For the Reynolds stress for ZF, one can calculate as

$$\begin{aligned}\delta\langle\tilde{V}_r\tilde{V}_\theta\rangle(x) =& -\sum_k \frac{\rho_s^2 k_r k_\theta c_s^2}{(1+k_\perp^2\rho_s^2)^2}\frac{2\omega_{*e}}{nT_e}\delta N_k(x) \\ \equiv& K\delta\langle V_E\rangle'(x)\end{aligned} \tag{2.62}$$

where

$$K \equiv \sum_k c_s^2\tau_{ZF}\frac{\rho_s^2 k_\theta^2}{(1+k_\perp^2\rho_s^2)^2}\left(-k_r\frac{\partial\langle\eta_k\rangle}{\partial k_r}\right), \tag{2.63}$$

$\eta_k \equiv (1+k_\perp^2\rho_s^2)^2|(e\phi_k)/T_e|^2$ is potential enstrophy and $\tau_{ZF} \equiv \nu_{eff}^{-1}$.

The growth rate is easily obtained with the momentum flux derived above and shown to be

$$\gamma_{flow} = q_r^2 K \tag{2.64}$$

The instability requires $K > 0$ or $-k_r(\partial\langle\eta_k\rangle/\partial k_r) > 0$, which is the same criteria for zonal flow growth.

For the residual stress in the parallel momentum flux $\Pi_{r\|}^{res}$, one can calculate as[30]

$$\begin{aligned}\Pi_{r\|}^{res} &= \frac{1}{m_i n}\sum_k v_{g,r}k_\| \delta N_k \\ &= \frac{c_s^2}{T_e n}\sum_k -\frac{2\rho_s^2 k_r k_\theta v_*}{(1+k\ \perp^2\ \rho_s^2)}k_\|\delta N_k \\ &\equiv \left\langle\frac{k_\|}{k_\theta}\right\rangle K\delta\langle V_E\rangle'(x)\end{aligned} \tag{2.65}$$

where

$$\left\langle\frac{k_\|}{k_\theta}\right\rangle \equiv \frac{1}{K}\sum_k \frac{k_\|}{k_\theta}c_s^2\tau_{ZF}\frac{\rho_s^2 k_\theta^2}{(1+k_\perp^2\rho_s^2)^2}\left(-k_r\frac{\partial\langle\eta_k\rangle}{\partial k_r}\right) \tag{2.66}$$

Acknowledgement

Chapter 2 is a reprint of material appearing in Y. Kosuga, P. H. Diamond and O.D. Gurcan, Phys Plasmas, **17**, 102313 (2010). The dissertation author was the primary investigator and author of this article.

Chapter 3

Drift hole structure and dynamics with turbulence driven flows

3.1 Introduction

A coherent structure is a frequently observed element in turbulent systems. While a coherent structure often forms in fluid turbulence in *real space*, such structures also form in *phase space*. In real space, a well-known example of such a coherent structure is a coherent vortex in fluid turbulence, especially those observed in quasi-2D fluids, including 'eyes' on Jupiter. Another example in real space turbulence is a density blob or a hole in tokamak plasmas[64, 65] (Fig.3.1). Density blobs or holes are generated at the plasma edge, where strong gradient perturbations generate an outgoing blob and an incoming hole. Once generated, the density hole (blob) can grow as it climbs (descends) the density gradient. This observation suggests that turbulence may be stirred by incoming nonlinear structures, as well as by local linear instability. Such structure driven turbulence may play a role in understanding the phenomenology of 'No Man's Land' in tokamak plasmas, a region that connects the tokamak core and edge.

A coherent structure in turbulence and its growth are not limited to real space, but also extend to phase space. The simplest example of such structures is that from 1D Vlasov plasmas, such as a BGK vortex[19], a phase space density

hole[20], and clump-hole pairs[31] in the context of the Berk-Breizman model[31] for energetic particle phenomenology. These coherent structures in phase space form due to strong wave-particle resonance, which generates a potential that can hold particles together in a trough. These trapped particles in turn generate a self-potential, leading to formation of a self-sustained structure. Once formed, such structures can grow by extracting free energy, as depicted in Fig.3.1. More precisely, the growth is made possible by momentum exchange with, and velocity scattering by other species[20] (for example, structures in ions must scatter electrons to maintain the quasi-neutrality). Such mechanisms allow a hole to be displaced up the phase space density gradient. The displacement leads to the growth of the hole, since phase space density is necessarily conserved along trajectory. Such growth of phase space density structures was predicted theoretically[20, 66] and confirmed in numerical simulations[67, 68, 31, 69, 70]. One of the striking features of the growth is that it can be subcritical, namely structures can extract free energy even when plasmas are predicted to be linearly stable[66]. Based on this, the fundamental role of linear stability theory was called into question[66].

A coherent structure in phase space also forms in more complex systems, such as inhomogeneous magnetized plasmas, a system of interest to the fusion community. Earlier study showed that BGK solutions can be obtained in such a system and thus a phase space density hole (dubbed drift hole[34]) forms. Due to the magnetic field, the drift hole has distinctive features in the parallel and the perpendicular directions. In the parallel direction, the structure is similar to the 1D Vlasov case, where trapping is provided by a potential field. In contrast, the drift hole has a perpendicular structure which can be viewed as a localized $E \times B$ vortex. Once formed, as with other phase space structures, drift holes can drive subcritical instability. As for the 1D Vlasov plasma, this is a consequence of the conservation of total phase space density, which necessitates that a localized depletion grows as it is displaced up the gradient (Fig.3.1). However, unlike the 1D problem, drift hole dynamics necessitates a spatial flux of particles. In particular, motion of an electron drift hole necessitates a spatial flux of ions. Intuitively, the displacement and the growth process of the electron drift hole may be understood in terms of

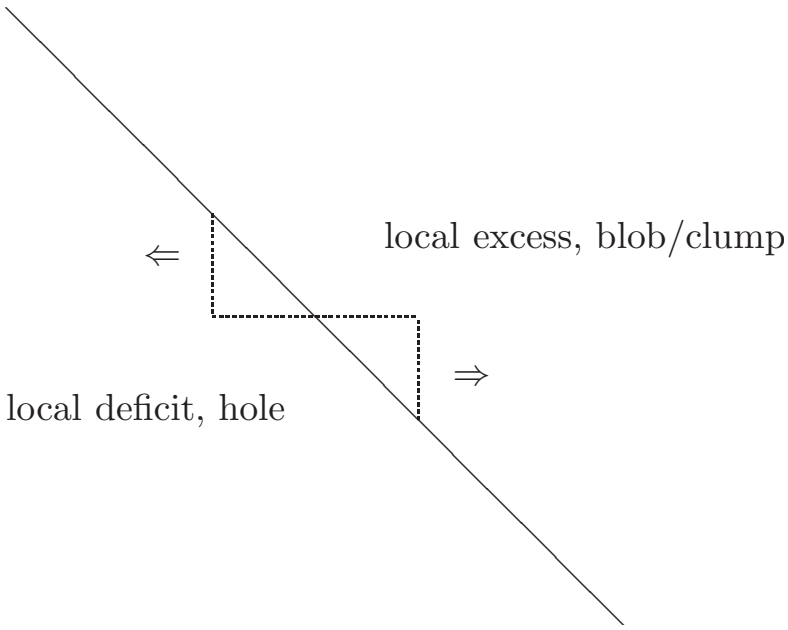

Figure 3.1: Formation and growth of structures. The flattening of the gradient leads to the formation of blobs (local excess) and holes (local deficit). Once formed, holes (blobs/clumps) can grow by propagating against (down) the gradient

its screening field. Namely, once the electron drift hole forms, it attracts a cloud of screening field. The screening field can spatially scatter ions, which forces the electron drift hole to move up the gradient, so as to satisfy the quasi-neutrality condition.

While early studies examined the basic structure and dynamics of drift holes, further development is still necessary. This is especially true regarding the issue of zonal flows[17]. The coupling of zonal flows in drift hole physics can be motivated from an analogy to dynamics of *drift wave* turbulence. It has been demonstrated that zonal flows have significant impact on fluctuation dynamics of drift wave turbulence via amplitude suppression and cross phase decorrelation[17]. This naturally leads us to the expectation that zonal flows could also impact *drift hole* driven relaxation processes. However, such zonal flow coupling was ignored in an earlier study[34]. This is partly because that study naively ignored mesoscales and envelope scales, and so treated $\langle \tilde{v}_x \nabla_\perp^2 \tilde{\phi} \rangle \sim \mathrm{Re} i k_y k_\perp^2 |\tilde{\phi}|_k^2 \to 0$. Note that the polarization charge flux is equivalent to the Reynolds force via the Taylor

identity[35, 71, 53] $\langle \tilde{v}_x \nabla_\perp^2 \tilde{\phi} \rangle \sim \partial_x \langle \tilde{v}_x \tilde{v}_y \rangle$.

The role of polarization charge flux in zonal flow coupling may be further clarified in the context of potential vorticity (PV) dynamics in the quasi-geostrophic (QG) system. The important physical meaning of the conservative PV dynamics is the conservation of a total charge[71, 72]. For example, in Hasegawa-Wakatani system[73], the PV is $q = n_e - \rho_s^2 \nabla_\perp^2 \phi$, where the total charge q consists of (guiding center) electron charge and polarization charge. The growth of the PV fluctuation is driven by transport of the total q. Since the transport of the total q contains polarization charge flux, and since the polarization charge flux is equivalent to Reynolds force[35, 71, 53], growth of fluctuation in the QG system *must* involve zonal flow acceleration. The point is depicted in Fig.3.2. Such coupled evolution was formulated as a momentum theorem[35, 74, 71] for the PV fluctuation and zonal flow. Similarly, in the drift hole dynamics, phase space density f is related to a total charge via $\int d^3v f_e = \int d^3v f_i^{GC} + \rho_s^2 \nabla_\perp^2 \phi$. Total charge conservation (or the quasi-neutrallity constraint) requires the screening cloud of a structure to scatter the oppositely charged particles, as well as polarization charge, during the growth process. Thus, we expect that the growth of the drift hole structure be accompanied by zonal flow growth, as for PV dynamics in Hasegawa-Wakatani system. As shown later, such polarization charge flux and thus zonal flow coupling in drift hole physics can be triggered by hole-flow resonance, which allows a non-zero cross-phase in the polarization charge flux, and hence the Reynolds force. That zonal flow coupling is made non-zero with hole-flow resonance is physically plausible, since the resonance allows the flow and the hole to exchange energy and momentum with each other.

In this paper, we present the theory of the structure and dynamics of drift holes with turbulence driven flows. Simply, drift hole structures are influenced by flows, since flows alter the medium response. The effect shows up in the screening length of the self-consistent drift hole potential. The flow correction in the screening leads to the shift of the $E \times B$ vortex produced by drift hole potential, analogous to a well known shear flow effect[75] on eigenmode structure[76]. In addition, the drift hole is coupled to flows via hole-flow resonance, which provides

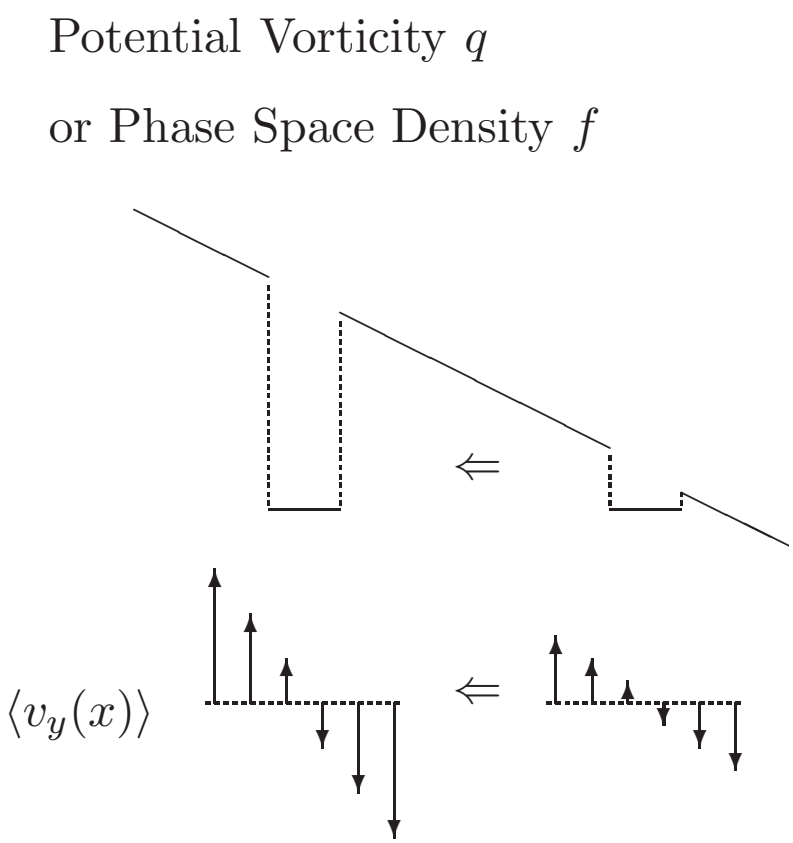

Figure 3.2: Growth of drift hole and zonal flow

the proper phase for non-zero polarization charge flux and hence Reynolds force. The non-zero flow coupling has an impact on drift hole dynamics as well. To access free energy and to grow, (electron) drift holes must move up the gradient by scattering guiding center ions, while the structure is coupled to zonal flows via the polarization charge flux. It is shown that drift hole growth is coupled to turbulence flow generation. The coupled dynamics of drift holes and zonal flows is analogous to that of drift wave-zonal flow turbulence[17, 55], in which waves and flows regulate one another. Since drift hole and zonal flow are coupled together, a stationary state with a finite zonal flow is possible. We argue that since even a single phase space structure can drive zonal flows, familiar concepts for zonal flow generation such as inverse cascade[77], Rhine's scale[78], and modulational instability[17] etc are maybe useful but are *not* fundamental. We also discuss the implication for the saturated amplitude of the drift hole. Since the drift hole and

zonal flow are coupled, a non-zero zonal flow can result in a stationary state. The resultant zonal flow in turn deforms the drift hole structure itself by modifying the screening effect. By requiring that *potential screening* is *finite* in the presence of the stationary zonal flow, an upper bound on drift hole amplitude in the drift hole-zonal flow system is calculated. The result indicates $|\phi|^2_{max} \sim (\nu_d/\omega_{ci})(k_\parallel/k_y)$, where the zonal flow damping appears as a control parameter.

The implication for the edge-core connection problem - the 'No Man's Land' phenomenology - is discussed as well. It has long been known that a strong perturbation at the tokamak edge can nucleate localized quasi-coherent structures (blobs and holes)[64, 65]. Once formed, such holes can propagate inward and bombard the 'No Man's Land' region. Since such structures will also tap free energy in a different way from linear instabilities driven by the local gradients, these structures can enhance the turbulence level in the 'No Man's Land' region. This is a potentially important step toward resolving the long standing problem of reconciling drift turbulence theories with observed levels of fluctuations and transport near the edge of the plasma.

The remainder of the paper is organized as follows. In section II, the radial structure of the drift hole potential is discussed in detail. The drift hole potential is determined in the plasma medium with flows. In section III, we show that drift hole growth is coupled to turbulence driven flows. The saturation dynamics is discussed as well, along with the calculation of an upper bound on the fluctuation amplitude at saturation. Section IV presents the discussion and conclusion.

3.2 Drift hole structure with flows

Here, we construct the drift hole potential and discuss its radial structure with flows in detail. Generally speaking, a drift hole will form at a strong resonance, which traps charged particles in a potential structure. In turn, the trapped charges produce a self-potential to reinforce the self-binding. Specifically, the drift hole has distinct structure both in the parallel and perpendicular directions. In the parallel direction, drift hole structure is characterized by trapping, and thus is similar to

the 1D problem. In contrast, in the perpendicular direction, the structure can be viewed as a $E \times B$ vortex. Mathematically, drift holes are BGK solutions of magnetized plasmas, which are constructed by solving both the kinetic and Poisson equations to determine the particle distribution and potential, self-consistently.

Assuming electron trapping here for definiteness, self-consistent potential is determined by solving the Gyrokinetic (GK) Poisson equation[39, 40, 34]:

$$\begin{aligned} &\frac{|e|\phi}{T_e} + \int_t dv_\parallel \left\{ f_e^t(\phi) - \langle f_e \rangle \right\} \\ &= -\left(\partial_t + \langle v_y \rangle \partial_y\right)^{-1} v_{*e} \frac{\partial}{\partial y} \frac{|e|\phi}{T_e} + \rho_s^2 \nabla_\perp^2 \frac{|e|\phi}{T_e}. \end{aligned} \tag{3.1}$$

Here, the lefthand side (electrons) consists of the screening by adiabatic electrons and the trapped electrons (hole). The righthand side (ions) contains the screening ions, including the guiding center ions with flows and the polarization ions. We can rewrite Eq.(3.1) in a form where the screening effect is more apparent:

$$(\partial_x^2 - \hat{\lambda}^{-2}) \frac{e\phi}{T_e} = \frac{1}{\rho_s^2} \int_t dv_\parallel \left\{ f_e^t(\phi) - \langle f_e \rangle \right\}. \tag{3.2}$$

Here we introduced the screening length $\hat{\lambda}^{-2} \equiv \rho_s^{-2} \hat{\chi}$ and $\hat{\chi}$ is the susceptibility defined as

$$\hat{\chi} \equiv 1 - \rho_s^2 \partial_y^2 + \left(\partial_t + \langle v_y \rangle \partial_y\right)^{-1} v_{*e} \frac{\partial}{\partial y}. \tag{3.3}$$

Eq.(3.2) takes the form of Poisson equation to determine the potential, with the source from the trapped electrons and the screening from the untrapped charges. Here, the screening appears as an effect of the shielding medium, which consists of the adiabatic electrons, the guiding center ions with flows, and the polarization charges. Loosely, structure corresponds to a localized potential $\phi \sim \exp(-x/\lambda)$, which requires $\lambda^{-2} > 0$. If $\lambda^{-2} < 0$, the potential is not localized and $\phi \sim \exp(ik_x x)$, which may be viewed as symptomatic of Cerenkov radiation of energy. If $\phi \sim \exp(ik_x x)$ then a localized structure does not form. We hereafter focus on the former case of the localized potential, $\phi \sim \exp(-x/\lambda)$.

To solve Eq.(3.2), we need to specify f_e^t. f_e^t is obtained as a stationary

solution for the drift kinetic equation:

$$\partial_t f_e^t + v_\parallel \nabla_\parallel f_e^t + \frac{c}{B}\hat{z} \times \nabla\phi \cdot \nabla f_e^t - \frac{|e|}{m_e} E_\parallel \frac{\partial f_e^t}{\partial v_\parallel} = 0. \tag{3.4}$$

Eq.(3.4) has a stationary solution with the form $f_e^t[m_e v_\parallel^2/2 - |e|\phi]$. The solution of Eq.(3.2) obtained for any $f_e^t[m_e v_\parallel^2/2 - |e|\phi]$ is the BGK solution for magnetized plasmas. As a subclass of such BGK solutions, hole solutions are constructed by maximizing entropy. The form of f_e^t which maximizes the entropy of system is derived by Dupree[20], and is:

$$f_e^t = \langle f_e \rangle \exp\left(\frac{E + |e|\phi_m}{\tau}\right). \tag{3.5}$$

Here $E \equiv m_e v_\parallel^2/2 - |e|\phi$ is the total energy of the electrons, $-|e|\phi < E < -|e|\phi_m$ for electrons trapped in the electrostatic potential, and τ is a temperature used as the Lagrange multiplier to maximize entropy[20]. f_e^t is called the Maxwell-Boltzman hole. The potential for the Maxwell-Boltzmann hole is obtained by substituting f_e^t in Eq.(3.2) with the Maxwell-Boltzmann hole, and by then solving the resultant equation:

$$\begin{aligned}(\partial_x^2 - \hat{\lambda}^{-2})\frac{e\phi}{T_e} =& \frac{2}{\rho_s^2}\int_{-|e|\phi_m}^{-|e|\phi} \frac{dE}{\sqrt{2m_e(E + |e|\phi)}} \langle f_e \rangle \\ & \times \left(\exp\left(\frac{E + |e|\phi_m}{\tau}\right) - 1\right).\end{aligned} \tag{3.6}$$

Although in principle the potential for the Maxwell-Boltzmann hole is obtained by solving Eq.(3.6), we note that Eq.(3.6) is a nonlinear integro-differential equation which cannot be solved except for special cases. Leaving the discussion of the exact solution for the special case to the appendix, we consider an approximate solution for Eq.(3.6) below. A useful approximation to the Maxwell-Boltzmann

hole is given by the box hole[20, 34] (Figs.3.3 and 3.4):

$$f_e^t = \begin{cases} \langle f_e \rangle + f_H & \text{for } \begin{cases} |v_\parallel - u_\parallel| < \Delta v_\parallel/2 \\ |x| < \Delta x/2,\ |y| < \Delta y/2 \end{cases} \\ \langle f_e \rangle & \text{for others} \end{cases} . \tag{3.7}$$

Namely, the electrons trapped in the parallel direction consist of those moving at the speed $u_\parallel$, within a range of velocities width $\Delta v_\parallel$. Electrons are localized in the perpendicular plane as well, within a spatial region of extent Δx and Δy, forming a $E \times B$ vortex. As discussed before, the box hole is a reasonable approximation to the Maxwell-Boltzmann hole[20, 34], in particular for $(E + |e|\phi_m)/\tau \ll 1$. For the box hole, the GK Poisson equation is

$$(\partial_x^2 - \hat{\lambda}^{-2})\frac{e\phi}{T_e} = \frac{1}{\rho_s^2} f_H \Delta v_\parallel. \tag{3.8}$$

In the Fourier representation,

$$(\partial_x^2 - \lambda_k^{-2}[\langle v_y \rangle])\frac{e\phi_k}{T_e} = \frac{1}{\rho_s^2} f_H \Delta v_\parallel \frac{\Delta y}{L_y} \frac{2}{k_y \Delta y} \sin\frac{k_y \Delta y}{2}. \tag{3.9}$$

Here L_y is the Fourier box size, $\lambda_k^{-2} = \rho_s^{-2}\chi(\mathbf{k}, k_\parallel u_\parallel)$, $\chi(\mathbf{k}, \omega) = 1 + k_y^2\rho_s^2 - \omega_{*e}/(\omega - k_y\langle v_y \rangle)$, and ω is evaluated at the hole doppler frequency $\omega = k_\parallel u_\parallel$.

Eq.(3.9) retains flow effects via the screening length or the susceptibility, $\lambda_k^{-2} \propto \chi$. Since the flow enters the susceptibility in the form $(k_\parallel u_\parallel - k_y\langle v_y \rangle)^{-1}$, it naturally raises the question of the singularity, or more physically, of the meaning and impact of the resonance between drift hole and shear flow. To treat the resonance properly, we employ the Plemelj formula,

$$\frac{1}{k_\parallel u_\parallel - k_y\langle v_y \rangle} = P\frac{1}{k_\parallel u_\parallel - k_y\langle v_y \rangle} - i\pi\delta(k_\parallel u_\parallel - k_y\langle v_y \rangle). \tag{3.10}$$

Here, the 'P' denotes the principal value of the integral. We note that, of course, the formula makes sense only when it appears inside an integral, such as that arises

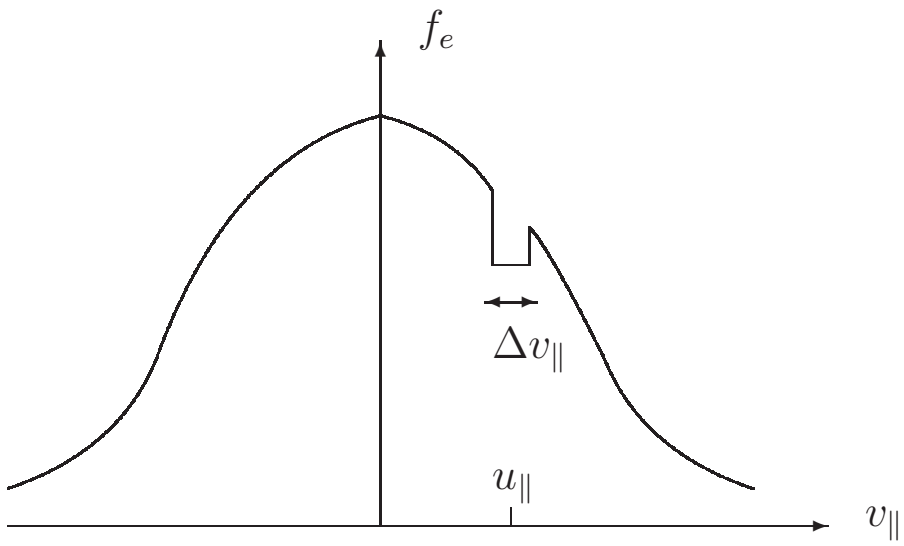

Figure 3.3: Hole in velocity space

in solving Eq.(3.9). Now, given the formula, the susceptibility becomes

$$\begin{aligned}\chi(\mathbf{k}, k_\parallel u_\parallel, \langle v_y \rangle) =& 1 + k_y^2 \rho_s^2 - P \frac{\omega_{*e}}{k_\parallel u_\parallel - k_y \langle v_y \rangle} \\ &+ i\omega_{*e} \pi \delta(k_\parallel u_\parallel - k_y \langle v_y \rangle) \qquad (3.11) \\ \cong& \chi^{(0)}(\mathbf{k}, k_\parallel u_\parallel) - \left(\frac{k_y c_s}{k_\parallel u_\parallel} \right)^2 \frac{\langle v_y \rangle}{c_s} \\ &+ i\omega_{*e} \pi \delta(k_\parallel u_\parallel - k_y \langle v_y \rangle), \qquad (3.12)\end{aligned}$$

where in the second line we assumed $k_\parallel u_\parallel > k_y \langle v_y \rangle$ and $\chi^{(0)}(\mathbf{k}, k_\parallel u_\parallel) \equiv 1 + k_y^2 \rho_s^2 - \omega_{*e}/(k_\parallel u_\parallel)$ is the susceptibility without flow. Thus, flow modifies the plasma response via the susceptibility, which changes the screening of the drift hole potential. Alternatively put, flow determines the structure and dynamics of the screening cloud of trapped particles. Finally, the flow-hole resonance gives an absorption mechanism, namely $\mathrm{Im}\chi \propto \delta(k_\parallel u_\parallel - k_y \langle v_y \rangle)$. The resonance allows the flow to absorb the energy in the screening field. As a consequence of the resonance process, 'cat's eye' patterns[79] are produced around the resonance location.

Having discussed the role of flow in plasma response, now we discuss the

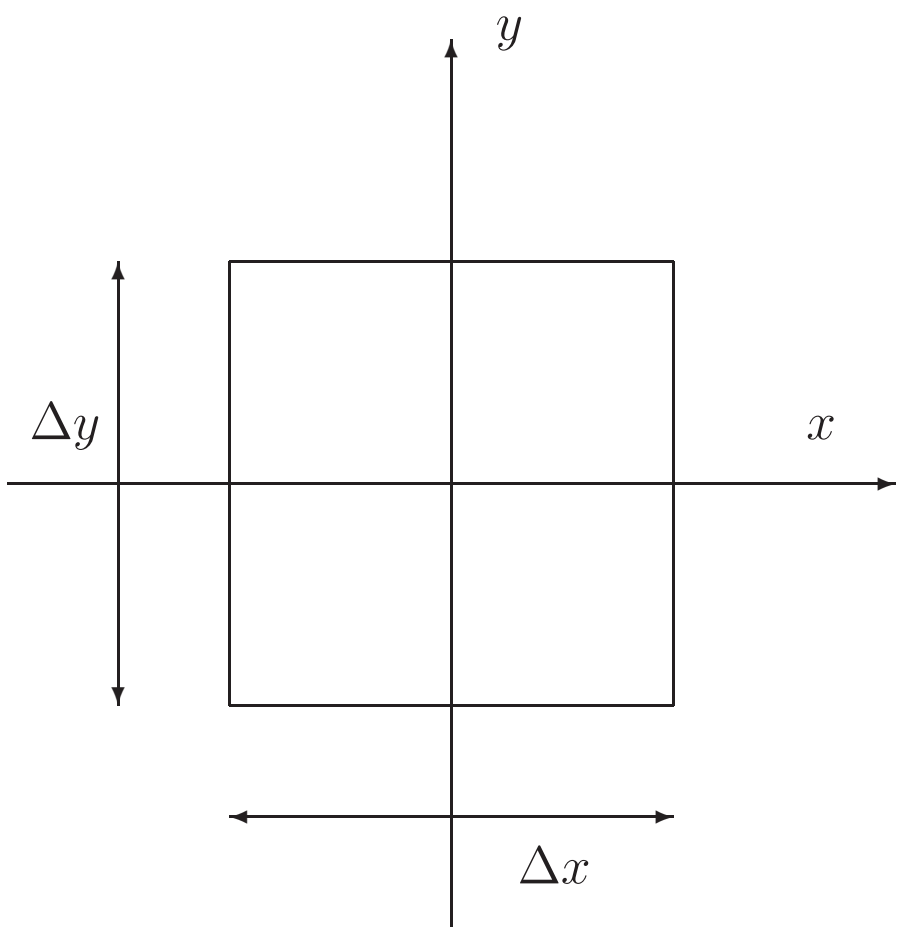

Figure 3.4: Box Hole

solution of Eq.(3.9). A general solution of Eq.(3.9) can be obtained as

$$\frac{|e|\phi_k}{T_e} = \int \frac{dx'}{\rho_s^2} G_k(x,x') f_H(x') \Delta v_\parallel \frac{\Delta y}{L_y} \frac{2}{k_y \Delta y} \sin \frac{k_y \Delta y}{2}, \tag{3.13}$$

where $G_k(x,x')$ is the Green's function which satisfies

$$(\partial_x^2 - \lambda_k^{-2}[\langle v_y \rangle]) G_k(x-x') = \delta(x-x'). \tag{3.14}$$

Note the Green's function here may be viewed as a renormalized propagator which includes the effect of flow in the medium. However, while the physical interpretation is clear, it is not an easy task to obtain the full renormalized $G_k(x,x')$, due

to the flow dependence in the screening length.

Thus, here we seek an approximate approach to obtain a solution ϕ_k. (As explained later, the approximation is analogous to the Born approximation in quantum mechanics[80].) Namely, rather than keeping the flow in the screening term, we rewrite Eq.(3.9) as

$$(\partial_x^2 - \lambda_k^{(0)-2})\frac{e\phi_k}{T_e} = \frac{1}{\rho_s^2} f_H \Delta v_\parallel \frac{\Delta y}{L_y}\frac{2}{k_y \Delta y}\sin\frac{k_y \Delta y}{2} + \left(\frac{k_y c_s}{k_\parallel u_\parallel}\right)^2 \frac{\langle v_y\rangle}{c_s}\frac{|e|\phi_k}{T_e} - i\omega_{*e}\pi\delta(k_\parallel u_\parallel - k_y\langle v_y\rangle)\frac{|e|\phi_k}{T_e}, \tag{3.15}$$

to obtain

$$\frac{|e|\phi_k}{T_e} = \int \frac{dx'}{\rho_s^2} G_k^{(0)}(x,x') f_H(x')\Delta v_\parallel \frac{\Delta y}{L_y}\frac{2}{k_y\Delta y}\sin\frac{k_y\Delta y}{2} + \int \frac{dx'}{\rho_s^2} G_k^{(0)}(x,x')\left(\frac{k_y c_s}{k_\parallel u_\parallel}\right)^2 \frac{\langle v_y(x')\rangle}{c_s}\frac{|e|\phi_k(x')}{T_e} - \int \frac{dx'}{\rho_s^2} G_k^{(0)}(x,x') i\omega_{*e}\pi\delta(k_\parallel u_\parallel - k_y\langle v_y(x')\rangle)\frac{|e|\phi_k(x')}{T_e}. \tag{3.16}$$

Here $G_k^{(0)}(x,x')$ is the 'bare' Green's function, which satisfies

$$(\partial_x^2 - \lambda_k^{(0)-2})G_k^{(0)}(x,x') = \delta(x-x'), \tag{3.17}$$

and thus

$$G_k^{(0)}(x,x') = -\frac{\lambda_k^{(0)}}{2}\exp\left(-\frac{|x-x'|}{\lambda_k^{(0)}}\right). \tag{3.18}$$

Simply put, the first term in Eq.(3.16) describes an isotropic $E\times B$ vortex, the second term describes a shift to the isotropic $E\times B$ vortex, and the third term accounts for flow-hole resonance and contributes to a non-zero momentum flux. We consider each term in detail in the following.

The first term in Eq.(3.16) describes an isotropic $E\times B$ vortex, which was

obtained in an earlier study[34]. The solution is

$$\frac{e\phi_k^{(0)}}{T_e} = -\frac{\Delta v_\parallel f_H}{\chi}\frac{\Delta y}{L_y}\frac{2}{k_y\Delta y}\sin\left(\frac{k_y\Delta y}{2}\right)X_k^{(0)}(x), \tag{3.19}$$

where $X_k^{(0)}(x)$ is a function which determines the radial profile of the potential field

$$X_k^{(0)}(x) = \begin{cases} \exp\left(-\dfrac{|x|}{\lambda_k}\right)\sinh\left(\dfrac{\Delta x}{2\lambda_k}\right) & \text{for } |x| > \Delta x/2 \\ 1-\cosh\left(\dfrac{x}{\lambda_k}\right)\exp\left(-\dfrac{\Delta x}{2\lambda_k}\right) & \text{for } |x| < \Delta x/2 \end{cases}. \tag{3.20}$$

Hereafter it is understood that the susceptibility and the screening length are evaluated without flow, $\lambda_k^{-2} = \rho_s^{-2}\chi$ and $\chi = 1 + k_y^2\rho_s^2 - \omega_{*e}/(k_\parallel u_\parallel) > 0$. The potential (Eq.(3.19)) is given by $\phi = \sum_{k_y}\phi_k\exp(ik_y y)$ and plotted in Fig.3.5; the drift hole potential leads to a localized, $E\times B$ vortex in 2D (x, y) plane.

Here, in contrast, we have the two additional terms in Eq.(3.16) due to the flow effects. Physically, as discussed in detail below, the second term describes the shift of the $E\times B$ vortex while the third term describes the flow-hole resonance which enables energy transfer between drift hole and shear flow. Technically, these terms are expressed in terms of the integration involving the solution ϕ. To proceed, we approximate the ϕ in the integrand by $\phi^{(0)}$. This is analogous to the Born approximation in quantum mechanical particle scattering, where the actual scattered wave function is replaced by the zeroth order plane wave solutions[80]. Further, for simplicity we assume $\langle v_y\rangle \cong Sx$ in the following. The approximation of the flow structure simplifies the analysis by allowing the spatial integral to be performed straightforwardly, while we note that as a caveat, the flow profile should be in principle determined from coupled evolution of the drift hole and zonal flow.

The second term in Eq.(3.16) describes the deformation and shift of the $E\times B$ vortex. Using the approximation discussed above, the second term in

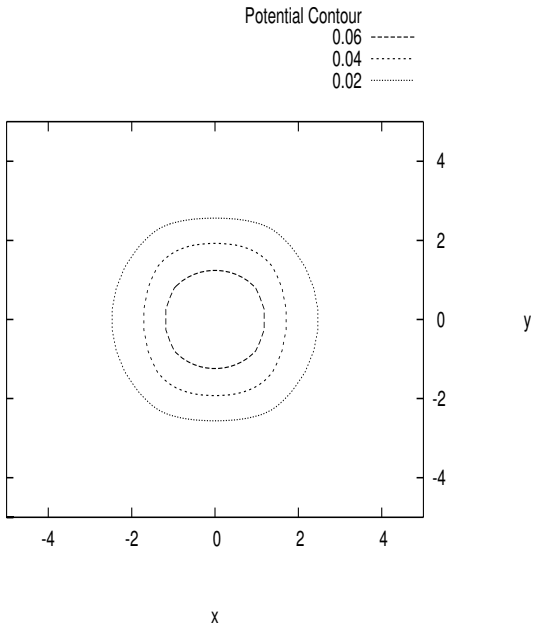

Figure 3.5: Potential contour without flow feedback. Here, length are normalized in ρ_s. The other parameters used are: $|f_H \Delta v_\parallel| = 0.1$, $\Delta x/\rho_s = \Delta y/\rho_s = 3.0$, $\rho_s/L_y = 0.03$, $\rho_* = 0.01$. The screening is symmetric and $E \times B$ vortex is symmetric.

Eq.(3.16) can be integrated to give

$$\frac{e\phi_k^{shift}}{T_e} = \frac{|f_H \Delta v_\parallel|}{2\chi^{3/2}} \left(\frac{k_y c_s}{k_\parallel u_\parallel}\right)^2 \frac{S}{\omega_{ci}} \rho_* \frac{\Delta y}{L_y} \frac{2}{k_y \Delta y} \times \sin\left(\frac{k_y \Delta y}{2}\right) X_k^{shift}(x), \tag{3.21}$$

where $X_k^{shift}(x)$ is a function which determines the radial structure of ϕ_k^{shift}. $X_k^{shift}(x)$ is defined as

$$X_k^{shift}(x) \equiv \left[I_{in} - \frac{1}{2}\left(\frac{\Delta x^2}{4\rho_s^2} - \frac{x^2}{\rho_s^2}\right) \exp\left(-\frac{\Delta x}{2\lambda_k}\right)\right] \sinh\frac{x}{\lambda_k} + \frac{2x}{\chi\lambda_k} - \frac{x}{2\rho_s\sqrt{\chi}} \exp\left(-\frac{\Delta x}{2\lambda_k}\right) \cosh\frac{x}{\lambda_k}, \tag{3.22}$$

for $|x| < \Delta x/2$ and

$$X_k^{shift}(x) \equiv \frac{x}{|x|} \exp\left(-\frac{|x|}{\lambda_k}\right) \times \left[I_{out} - \frac{1}{2}\left(\frac{\Delta x^2}{4\rho_s^2} - \frac{x^2}{\rho_s^2}\right) \sinh\frac{\Delta x}{2\lambda_k} + \frac{|x|}{2\sqrt{\chi}\rho_s} \sinh\frac{\Delta x}{2\lambda_k}\right], \tag{3.23}$$

for $|x| > \Delta x/2$. The constants I_{in} and I_{out} are defined as

$$I_{in} \equiv \frac{1}{2\chi}\left(1 + \frac{\Delta x}{\lambda_k}\right) \exp\left(-\frac{\Delta x}{\lambda_k}\right) - \frac{1}{\chi}\left(\frac{7}{4} + \frac{\Delta x}{\lambda_k}\right) \exp\left(-\frac{\Delta x}{2\lambda_k}\right) \tag{3.24}$$

$$+ \frac{1}{4\chi}\left(1 + \frac{\Delta x}{\lambda_k}\right) \exp\left(-\frac{3\Delta x}{2\lambda_k}\right), \tag{3.25}$$

and

$$I_{out} \equiv -\frac{1}{4\chi}\left[7 + \left(1 + \frac{\Delta x}{\lambda_k}\right) \exp\left(-\frac{\Delta x}{\lambda_k}\right)\right] \sinh\frac{\Delta x}{2\lambda_k} + \frac{1}{4\chi} \exp\left(-\frac{\Delta x}{2\lambda_k}\right) \sinh\frac{\Delta x}{\lambda_k} + \frac{\Delta x}{\chi\lambda_k}\left(\cosh\frac{\Delta x}{2\lambda_k} - \frac{1}{4} \exp\left(-\frac{\Delta x}{2\lambda_k}\right) \cosh\frac{\Delta x}{\lambda_k}\right). \tag{3.26}$$

To see the effect of ϕ^{shift}, we plot $\phi = \sum_{k_y} (\phi_k^{(0)} + \phi_k^{shift}) \exp(ik_y y)$ in Fig.3.6. As compared to $\phi^{(0)}$ (Fig.3.5), the potential is clearly deformed by the shear flow. In particular, the potential lacks reflectional symmetry in x, and is shifted radially.

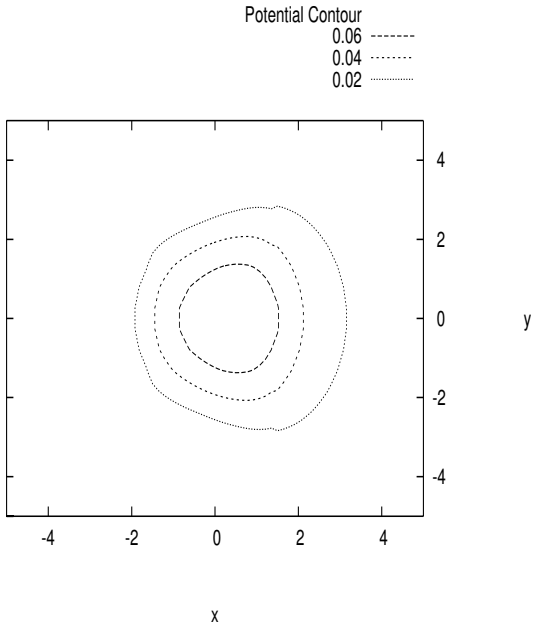

Figure 3.6: Potential contour with flow feedback ($\langle v_y \rangle = Sx$, external flow). Here, length are normalized in ρ_s. The other parameters used are: $|f_H \Delta v_\parallel| = 0.1$, $\Delta x/\rho_s = \Delta y/\rho_s = 3.0$, $\rho_s/L_y = 0.03$, $\rho_* = 0.01$, $\rho_* \omega_{ci}/(k_\parallel u_\parallel) = 1.0$, $S/\omega_{ci} = 0.05$. The potential is screened more strongly for $x < 0$ than for $x > 0$, resulting in a shifted, deformed $E \times B$ vortex.

This is because the shear flow introduces a spatial dependence to the screening length $\lambda[\langle v_y(x) \rangle]$. The spatial dependence leads to different screening responses for $x > 0$ and $x < 0$, which leads to the overall radial shift of the $E \times B$ vortex. We note that the analysis and the result given here are analogous to the well-known shear flow effect[75] on the eigenmode structure of drift waves[76], where a shear flow breaks the eigenfunction symmetry around the rational surface and shifts the eigenmode potential radially.

The third term in Eq.(3.16) is related to flow-hole resonance. The integra-

tion can be performed to give

$$\frac{|e|\phi_k^{res}}{T_e} = \frac{i\pi}{2\sqrt{\chi}} \exp\left(-\frac{|x-x_c|}{\lambda_k}\right) \frac{c_s}{|S||L_n|} \frac{k_y}{|k_y|} \frac{|e|\phi_k^{(0)}(x_c)}{T_e}. \tag{3.27}$$

where x_c is the location of the hole-flow resonance (i.e. the location of the critical layer), i.e.

$$x_c = \frac{k_\parallel}{k_y} \frac{u_\parallel}{S}. \tag{3.28}$$

This term physically describes the coupling of the drift hole structure to the plasma flow via a dissipative resonance. The localized structure produces a screening field, as depicted in Fig.3.7. The resonance allows the energy in the screening field to be radiated and absorbed into the flow. As a result, the localized structure feels the presence of the flow through the screening field, whose effect appears as ϕ^{res}. Stated differently, the structure and the flow form a single entity through the absorption process.

An important feature of the resonance process is that it enables the coupling between drift holes and zonal flows by allowing the necessary finite cross phase in the Reynolds stress, to produce a momentum flux. The momentum is ($\langle ... \rangle$ denotes average in y and z direction)

$$\begin{aligned}\langle \tilde{v}_x \tilde{v}_y \rangle = \frac{c^2}{B^2} \mathrm{Re} \sum_k & ik_y(\phi_{-k}^{(0)} + \phi_{-k}^{shift} + \phi_{-k}^{res}) \\ & \times \partial_x(\phi_k^{(0)} + \phi_k^{shift} + \phi_k^{res}).\end{aligned} \tag{3.29}$$

Noting $\phi_k^{(0)}$ and ϕ_k^{shift} are purely real and ϕ_k^{res} is purely imaginary, the non-zero contribution comes from the terms involving ϕ_k^{res} as

$$\begin{aligned}\langle \tilde{v}_x \tilde{v}_y \rangle =& \frac{c^2}{B^2} \mathrm{Re} \sum_k ik_y(\phi_{-k}^{(0)} + \phi_{-k}^{shift}) \partial_x \phi_k^{res} \\ & + \frac{c^2}{B^2} \mathrm{Re} \sum_k ik_y \phi_{-k}^{res} \partial_x(\phi_k^{(0)} + \phi_k^{shift}).\end{aligned} \tag{3.30}$$

The fact that the drift hole is coupled to zonal flows requires us to incorporate zonal flows into the dynamics of the drift hole as well. The dynamical dependence

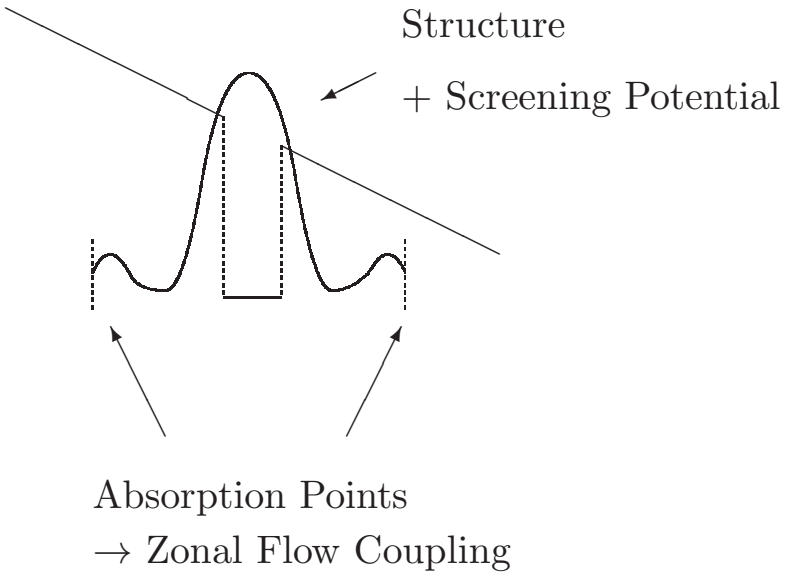

Figure 3.7: Drift hole and zonal flow coupling.

of drift hole growth on zonal flows is discussed in the next section.

To summarize, the total potential was obtained as

$$\frac{|e|\phi_k}{T_e} = \frac{|e|\phi_k^{(0)}}{T_e} + \frac{|e|\phi_k^{shift}}{T_e} + \frac{|e|\phi_k^{res}}{T_e}. \tag{3.31}$$

$\phi^{(0)}$ describes the isotropic $E \times B$ vortex, Fig.3.5. ϕ^{shift} and ϕ^{res} arise due to flow, which influences drift hole potential structure by changing the plasma medium response and thus the screening effect. ϕ^{shift} gave a shift to the isotropic $E \times B$ vortex (Fig.3.6), which is similar to the shift of drift wave eigenmode structure. ϕ^{res} is related to the flow-hole resonance, which allows the zonal flow to absorb energy or momentum of the screening field.

3.3 Drift hole dynamics and turbulence driven flows

Once formed, drift hole structure can grow by extracting free energy. Simply put, the growth is caused by a hole being displaced up the background gradient, as

depicted in Fig.3.8. As a hole is displaced up the gradient, since f_e is conserved, its depth $\delta f_e = f_e - \langle f_e \rangle$ must grow[20, 66, 34]. For an electron drift hole, the displacement is made possible by scattering off ions. The scattering of ions requires the electron structure to move up the gradient so as to maintain the quasi-neutrality constraint. This enables the electron hole to be displaced in phase space and to grow.

3.3.1 Drift hole growth with turbulence driven flows

To describe the growth of a drift hole, we consider a displacement of the drift hole in phase space from $(x_0, u_\parallel)$ to $(x, v_\parallel)$. Let phase space density at the initial position $\langle f_e \rangle|_0 + f_{H0}$ and at the displaced position $\langle f_e \rangle + f_H$ (Fig.3.8). Since phase space density is conserved along trajectory, the two values must be same:

$$\langle f_e \rangle|_0 + f_{H0} = \langle f_e \rangle + f_H. \tag{3.32}$$

From this, the increment in the depth of the hole $\delta f_e \equiv f_H - f_{H0}$ is calculated to be

$$\begin{aligned} \delta f_e &= \langle f_e \rangle|_0 - \langle f_e \rangle \\ &\simeq -(x - x_0) \left. \frac{\partial \langle f_e \rangle}{\partial x} \right|_0 - (v_\parallel - u_\parallel) \left. \frac{\partial \langle f_e \rangle}{\partial v_\parallel} \right|_0 . \end{aligned} \tag{3.33}$$

The growth of the depth along the trajectory is then

$$\frac{d}{dt} \delta f_e^2 = 2 \delta f_e \frac{d}{dt} \delta f_e \tag{3.34}$$

$$= 2 \delta f_e \left(-\tilde{v}_x \left. \frac{\partial \langle f_e \rangle}{\partial x} \right|_0 + \frac{|e|}{m_e} \tilde{E}_\parallel \left. \frac{\partial \langle f_e \rangle}{\partial v_\parallel} \right|_0 \right), \tag{3.35}$$

where we used

$$\frac{d}{dt}(x - x_0) = \tilde{v}_x = \frac{c}{B} \tilde{E}_y, \ \frac{d}{dt}(v_\parallel - u_\parallel) = -\frac{|e|}{m_e} \tilde{E}_\parallel. \tag{3.36}$$

Integrating over $v_\parallel$ and averaging over y and z, we obtain

$$\frac{\partial}{\partial t}\int dv_\parallel \frac{\langle \delta f_e^2\rangle}{2} = -\left\langle \tilde{v}_x \frac{\delta n_e}{n_0}\right\rangle \left.\frac{\partial\langle f_e\rangle}{\partial x}\right|_0 + \frac{|e|}{m_e}\left\langle \tilde{E}_\parallel \frac{\delta n_e}{n_0}\right\rangle \left.\frac{\partial\langle f_e\rangle}{\partial v_\parallel}\right|_0 . \tag{3.37}$$

Now, the electron drift hole growth is constrained by other charges via the quasi-neutrality condition. Since $\delta n_e = \delta n_i^{GC} + n_0\rho_s^2\nabla_\perp^2 e\tilde{\phi}/T_e$, the evolution of drift hole perturbation is given by

$$\begin{aligned}\frac{\partial}{\partial t}\int dv_\parallel \frac{\langle \delta f_e^2\rangle}{2} &= -\left\langle \tilde{v}_x \frac{\delta n_i^{GC}}{n_0}\right\rangle \left.\frac{\partial\langle f_e\rangle}{\partial x}\right|_0 \\ &+ \frac{|e|}{m_e}\left\langle \tilde{E}_\parallel \frac{\delta n_i^{GC}}{n_0}\right\rangle \left.\frac{\partial\langle f_e\rangle}{\partial v_\parallel}\right|_0 - \left\langle \tilde{v}_x\rho_s^2\nabla_\perp^2\frac{e\tilde{\phi}}{T_e}\right\rangle \left.\frac{\partial\langle f_e\rangle}{\partial x}\right|_0 \\ &+ \frac{|e|}{m_e}\left\langle \tilde{E}_\parallel\rho_s^2\nabla_\perp^2\frac{e\tilde{\phi}}{T_e}\right\rangle \left.\frac{\partial\langle f_e\rangle}{\partial v_\parallel}\right|_0 .\end{aligned} \tag{3.38}$$

Thus, the overall growth is determined by the spatial and velocity scattering of guiding center ion and polarization charge. Simply put, to climb up the gradient, electron drift hole must scatter guiding center ion and polarization charge to satisfy quasi-neutrality.

The first two terms due to the guiding center ions are the drive of drift hole instability, as discussed in an earlier study. Writing $\delta n_i^{GC}/n_0 = \chi_i(e\phi/T_e)$, we have

$$\begin{aligned}&-\left\langle \tilde{v}_x \frac{\delta n_i^{GC}}{n_0}\right\rangle \left.\frac{\partial\langle f_e\rangle}{\partial x}\right|_0 + \frac{|e|}{m_e}\left\langle \tilde{E}_\parallel \frac{\delta n_i^{GC}}{n_0}\right\rangle \left.\frac{\partial\langle f_e\rangle}{\partial v_\parallel}\right|_0 \\ &= -\langle f_e\rangle|_0 \sum_{\mathbf{k}}(\omega_{*e}|_0 - k_\parallel u_\parallel)\mathrm{Im}\chi_i(\mathbf{k}, k_\parallel u_\parallel)\left|\frac{e\tilde{\phi}}{T_e}\right|_{\mathbf{k}}^2 .\end{aligned} \tag{3.39}$$

Here, $\omega_{*e}|_0 = -k_y\rho_s c_s\partial_x \ln\langle f_e\rangle|_0 \simeq \omega_{*e}(1-\eta_e/2)$ ($u_\parallel < v_{the}$ was assumed), the frequency ω is evaluated at hole Doppler frequency $\omega = k_\parallel u_\parallel$, $\mathbf{k}$ refers to modes excited by the drift hole, and $\mathrm{Im}\chi_i$ is the imaginary part of the guiding center ion susceptibility. Note that here ion dissipation $\mathrm{Im}\chi_i$ acts as a trigger of instability. This is quite different from the usual drift wave instability, where ion dissipation

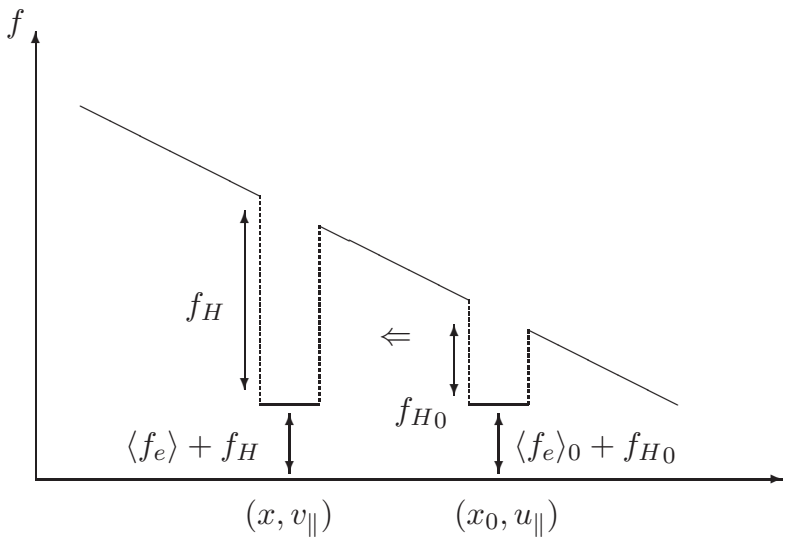

Figure 3.8: Configuration of hole displacement

is a stabilizing effect. The dissipation $\mathrm{Im}\chi_i$ is a necessary ingredient for drift hole instability, since such instability requires the irreversible scattering of guiding center ions via the quasi-neutrality constraint.

The third and the fourth terms in Eq.(3.38) are associated with polarization charge. Physically, these terms are related to zonal and toroidal flows. The connection may be best seen by noting the identities:

$$\langle \tilde{v}_x \nabla_\perp^2 \tilde{\phi} \rangle = -\frac{c}{B} \partial_x \langle \partial_y \tilde{\phi} \partial_x \tilde{\phi} \rangle = \frac{B}{c} \partial_x \langle \tilde{v}_x \tilde{v}_y \rangle, \tag{3.40}$$

and

$$\begin{aligned} \langle \tilde{E}_\parallel \nabla_\perp^2 \tilde{\phi} \rangle = & -\partial_x \langle \partial_z \tilde{\phi} \partial_x \tilde{\phi} \rangle + \frac{1}{2} \partial_z \langle (\partial_x \tilde{\phi})^2 \rangle \\ & -\partial_y \langle \partial_z \tilde{\phi} \partial_y \tilde{\phi} \rangle + \frac{1}{2} \partial_z \langle (\partial_y \tilde{\phi})^2 \rangle \\ = & -\partial_x \langle \tilde{E}_x \tilde{E}_\parallel \rangle. \end{aligned} \tag{3.41}$$

The first identity relates polarization charge flux (vorticity flux) to the Reynolds force on zonal flow[35, 71], while the second one is related to the parallel acceleration of toroidal flow due to charge separation[81, 82]. Thus, the drift hole

instability is coupled to the generation of both zonal and toroidal flows. Of course, a finite cross-phase is required for non-zero contribution. The cross-phase of polarization charge scattering is set by flow-hole resonance, as follows. The spatial flux of polarization charge is written using the potential structure derived above as

$$\langle \tilde{v}_x \nabla_\perp^2 \tilde{\phi} \rangle = \frac{c}{B} \mathrm{Re} \sum_k i k_y (\phi_{-k}^{(0)} + \phi_{-k}^{shift} + \phi_{-k}^{res}) \times \partial_x^2 (\phi_k^{(0)} + \phi_k^{shift} + \phi_k^{res}). \tag{3.42}$$

Due to its radial structure and phase, we have a non-zero contribution from the combination of ϕ^{shift} (pure real) and ϕ^{res} (pure imaginary) as

$$\langle \tilde{v}_x \nabla_\perp^2 \tilde{\phi} \rangle = \frac{c}{B} \mathrm{Re} \sum_k i k_y (\phi_{-k}^{shift} \partial_x^2 \phi_k^{res} + \phi_{-k}^{res} \partial_x^2 \phi_k^{shift}). \tag{3.43}$$

which leads to non-zero Reynolds forcing. Thus, the proper phase for polarization charge flux and thus Reynolds forcing is provided by the flow-hole resonance. A similar argument applies to the velocity scattering of polarization charge.

Having discussed each term in Eq.(3.38), we now discuss the implication for drift hole growth. Collecting the result, Eq.(3.38) now becomes

$$\begin{aligned} \frac{\partial}{\partial t} \int dv_\parallel \frac{\langle \delta f_e^2 \rangle}{2} = & - \langle f_e \rangle |_0 \sum_{\mathbf{k}} (\omega_{*e}|_0 - k_\parallel u_\parallel) \mathrm{Im} \chi_i \left| \frac{e\tilde{\phi}}{T_e} \right|_{\mathbf{k}}^2 \\ & - \frac{1}{\omega_{ci}} \partial_x \langle \tilde{v}_x \tilde{v}_y \rangle \left. \frac{\partial \langle f_e \rangle}{\partial x} \right|_0 \\ & - \frac{m_i}{m_e} \frac{c^2}{B^2} \partial_x \langle \tilde{E}_x \tilde{E}_\parallel \rangle \left. \frac{\partial \langle f_e \rangle}{\partial v_\parallel} \right|_0 . \end{aligned} \tag{3.44}$$

The first term is due to the scattering of guiding center ions, while the second and the third terms are due to the scattering of polarization charge. Here, we first consider a 'bare' growth, i.e. without flow coupling, and later come back to the issue of flows. For the growth rate, we derive its scaling property. Using $|e\tilde{\phi}/T_e|_k^2 \sim \int dv_{\parallel,1} dv_{\parallel,2} \langle \delta f_e(1) \delta f_e(2) \rangle_k / |\chi|^2$ via the GK Poisson equation, $\int dv_\parallel \delta f_e \sim \Delta v_\parallel \delta f_e$,

and $\mathrm{Im}\chi_i < 0$ for ion Landau damping, we have

$$\gamma \Delta v_\parallel \langle \delta f_e^2 \rangle \sim \langle f_e \rangle|_0 (\omega_{*e}|_0 - k_\parallel u_\parallel)(|\mathrm{Im}\chi_i|) \frac{\Delta v_\parallel^2 \langle \delta f_e^2 \rangle}{|\chi|^2}. \tag{3.45}$$

This estimate then yields a scaling form of the growth rate as

$$\gamma \sim \langle f_e \rangle|_0 \Delta v_\parallel (\omega_{*e}|_0 - k_\parallel u_\parallel) \frac{|\mathrm{Im}\chi_i|}{|\chi|^2} \sim k_\parallel \Delta v_\parallel \frac{|\mathrm{Im}\chi_e \mathrm{Im}\chi_i|}{|\chi|^2}. \tag{3.46}$$

We can extract several features of drift hole instability from Eq.(3.46). First of all, the growth rate is nonlinear, as it depends on amplitude via $\Delta v_\parallel \sim \sqrt{\tilde{\phi}}$. This allows explosive, rather than linear exponential growth, of fluctuations. Secondly, the instability requires a free energy, $\gamma \propto \omega_{*e}|_0 - k_\parallel u_\parallel$. The requirement that $\omega_{*e}|_0 - k_\parallel u_\parallel > 0$ for instability means that spatial scattering has to release more energy than the cost due to velocity scattering, similar to $\omega < \omega_{*e}$ for drift wave instability. Finally, the drift hole instability is triggered by ion dissipation $\mathrm{Im}\chi_i$. Ion dissipation is essential for drift hole instability since it allows irreversible scattering of ions and thus non-zero ion flux. Due to the quasi-neutrallity condition, the non-zero ion flux allows an electron hole to be displaced up the gradient, and thereby to access free energy, as depicted in Fig.3.8.

The feature of the drift hole instability can be further clarified by comparing it to the linear growth of drift waves, Table 3.1. Both instabilities require free energy to grow, i.e. $\omega_{*e}|_0 > k_\parallel u_\parallel$ for the drift hole instability and $\omega_{*e} > \omega$ for the linear drift wave instability. On the other hand, the drift hole instability is distinctive in that it is nonlinear and triggered by ion dissipation. The drift hole instability is amplitude dependent $\gamma \sim \Delta v_\parallel$ and thus allows nonlinear explosive growth, while the electron drift wave instability is independent of amplitude and thus gives exponential linear growth. In addition, the drift hole instability is triggered by $\mathrm{Im}\chi_i$, while the linear instability is damped by $\mathrm{Im}\chi_i$. Due to the different dependence on $\mathrm{Im}\chi_i$, we note that the growth of the hole can be subcritical, i.e. $\gamma > 0$ even when $\gamma_L \lesssim 0$. This allows release of free energy even when plasmas are linearly stable or only weakly unstable, and thus drift hole structures can be more efficient at tapping free energy than drift wave eigenmodes.

Table 3.1: Comparison between linear and nonlinear instabilities.

	Electron drift wave	Electron drift hole
Growth rate	$\gamma_L \sim \lvert\partial\chi/\partial\omega_k\rvert^{-1}$ $\times(\lvert\mathrm{Im}\chi_e\rvert - \lvert\mathrm{Im}\chi_i\rvert)$	$\gamma \sim k_\parallel \Delta v_\parallel \lvert\mathrm{Im}\chi_e \mathrm{Im}\chi_i\rvert/\lvert\chi\rvert^2$
Access to free energy	$\omega_* > \omega$	$\omega_{*e}\lvert_0 > k_\parallel u_\parallel$
Amplitude dependence	No	Yes, $\propto \Delta v_\parallel \sim \sqrt{\tilde{\phi}}$
Ion Landau Damping	Stabilizing	Destabilizing
Type of instability	Supercritical Exponential growth	Subcritical Explosive growth

Table 3.2: Growth in 1D Vlasov v.s. Gyrokinetic plasma. For 1D Vlasov plasma, 'BOT' is 'bump-on-tail,' γ_d is a generic background dissipation, u is a resonant velocity, ω_p is the plasma frequency.

	1D Vlasov plasma	Gyrokinetic plasma
Linear growth rate γ_L	$\gamma_{BOT} - \gamma_d$	$\lvert\partial\chi/\partial\omega_k\rvert(\lvert\mathrm{Im}\chi_e\rvert - \lvert\mathrm{Im}\chi_i\rvert)$
Nonlinear growth rate γ_{NL}	$\Delta v(\partial f_0/\partial v)\lvert_u u\gamma_d$ $\times(\omega_p^2/(k^2u^2 + 4\gamma_d^2))$	$f_e^{(0)}\Delta v_\parallel(\omega_{*e}\lvert_0 - k_\parallel u_\parallel)$ $\lvert\mathrm{Im}\chi_i\rvert/\lvert\chi\rvert^2$
Dissipation	γ_d	$\mathrm{Im}\chi_i$
Subcritical growth	Yes	Yes

We also note that a similar scaling form as Eq.(3.46) is obtained for a subcritical hole instability in 1D Vlasov system with a bump on tail and a generic background dissipation[31]. The result for the 1D Vlasov system qualitatively agrees with a simulation result[69]. Table 3.2 shows a comparison between the results from the GK calculation and the 1D Vlasov calculation.

The drift hole instability is coupled to zonal and toroidal flows, as explicitly seen in Eq.(3.44). This leaves a footprint on the drift hole growth. Namely, by scattering polarization charges, the drift hole is coupled to zonal flows (and toroidal flows). The coupling is made possible via hole-flow resonance, which provides the proper phase for polarization scattering. The flow coupling makes structure-induced mixing more difficult, resulting in the reduction of instability drive. The effect explicitly appears in Eq.(3.44), from which we can see that the dissipation drive via ion Landau damping must overcome the energy penalty due to the flow

coupling.

Eventually, the flow coupling can saturate drift hole instability. Namely, while drift hole grows by extracting free energy, the growing hole keeps pumping turbulence driven flows via absorption arising from hole-flow resonance. The pumping amplifies the hole-flow resonance, and eventually makes the polarization scattering comparable to the guiding center ion scattering. This leads to the saturation of drift hole growth. In the following, we discuss a more precise treatment of the coupled dynamics of the drift hole-zonal flow system and its implication for the saturation of the drift hole growth.

3.3.2 Saturation of drift hole growth with turbulence driven flows and an upper bound on fluctuation amplitude

Here, we discuss the saturation of the nonlinear instability. Since the quasi-neutrality constraint on drift hole growth requires the scattering of polarization charge, drift hole turbulence is dynamically coupled to turbulence driven flows. Thus, the saturation of drift hole instability is a highly nonlinear phenomena involving the interplay between dynamically evolving turbulent fluctuations and turbulence driven flows. Explicitly, as seen in Eq.(3.44), the evolution of drift hole turbulence contains both the Reynolds force on the zonal flow and the polarization force on the toroidal flow. To describe the fully nonlinear dynamics of the coupled system, we need an evolution equation for the flows. For the zonal flow momentum balance, we employ a simplified model:

$$\partial_t \langle v_y \rangle = -\partial_x \langle \tilde{v}_x \tilde{v}_y \rangle - \nu_d^{\perp} \langle v_y \rangle. \tag{3.47}$$

Here, the drive is given by the Reynolds force, and the damping is accounted for by $\nu_d^{\perp}$. For the toroidal flow, we note that forcing arises from *both* the momentum flux and the polarization forcing[81, 82]. Since the toroidal flow coupling in Eq.(3.44) describes a part of the toroidal flow drive, fully coupled dynamics of the drift hole growth and toroidal flow generation requires modeling of the momentum flux

(including residual stress) driven by the drift hole potential. However, this is beyond the scope of the paper and hereafter we focus on the zonal flow coupling in drift hole dynamics. Note that neglecting the toroidal flow feedback is consistent with restricting the analysis to $\omega_*|_0 > k_\parallel u_\parallel$, since the ratio of zonal flow feedback to toroidal flow feedback in $\langle \delta f_e^2 \rangle$ evolution is

$$\left| -\frac{1}{\omega_{ci}} \partial_x \langle \tilde{v}_x \tilde{v}_y \rangle \left. \frac{\partial \langle f_e \rangle}{\partial x} \right|_0 \right| : \left| -\frac{m_i}{m_e} \frac{c^2}{B^2} \partial_x \langle \tilde{E}_x \tilde{E}_\parallel \rangle \left. \frac{\partial \langle f_e \rangle}{\partial v_\parallel} \right|_0 \right|$$
$$\sim |\omega_*| : |k_\parallel u_\parallel|. \tag{3.48}$$

Eliminating the Reynolds force, we obtain the coupled evolution equation for drift hole turbulence and turbulence driven zonal flows:

$$\frac{\partial}{\partial t} \left(\int dv_\parallel \frac{\omega_{ci} \langle \delta f_e^2 \rangle}{2 \partial \langle f_e \rangle / \partial x|_0} - \langle v_y \rangle \right)$$
$$= \frac{c_s^2}{v_*} \sum_{\mathbf{k}} (\omega_{*e}|_0 - k_\parallel u_\parallel) \mathrm{Im} \chi_i \left| \frac{e\tilde{\phi}}{T_e} \right|_{\mathbf{k}}^2 + \nu_d^\perp \langle v_y \rangle, \tag{3.49}$$

where $v_* = (\rho_s/|L_n|) c_s (1 - \eta_e (1 - u_\parallel^2/v_{the}^2)/2)$. In the presence of flows, the growth of the structure must accompany the acceleration of zonal flow, as depicted in Fig.3.2. The coupled evolution of the drift hole and zonal flow is analogous to the coupled evolution of turbulence and flows in a potential vorticity conserving, quasi-geostrophic system. For example, in the Hasewaga-Wakatani system[73] the coupled evolution is described by a momentum theorem[71],

$$\frac{\partial}{\partial t} \left\{ \frac{\langle \delta q^2 \rangle}{2 \langle q \rangle'} + \langle v_\theta \rangle \right\} = -\langle \tilde{v}_r \tilde{n}_e \rangle$$
$$- \frac{1}{\langle q \rangle'} \left(\frac{\partial}{\partial r} \left\langle \tilde{v}_r \frac{\delta q^2}{2} \right\rangle + D_0 \langle (\nabla \delta q)^2 \rangle \right) - \nu \langle v_\theta \rangle. \tag{3.50}$$

Here $q = n - \rho_s^2 \nabla_\perp^2 (e\phi/T_e)$, $\langle \delta q^2 \rangle / \langle q \rangle'$ is the wave activity density, D_0 is the diffusivity of potential vorticity, and ν is a collisional drag on the flow. Here for simplicity the particle diffusivity (D_0) and the viscosity (μ) were assumed to be equal. The wave activity density is related to fluctuation pseudomomentum[83], since in weak turbulence limit $\langle \delta q^2 \rangle / \langle q \rangle' \sim -|v_*|^{-1} \sum_k (1 + \rho_s^2 k_\perp^2)^2 |\hat{\phi}|_k^2 \sim -\sum_k k_\theta (\mathcal{E}_k/\omega_k)$ which

is recognizable as the negative of the wave momentum density. The theorem relates the coupled evolution of zonal flow momentum and fluctuation psedomomentum to the driving flux of turbulence, the local collisional dissipation of turbulence, turbulence spreading (the triplet term), and drag on zonal flow. Note that the turbulence spreading term can act as an effective local drive or dissipation of turbulence, depending on whether there is a local convergence or divergence of the potential enstrophy flux. The correspondence between the theorem and Eq.(3.49) is apparent. Here, Eq.(3.49) describes the coupled evolution of zonal flow momentum and the pseudomomentum of the drift hole. The drift hole pseudomomentum is given by $\langle \delta f_e^2 \rangle / \langle f_e \rangle'$, which can be viewed as a kinetic extension of the wave activity density. It may by interesting to note that the kinetic pseudomomentum is related to several other quantities such as the phasetrophy[30, 37] $\langle \delta f_e^2 \rangle$ (potential enstrophy in phase space), fluctuation entropy $\int dv_\parallel \langle \delta f_e^2 \rangle / \langle f_e \rangle$, as well as the fluctuation dynamic pressure $\int dv_\parallel \langle \delta f_e^2 \rangle / (2\partial \langle f_e \rangle / \partial E|_0)$, defined in the context of the kinetic energy principle for the Jean's instability for self-gravitating matter[84].

At this point, it may be appropriate to clarify the flow of free energy in the coupled dynamics of drift hole structure and zonal flow. The free energy channel is depicted in Fig.3.9. Note Fig.3.9 is specifically to an electron drift hole. The electron drift hole extracts free energy from the mean distribution function $\langle f_e \rangle$ by scattering guiding center ions and polarization charges. Scattering of guiding center ions leads to the growth of the drift hole structure, and hence releases the free energy. On the other hand, the quasi-neutrality constraint requires the structure to scatter polarization charge as well. This allows a part of the free energy to be coupled to zonal flows. Note zonal flows are a 'benign' repository of the free energy, since they cannot cause any transport. Note also that once accelerated, zonal flows reinforce the free energy coupling to the zonal flow channel. This is because the accelerated zonal flows can enhance the resonant absorption of drift holes. Zonal flow shears shift phases in the polarization charge flux further, and hence promote free energy coupling to the zonal flow channel.

The partition of the free energy leads to a self-regulating, predator-prey behavior of the drift hole and zonal flow. Here the prey is the drift hole, while the

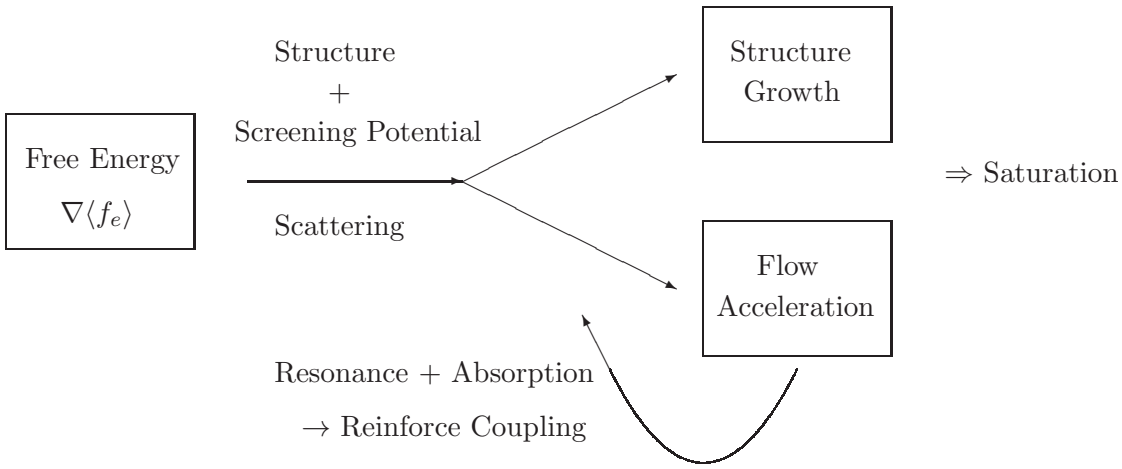

Figure 3.9: Flow of free energy

predator is the zonal flow. To address the point, it is useful to recall the predator-prey behavior of the *drift wave* and zonal flow system. A simplified model of drift wave and zonal flow turbulence is given as:

$$\partial_t \mathcal{E}_{DW} = \gamma_L \mathcal{E}_{DW} - \alpha \mathcal{E}_{DW} {V'_{ZF}}^2 - \Delta\omega(\mathcal{E}_{DW})\mathcal{E}_{DW}, \tag{3.51a}$$

$$\partial_t {V'_{ZF}}^2 = \alpha \mathcal{E}_{DW} {V'_{ZF}}^2 - \nu {V'_{ZF}}^2. \tag{3.51b}$$

Here, $\mathcal{E}_{DW}$ is the energy of the drift wave, ${V'_{ZF}}^2$ is the energy of the zonal flow, γ_L is a linear growth rate of the drift wave, α is a coupling constant, $\Delta\omega$ is a nonlinear damping of the drift wave, and ν is a collisional damping of the zonal flow. The drift wave behaves as a prey, while the zonal flow behaves as a predator. The prey is excited by the linear growth. The damping of the prey is two fold; dissipation by itself and dissipation by coupling to the predator. The predator is supported by the prey, while the predator reduces its population by collisional damping. Through the coupling process, the total energy between the prey and the predator is conserved. The conservation is explicitly manifested by adding the coupled equations:

$$\partial_t (\mathcal{E}_{DW} + {V'_{ZF}}^2) = \gamma_{eff} \mathcal{E}_{DW} - \nu {V'_{ZF}}^2. \tag{3.52}$$

Here, $\gamma_{eff} \equiv \gamma_L - \Delta\omega(\mathcal{E}_{DW})$ is the difference between the linear growth rate and the nonlinear damping of the drift waves. Note that similar conservation relation holds for the coupled drift hole and zonal flow system (Eq.(3.49)), albeit Eq.(3.49) describes the momentum budget.

The coupling between drift hole and zonal flow can impact the saturation of drift hole growth. Due to the coupling, a stationary state is achieved with a non-zero zonal flow. The stationary state is achieved when the competing effects on the righthand side of Eq.(3.49) balance, i.e.:

$$0 = \frac{c_s^2}{v_*} \sum_{\mathbf{k}} (\omega_{*e}|_0 - k_\parallel u_\parallel) \mathrm{Im}\chi_i \left| \frac{e\tilde{\phi}}{T_e} \right|_{\mathbf{k}}^2 + \nu_d^\perp \langle v_y \rangle .$$

We note that in principle, $\mathrm{Im}\chi_i$ can be a function of flows. Such flow dependence may allow a bifurcated flow solution. However, a detailed analysis of the bifurcated flow solution is beyond the scope of the paper and will be pursued in a future publication. Here, for simplicity, we assume $\mathrm{Im}\chi_i$ is set by ion Landau damping and is independent of the flow velocity. Given the caveat, stationary solution for the zonal flow is given by

$$\frac{\langle v_y \rangle}{c_s} = -\frac{1}{\nu_d^\perp} \frac{c_s}{v_*} \sum_{\mathbf{k}} (\omega_{*e}|_0 - k_\parallel u_\parallel) \mathrm{Im}\chi_i \left| \frac{e\tilde{\phi}}{T_e} \right|_{\mathbf{k}}^2 . \tag{3.53}$$

Several remarks on the saturation and the resultant zonal flows are in order. First, the physical picture of saturation is that drift hole growth saturates when the mixing of phase space density with ion dissipation is suppressed by large enough dynamical friction from flows. This follows from the fact that since the total momentum is conserved, flows are accelerated from drift hole turbulence. Secondly, all that is required for flow generation is a drift hole - a localized single phase space structure - and the absorption of its momentum by the flow at the resonance. This is sharp contrast to the familiar concepts for zonal flow generation by turbulence, such as inverse cascade[77], Rhine's scale[78], modulational instability[17] etc. This suggests that while the above mentioned familiar concepts are useful to understand zonal flow physics, none of them are fundamental. Finally, since drift

holes and zonal flows form a self-regulating predator-prey system, the saturated state discussed here with non-zero zonal flow can be viewed as the stationary state of predator-prey system with a non-zero predator population.

We can extract the maximal saturation amplitude for drift hole-zonal flow turbulence from the saturated zonal flow velocity Eq.(3.53). The amplitude is obtained as follows. Namely, at saturated state, non-zero flows are required, while the resultant zonal flow can feedback on drift hole structure through its screening length. If the flows were strong enough to make $\mathrm{Re}\chi[\langle v_y\rangle] < 0$ or at least $\mathrm{Re}\chi[\langle v_y\rangle] \to 0$, then the screening potential is not localized, and hence a self-bound drift hole does not form. Hence, to have a stationary state with non-zero flows, the resultant flow speed must not exceed the limit for the formation of the self-bound drift hole. The condition for drift hole to be self-bound is expressed in terms of the susceptibility as $\mathrm{Re}\chi[\langle v_y\rangle] > 0$, which gives

$$\frac{\langle v_y\rangle}{c_s} < \min\left(\frac{u_\parallel}{c_s}\frac{k_\parallel}{k_y}\frac{\chi^{(0)}}{1+k_y^2\rho_s^2}\right). \tag{3.54}$$

Here the minimum value ensures $\lambda_k^{-2} \propto \mathrm{Re}\chi[\langle v_y\rangle] > 0$ for each k. The condition Eq.(3.54) can be restated that hole-flow resonance is not strong, since the condition loosely says $k_y\langle v_y\rangle < k_\parallel u_\parallel$. This is physically plausible since if the resonance is strong, then the energy in the screening field is radiated and absorbed into the flows. In such cases, since the screening field is radiated away, the drift hole cannot self-bind itself.

The bounds on potential amplitude are then set by the condition Eq.(3.54), since the zonal flow is a function of fluctuation, i.e. $\langle v_y\rangle = \langle v_y\rangle[|\tilde{\phi}|^2]$ (See Eq.(3.53)). To be specific, we consider the saturation in the limit $\omega_{*e}|_0 \gg k_\parallel u_\parallel$, i.e. above threshold for drift hole growth. In this limit, the zonal flow level obtained from Eq.3.49 is

$$\frac{\langle v_y\rangle}{c_s} \cong -\frac{\omega_{ci}}{\nu_d^\perp}\sum_{\mathbf{k}} k_y\rho_s \mathrm{Im}\chi_i \left|\frac{e\tilde{\phi}}{T_e}\right|_{\mathbf{k}}^2. \tag{3.55}$$

Applying the condition $\langle v_y\rangle < \langle v_y\rangle_{max}$, the bound on potential amplitude in drift

hole-zonal flow turbulence then is:

$$\left|\frac{e\tilde{\phi}}{T_e}\right|^2 < \left|\frac{e\tilde{\phi}}{T_e}\right|^2_{max}, \tag{3.56}$$

where, the maximum amplitude is estimated to be:

$$\left|\frac{e\tilde{\phi}}{T_e}\right|^2_{max} \equiv \frac{\nu_d^{\perp}}{\omega_{ci}} \frac{1}{\overline{\rho_s k_y \mathrm{Im}\chi_i}} \min\left(\frac{u_{\parallel}}{c_s}\frac{k_{\parallel}}{k_y}\frac{\chi^{(0)}}{1+k_y^2\rho_s^2}\right). \tag{3.57}$$

Here $\overline{(...)}$ denotes the spectral average. Note the zonal flow damping $\nu_d^{\perp}$ appears as a control parameter for the maximum amplitude. This is similar to the case in predator-prey models[17, 72], where the damping of the predator (zonal flow) controls the population of the prey (drift hole). Physically put, this is because a larger collisional damping damps the zonal flow more strongly. The strong damping of the zonal flow allows the drift hole to easily extract the free energy, which in turn leads to a larger fluctuation amplitude. As a caveat, however, we note that there are both an upper and lower limit on the collisional damping $\nu_d^{\perp}$. The upper bound[85] is necessary since if the collisional damping is too strong, then zonal flows are completely damped, and hence cannot act as a repository of free energy. On the other hand, the lower bound is tied to stability of the zonal flow. If the collisional damping is too weak, then the free energy coupling to zonal flow is so strong that the resultant zonal flow can become Kelvin-Helmholtz unstable[86].

3.4 Conclusions

In this paper, we discussed the theory of drift hole structure and dynamics in the presence of zonal flows. In contrast to a previous study[34], we emphasized, throughout, the role of self-consistent turbulence driven flows in determining the radial structure of drift hole potential and in describing nonlinear dynamics of drift hole growth. (See Table.3.3 for comparison to the previous study.) The principal results of the paper are:

1. The drift hole potential was determined as $\phi = \phi^{(0)} + \phi^{shift} + \phi^{res}$ by solving

Table 3.3: Comparison between a previous study and this work.

	Previous study[34]	This work
Drift hole potential	$\phi^{(0)}$	$\phi^{(0)} + \phi^{shift} + \phi^{res}$
Time evolution	$\partial_t \int dv_\parallel \langle \delta f_e^2 \rangle$	$\frac{\partial}{\partial t}\left(\int dv_\parallel \frac{\omega_{ci}\langle \delta f_e^2 \rangle}{2\partial \langle f_e \rangle / \partial x|_0} - \langle v_y \rangle \right)$
Saturated amplitude	$\left\lvert \frac{e\tilde{\phi}}{T_e} \right\rvert \sim \frac{1}{\chi^{(0)}} \frac{\Delta x}{\lvert L_n \rvert}$	$\left\lvert \frac{e\tilde{\phi}}{T_e} \right\rvert^2_{max} = \frac{\nu_d^\perp}{\omega_{ci}} \frac{1}{\overline{\rho_s k_y \mathrm{Im}\chi_i}}$ $\times \min\left(\frac{u_\parallel}{c_s} \frac{k_\parallel}{k_y} \frac{\chi^{(0)}}{1 + k_y^2 \rho_s^2} \right)$

the Gyrokinetic Poisson equation with flow coupling. $\phi^{(0)}$ is the potential without flow coupling. This term describes an isotropic $E \times B$ vortex, as discussed in a previous study. In addition to $\phi^{(0)}$, here we have novel pieces due to flow coupling, i.e. ϕ^{shift} and ϕ^{res}. ϕ^{shift} originates from the expansion of the plasma susceptibility in terms of flow. Physically ϕ^{shift} describes radial shift of the isotropic $E \times B$ vortex, which is analogous to a flow shear effect on radial eigenmode structure of drift waves. ϕ^{res} originates from hole-flow resonance. This term gives rise to a cross-phase for Reynolds force, $\partial_x \langle \tilde{v}_x \tilde{v}_y \rangle$.

2. The theory of fully nonlinear dynamics of a drift hole and zonal flow was formulated. The dynamical evolution of the drift hole was coupled to the zonal flow, since the quasi-neutrallity constraint requires the drift hole to scatter polarization charge during hole growth. Since the polarization charge scattering is equivalent to Reynolds force on zonal flow, drift hole growth must be dynamically coupled to zonal flows. The coupled evolution of the

drift hole and zonal flow is described by:

$$\frac{\partial}{\partial t}\left(\int dv_{\parallel}\frac{\omega_{ci}\langle\delta f_e^2\rangle}{2\partial\langle f_e\rangle/\partial x|_0}-\langle v_y\rangle\right)$$
$$=\frac{c_s^2}{v_*}\sum_{\mathbf{k}}(\omega_{*e}|_0-k_{\parallel}u_{\parallel})\mathrm{Im}\chi_i\left|\frac{e\tilde{\phi}}{T_e}\right|_{\mathbf{k}}^2+\nu_d^{\perp}\langle v_y\rangle.$$

The coupled evolution describes a momentum budget of the drift hole and zonal flow. Due to the zonal flow coupling, it is the coupled momentum that evolves in time. Note this reduces to the expression for drift hole growth without flow coupling derived in an earlier study:

$$\frac{\partial}{\partial t}\int dv_{\parallel}\frac{\langle\delta f_e^2\rangle}{2}$$
$$=-\langle f_e\rangle|_0\sum_{\mathbf{k}}(\omega_{*e}|_0-k_{\parallel}u_{\parallel})\mathrm{Im}\chi_i\left|\frac{e\tilde{\phi}}{T_e}\right|_{\mathbf{k}}^2.$$

We note that the drift hole growth (up to flow) is subcritical, with the growth rate $\gamma_{NL}\sim k_{\parallel}\Delta v_{\parallel}|\mathrm{Im}\chi_i\mathrm{Im}\chi_e|/\chi^2$. This is quite different from the expression for the linear growth of drift waves, $\gamma_L\sim|\omega_*|(|\mathrm{Im}\chi_e|-|\mathrm{Im}\chi_i|)$.

3. The coupled evolution equation for the drift hole and zonal flow was analogous to momentum theorems which describe the coupled evolution of fluctuation pseudomomentum and flow momentum. $\int dv_{\parallel}\langle\delta f_e^2\rangle/\langle f_e\rangle'$ is pseudemomentum of an electron drift hole, a kinetic expression similar to wave activity density for quasi-geostrophic turbulence. As a consequence of the coupling, it is not the drift hole pseudomomentum but the total momentum, including zonal flow momentum, that evolves in time. We argued that a stationary state is achieved when the total momentum is constant in time.

4. The coupled evolution equation for the drift hole and zonal flow was also interpreted in the context of a predator-prey system. Here, the drift hole is the prey, and the zonal flow is the predator. The self-regulating behavior was analogous to that for the drift wave-zonal flow system.

5. As a consequence of the coupled evolution, a stationary state is possible with flow coupling. At the stationary state, non-zero zonal flow is supported, and is given by:

$$\frac{\langle v_y \rangle}{c_s} = -\frac{1}{\nu_d^{\perp}} \frac{c_s}{v_*} \sum_{\mathbf{k}} (\omega_{*e}|_0 - k_{\parallel} u_{\parallel}) \mathrm{Im}\chi_i \left| \frac{e\tilde{\phi}}{T_e} \right|_{\mathbf{k}}^2 .$$

The saturated state is analogous to a state in the predator-prey system with non-zero predator population.

6. An upper bound on the drift hole potential amplitude in the coupled drift hole-zonal flow system was calculated. The derivation was based on physical arguments that; i) energy in the screening field of a drift hole is absorbed into flows and thus excites zonal flow. ii) the coupling leads to a non-zero zonal flow at stationary state, and iii) the resultant zonal flow velocity must not exceed the flow velocity above which a self-bound drift hope cannot form. The result predicts that

$$\left| \frac{e\tilde{\phi}}{T_e} \right|_{max}^2 = \frac{\nu_d^{\perp}}{\omega_{ci}} \frac{1}{\rho_s k_y \mathrm{Im}\chi_i} \min \left(\frac{u_{\parallel}}{c_s} \frac{k_{\parallel}}{k_y} \frac{\chi^{(0)}}{1 + k_y^2 \rho_s^2} \right).$$

Note the appearance of the damping of zonal flow as a control parameter. The result can be compared to a saturation amplitude in a previous study[34] without flow coupling:

$$\frac{\tilde{n}}{n_0} \sim \frac{\tilde{f}}{f_0} \sim \chi^{(0)} \left| \frac{e\tilde{\phi}}{T_e} \right| \sim \frac{\Delta x}{|L_n|}.$$

This is essentially the mixing length estimate. The result obtained here shows that the zonal flow enters saturation dynamics as a critical element. In particular, the zonal flow damping appears as a control parameter of the saturation amplitude.

In a nutshell, we discussed the structure and dynamics of drift hole structure with the dissipative resonance with zonal flows. The drift hole solution was

obtained as a BGK solution for 3D magnetized plasmas. As explained above, the drift hole structure can tap free energy. Also, being a BGK solution, the drift hole can be viewed as analogous to a soliton. In this sense, the drift hole structure discussed here may be viewed as that analogous to a soliton solution in drift wave-zonal flow system[87, 88], which can spread turbulence. However, the drift hole solution obtained in this work is more general than the soliton solutions described in the references[87, 88], since the drift hole solution includes resonant coupling with zonal flows. As shown above, such resonant coupling with zonal flows significantly influences the dynamical evolution of the drift hole soliton. This raises a question regarding the effect of the resonant coupling with zonal flows on drift wave-zonal flow solitons. The role of such dissipative resonant coupling of zonal flows in the soliton solutions in drift wave-zonal flow system will be pursued in a future publication.

As a caveat, we note that the analysis presented here was concerned with a single coherent structure. Differently put, we considered *coherent* trapping. In contrast, as a complementary case, we can also have *turbulent* trapping, in which case structures form, but also break apart, leading to incoherent granular fluctuations[21, 32, 33, 89, 38]. While the analysis with the granulation requires a statistical treatment, rather than consideration of displacement of a single structure, the role of the granulation in driving relaxation is quite similar to the role of drift holes discussed here. Namely, the granulation evolves in time via dynamical friction due to the quasi-neutrality constraint, and can extract free energy even when plasmas are linearly stable. The granulation can also drive zonal flow by scattering polarization charge.

Taken together, we conclude that structures which form with either coherent or turbulent trapping are important players in relaxation in turbulent plasmas. *Structures can directly extract free energy, which leads to profile relaxation. Structures (even a single structure) also can excite zonal flows, and possibly toroidal flows. These findings are in sharp contrast to profile relaxation and flow generation by quasi-linear drift wave turbulence, a paradigm which is often assumed in the fusion community.*

The paradigm presented here may be applied to several issues in tokamak phenomenologies. As an example, we here discuss the application of this paradigm to the phenomenology of 'No Man's Land.' 'No Man's Land' is a region that connects the tokamak core region to the tokamak edge-pedestal region(Fig.3.10). An issue in the phenomenology of 'No Man's Land' is that while the turbulence level is observed to increase from the core to the edge region, most theoretical predictions based on the local gradient driven instabilities cannot reproduce the observed turbulence profile. In particular, most theoretical predictions reproduce the core turbulence level, while the prediction of the turbulence level deviates from the observed level in the 'No Man's Land' region. Here we argue that structures may enhance the turbulence level in the 'No Man's Land' region as follows. At the tokamak edge, a strong perturbation can nucleate structures such as density blobs or holes[64, 65] (Fig.3.10). Once formed, the blob propagates down the gradient, while the hole can propagate *up* the gradient. So, the hole can propagate *inward* from the edge and bombard the 'No Man's Land' region. As discussed above, since such incoming holes can tap free energy stored in the local gradient, such incoming holes can increase the turbulence level in 'No Man's Land' by feeding off the local gradient drive. Of course, the density holes may be self-regulated by zonal flows due to the total charge conservation. If this is the case, the fluctuation level associated with the density holes will be controlled, in part, by the collisional damping of zonal flows, $\langle \delta n_{hole}^2 \rangle \propto \nu_d$. Since ν_d typically increases towards the edge, it seems that even with the zonal flow coupling the fluctuation drive by the incoming hole structures becomes increasingly important in 'No Man's Land'.

The paradigm presented here may be also applied to several other relevant issues, such as i) anomaly of electron heat transport in the linear ohmic regime with large electron drift velocity[90], where linear eigenmodes of interest (current driven drift waves) are predicted to be marginal[91], ii) intrinsic rotation drive, where structure driven turbulence may leads to a source of residual stress and acts as a heat engine[36] to convert radial inhomogeneity to rotation, and iii) energetic particle confinement where strong wave-particle resonance is expected[92]. These are pursued in future publications.

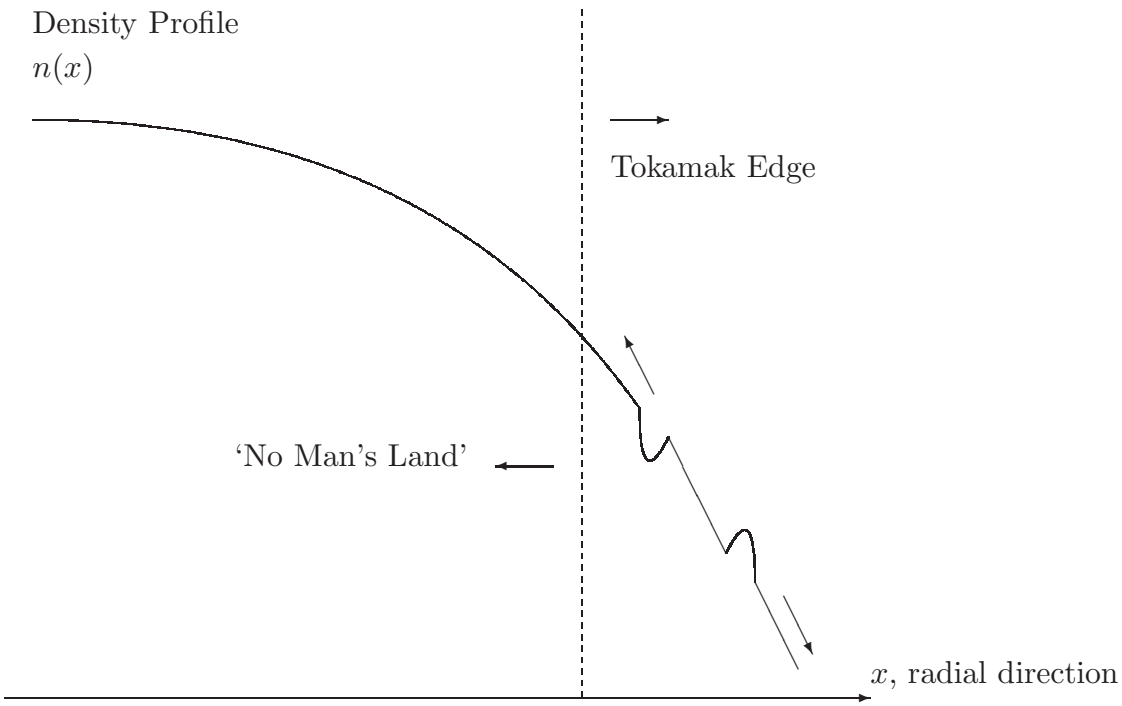

Figure 3.10: Incoming structures and turbulence in 'No Man's Land'

3.A Maxwell-Boltzmann hole and axisymmetric solution

The axisymmetric ($\partial_y = 0$) solution of the GK Poisson equation with the Maxwell-Boltzmann hole is analyzed. This solution physically describes an anisotropic $E \times B$ vortex extended in y direction. As such, the solution so obtained may be viewed as a 'zonal'; however, we note that a finite $k_\parallel \neq 0$ is required for a non-trivial parallel dynamics, including adiabatic electron response as well as electron trapping. Given the caveat, we refer the axisymmetric solution as the 'quasi'-zonal hole. Now, the axisymmetric condition $\partial_y = 0$ reduces the GK Poisson equation to a 1D problem by reducing the screening length to

$$\hat{\lambda}^{-2} = \rho_s^{-2} \tag{3.58}$$

In this case, the screening is determined solely by adiabatic electrons. Note the screening feedback of zonal flow is absent here. Now, to proceed further, we also assume a small hole $(E + |e|\phi_m)/\tau \ll 1$. In this case, the GK Poisson equation reduces to a 1D, albeit nonlinear, equation

$$\begin{aligned} &\partial_x^2 \frac{|e|\phi}{T_e} - \frac{1}{\rho_s^2}\frac{|e|\phi}{T_e} \\ &\cong -\frac{1}{\rho_s^2}\frac{4\sqrt{2}}{3}\langle f_e\rangle_0 v_{the}\frac{T_e}{\tau}\left(\frac{|e|\phi}{T_e} - \frac{|e|\phi_m}{T_e}\right)^{3/2} \end{aligned} \tag{3.59}$$

With dimensionless variables

$$w \equiv \left(\frac{16\sqrt{2}}{15}\langle f_e\rangle_0 v_{the}\frac{T_e}{\tau}\right)^2 \frac{|e|\phi}{T_e},\ \xi \equiv \frac{x}{\rho_s} \tag{3.60}$$

we have

$$\partial_\xi^2 w - w + \frac{5}{4}(w - w_m)^{3/2} = 0 \tag{3.61}$$

We seek for a localized solution with $w, \partial_\xi w \to 0$ as $\xi \to \pm\infty$. We also set $w_m = 0$ hereafter, which fix the trapping energy to zero (i.e. $E < -|e|\phi_m = 0$ for trapping). Interestingly, Eq.(3.61) can be viewed as the equation of motion for a point particle with nonlinear spring constant. The analogy is clear if we take ξ as time and w as a displacement. Then, we can see that Eq.(3.61) is the equation of motion with the nonlinear spring constant $1 - 5/4w^{1/2}$. To gain an insight into the 'trajectory' produced by Eq.(3.61), it is useful to note 'energy' is conserved:

$$\frac{\partial}{\partial\xi}\left[\frac{1}{2}\left(\frac{\partial w}{\partial\xi}\right)^2 - \frac{1}{2}w^2 + \frac{1}{2}w^{5/2}\right] = 0 \tag{3.62}$$

or

$$\left(\frac{\partial w}{\partial\xi}\right)^2 + V(w) = 0 \tag{3.63}$$

where $V(w) = -w^2 + w^{5/2}$ is the Sagdeev potential[93]. $V(w)$ is plotted in Fig.3.11. From the figure, we can see that $V(w)$ has a trough which allows a localized, bound solution for the electrostatic potential w. The solution is obtained via quadrature

as follows. The energy conservation yields

$$\xi = \pm \int_{w_0}^{w} \frac{dw'}{\sqrt{w'^2 - w'^{5/2}}} \tag{3.64}$$

where w_0 is the value of potential at $\xi = 0$, which is a maximum and $w_0 = 1$ from Fig.3.11. The integral can be performed by setting $w' = \sin^4 \theta'$, leading to

$$w = \mathrm{sech}^4 \left(\frac{\xi}{4} \right) \tag{3.65}$$

The quasi-zonal solution w is a localized potential in x, with the spatial extent of $\sim 4\rho_s$. Note $w > 0$, which is amenable to electron trapping. By its construction, Eq.(3.65) can be thought of as a soliton solution of GK-Poisson system, while it differs from usual solitons, such as ion acoustic solitons, in that the amplitude and the spatial extent is independent.

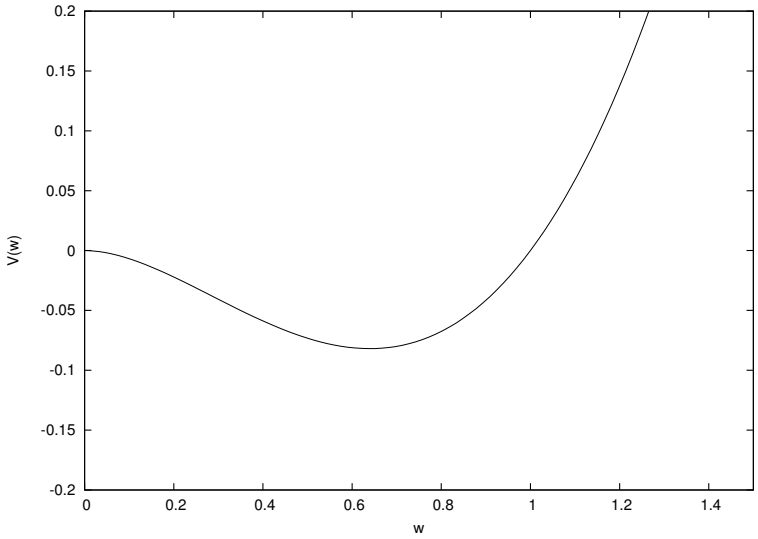

Figure 3.11: Sagdeev Potential $V(w)$.

Acknowledgement

Chapter 3 is a reprint of material submitted to Phys Plasmas, (2012). The dissertation author was the primary investigator and author of this article.

Chapter 4

Relaxation and transport in gyrokinetic drift wave turbulence with zonal flow

4.1 Introduction

Turbulent relaxation and transport are important issues for fusion plasmas. Conventionally, the relaxation process is thought to begin with free energy stored in plasma inhomogeneity being released by linear instability of drift waves. Transport or mean field evolution due to the instability is usually described via a quasilinear calculation[27], which assumes a spectrum of eigenmodes only, and thus treats turbulence as an ensemble of waves[10]. In terms of dimensionless numbers, this conventional approach is valid for Kubo number $K \equiv \tilde{v}\tau_c/\Delta_c \ll 1$ where $\tilde{v}$ is the typical velocity, τ_c is the correlation time, Δ_c is the correlation length. Despite usual practice, the conventional approach is not compatible with the mixing length theory[10] predictions - which are standard estimates for saturation levels - since in the saturated state we expect from mixing length theory that $\tilde{v} \sim \Delta_c/\tau_c$, so turbulence is characterized by $K \sim 1$. Moreover, $K \gtrsim 1$ can result for turbulence with non-mode like fluctuations such as vortices, eddys, blobs etc with $\tau_L \gtrsim \tau_{cir}$ (Fig.4.1), where $\tau_L \sim \tau_c$ is a life time of field pattern and $\tau_{cir} \sim \Delta_c/\tilde{v}$ is an eddy

circulation time. Thus, since turbulence is often in a state with $K > 1$ or at least $K \sim 1$, turbulence driven relaxation and transport should be analyzed in such regimes. There exist attempts[94, 95] to characterize transport in such a case; however, they usually study transport for a given, fixed spectrum of turbulence, without linking the structures inherent to $K \gtrsim 1$ with the turbulence *dynamics*. Since transport necessarily evolves profiles which in turn evolves turbulence, we need a self-consistent model of turbulent transport for $K \gtrsim 1$.

For $K \gtrsim 1$, kinetic plasma turbulence models, such as 1D Vlasov or gyrokinetic (GK) models used heavily in the fusion community, exhibit the existence of phase space structures. In the 1D Vlasov plasmas, $K \gtrsim 1$ corresponds to the state where the effect of particle trapping is important, since the Kubo number can be recast as $K = \tilde{v}\tau_c/\Delta_c \sim \tau_{ac}/\tau_b$ where $\tau_{ac}^{-1} = |d\omega/dk - \omega/k|\Delta k$ is the auto-correlation time of a packet and $\tau_b^{-1} \sim \tilde{v}/\Delta_c \sim k\sqrt{(q\phi/m)}$ is bounce frequency of particles trapped in potential trough (for 1D Vlasov models). Particle trapping leads to formation of phase space structures, such as BGK eddys[19], phase space holes[20, 96, 97], clumps or granulations[21, 96, 97], etc, which can be important players for relaxation and transport. As argued by Dupree[22] and Kadomtsev[98], phase space structures can emit a wake of waves via Cerenkov emission, an effect which necessarily appears as dynamical friction in the phase space density evolution equation (Fig.4.2). In this view, the emission is treated much like that from a test particle[30] and the emitting structure is viewed as a kind of macro particles, albeit one with a finite lifetime. Thus, turbulence driven mean field evolution equation is altered from a pure diffusive type to a Lenard-Balescu type, with *both diffusion and dynamical friction entering the evolution of* $\langle f \rangle$ *(Table 4.1).* The mean field evolution has been applied to current carrying Vlasov plasma, and the origin of anomalous resistivity has been linked to momentum exchange mediated by structures[22], in addition to the conventional approach based on waves[28].

The formation of structures[34, 96, 97] and its effect on transport[32, 33] are also discussed for inhomogeneous phase space turbulence, which is relevant to the problems in confined plasma transport. The ideas of phase space density granulation and dynamical friction are applied to collisionless ITG turbulence[33].

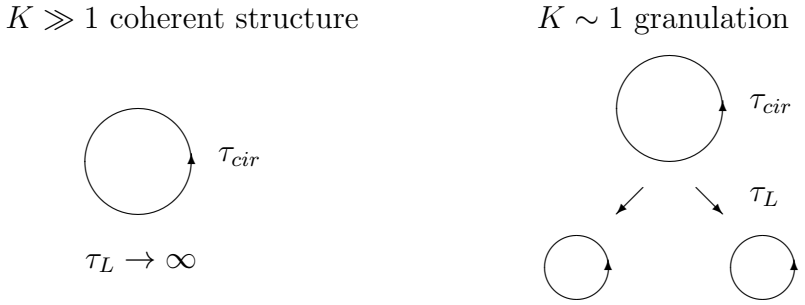

Figure 4.1: $K \gg 1$ and $K \simeq 1$

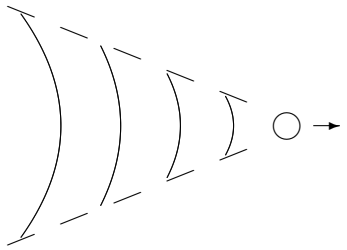

Figure 4.2: Cerenkov emission and wake.

In that analysis, the authors argued that the relaxation process inherently produces ion phase space density granulations, which then experience dynamical friction via the wake effect due to Cerenkov emission. The dynamical friction due to dissipative electrons is found to cause anomalous transport of ion energy and particles. On the other hand, the dynamical friction due to polarization charge is not included in that analysis, as the authors naively thought that the mixing of ion guiding center phase space is not coupled to polarization charge mixing; $\langle \tilde{v}_r \delta f_i \rangle \sim \langle \tilde{v}_r \tilde{n}_{GC,i} \rangle \sim \langle \tilde{v}_r \nabla_\perp^2 \tilde{\phi} \rangle$ and $\langle \tilde{v}_r \nabla_\perp^2 \tilde{\phi} \rangle \sim \mathrm{Re} \sum_k i k_\theta k_\perp^2 |\tilde{\phi}|_k^2 \to 0$.

However, *we do know that the polarization charge flux is tied to Reynolds*

Table 4.1: Turbulence with waves v.s. turbulence with structures

	Turbulence with waves	Turbulence with structures
Fluctuations	Eigenmode Drift wave, ...	Non-mode like BGK eddy, Clump, Hole, ...
Instability	Growth of mode	Growth of structure
Mean Evolution	Quasilinear diffusion	Diffusion + Dynamical friction, Drag

force via the identity[35, 71], $\langle \tilde{v}_r \nabla_\perp^2 \tilde{\phi} \rangle = \partial_r \langle \tilde{v}_r \tilde{v}_\theta \rangle$*, which usually is non-zero.* The analysis of the reference[33] overlooked the envelope and zonal flow scale. The issue may be clarified by noting that there are several spatial scales inherent to drift wave turbulence, which are:

- Mode fluctuation scale $l_c \sim k_r^{-1}$, where l_c is the typical correlation scale and k_r is the mode wave number
- Fluctuation spatial envelope scale of fluctuation Δ_{env}, where

$$\Delta_{env} \sim (|\tilde{\phi}_k|^{2'}/|\tilde{\phi}_k|^2)^{-1}$$

- Avalanche size Δ_{ava}, where $\Delta_{ava} > l_c$. An avalanche involves intermittent interaction of several neighboring fluctuation envelopes.
- Profile scale, L_f where $L_f \equiv (\langle f \rangle'/\langle f \rangle)^{-1}$

Usually $k_r^{-1} < \Delta_{env} \lesssim \Delta_{ava} < L_f$. Since the wake has a finite spatial extent, Fig.4.2, it naturally introduces an effective envelope scale to the fluctuation dynamics. The envelope scale can also be set by mode propagation and absorption points, the excitation profile, plasma profile curvature, etc. The envelope dependence alters the radial variation of the fluctuations from $\partial_r \tilde{\phi} \sim i k_r \phi_k e^{i k_r r}$ to $\partial_r \tilde{\phi} \sim (i k_r + \partial_R)\phi_k(R) e^{i k_r r}$, where $|i k_r| \gg |\partial_R|$ and r, R are associated with fast fluctuation variation and slow envelope variation respectively. Hence the envelope dependence replaces $k_r \to k_r - i\partial_R$, which effectively can be thought of as an $\mathrm{Im} k_r$. This leads to $\mathrm{Im} k_\perp^2 \neq 0$ and thus $\langle \tilde{v}_r \nabla_\perp^2 \tilde{\phi} \rangle \neq 0$. This is plausible since the envelope variation also implies a non-zero Reynolds force, $\partial_r \langle \tilde{v}_r \tilde{v}_\theta \rangle$. Thus, by accounting for the slow envelope variation, dynamical friction appears from the polarization charge, which induces direct zonal flow coupling to relaxation and transport by phase space density granulation. We note that Δ_{ava} could also be a relevant scale for zonal flow variation[99]; however, we do not further consider avalanching here.

In this paper, we discuss relaxation and transport in inhomogeneous phase space turbulence with zonal flow in the limit $K \gtrsim 1$. We consider a simple

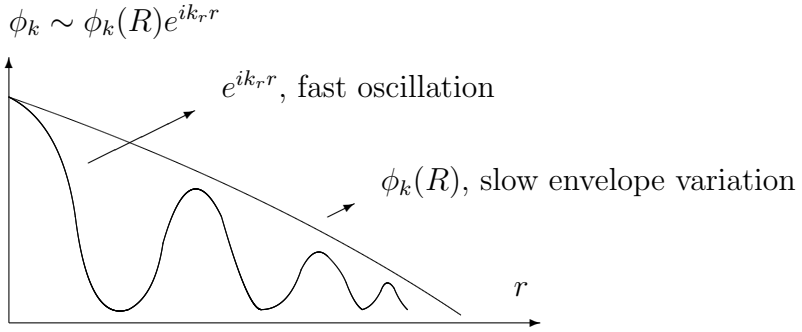

Figure 4.3: Envelope modulation

model[100] for GK drift wave turbulence:

$$\partial_t f + v_d \partial_y f + \{\phi, f\} = C(f) \tag{4.1a}$$

$$\alpha_e(\phi - \langle\phi\rangle_y) - \rho^2 \nabla_\perp^2 \phi = \frac{2}{n_{eq}\sqrt{\pi}} \int_0^\infty dE\sqrt{E} f - 1 \tag{4.1b}$$

with heat flux Q matched according to:

$$Q = -\chi_{coll}\langle T\rangle' + \frac{2}{\sqrt{\pi}} \int dE\sqrt{E} E \langle \tilde{V}_r \delta f\rangle \tag{4.1c}$$

where χ_{coll} is a collisional thermal conductivity. The model describes basically 2D drift wave dynamics, with a trapped particle precession resonance. Parallel acceleration is annihilated by bounce averaging, which enables us to focus on pure spatial mixing due to $E \times B$ drift. Eq.(4.1a) is bounce averaged kinetic equation for trapped ions. $v_d = v_{d,0}E/T_i$ is an energy dependent magnetic precession drift velocity[101]. The Poisson bracket accounts for $E \times B$ convection. Eq.(4.1b) is GK Poisson equation[39, 40], which accounts for polarization charge. Although the model is very simplified as compared to the full GK description, it does contain a minimal representation of all the relevant effects we need here. Namely, polarization charge introduces zonal flow coupling to the model, since any mixing of f leads to the mixing of $\nabla^2\phi$, which in turn leads to Reynolds forcing via the Taylor identity[35]; $\langle \tilde{v}_r \delta f_i\rangle \sim \langle \tilde{v}_r \tilde{n}_{GC,i}\rangle \sim \langle \tilde{v}_r \nabla_\perp^2 \phi\rangle = \partial_r \langle \tilde{v}_r \tilde{v}_\theta\rangle$. Also, $K \gtrsim 1$ is easily possible in the model, since the correlation time for particle and spectra can

become long, i.e. since

$$\Delta(\omega - \omega_d) \cong \Delta k_\theta \left| \frac{d\omega}{dk_\theta} - \frac{\omega}{k_\theta} \right| \tag{4.2}$$

then $\tau_{ac} \sim (|d\omega/dk_\theta - \omega/k_\theta|\Delta k_\theta)^{-1}$. Given the weakly dispersive nature of long wavelength drift wave turbulence, it is very easy to have long τ_{ac} and thus Kubo number $K = \tau_{ac}\tilde{v}/\Delta_c \gtrsim 1$ is possible. Hence phase space structure formation can be expected in this model.

In the remainder of the paper, we consider the two different limits of the model described above, $K \gg 1$ and $K \sim 1$. First we consider the strongly resonant limit for $K \gg 1$, which is applicable when a single structure can form(Fig.4.1). In this strongly resonant limit, we show that a phase space structure, as well as a wave, carries a pseudomomentum[83], and can exchange it with the zonal flow. To see this, we consider the growth of a single structure in the ion phase space density, in the presence of electrons and polarization charges. There, based on the invariance of the total dipole moment, we show that a single ion phase space density structure cannot avoid zonal flow coupling. The pseudomomentum associated with structures is identified as the negative of the kinetic wave activity density, $-\int dE\sqrt{E}\langle \delta f_i^2 \rangle / \langle f \rangle'|_0$. The structure growth equation with zonal flow is shown to be closely related to the Charney-Drazin (C-D) theorem[74, 16, 71] for potential vorticity (PV) conserving quasigeostrophic (QG) system, which is the fundamental momentum constraint for a system with turbulence and zonal flows. This is due to the fact that even single structure dynamics is necessarily tightly coupled to zonal flows.

Then we move to the limit $K \sim 1$, where structures can form but also break up(Fig.4.1), thus forming a statistical ensemble of granulations[21, 30, 32, 33]. Granulations are similar to fluid eddys, albeit in phase space, and constitute an incoherent part of fluctuations which enters relaxation and transport process as dynamical friction. We consider the dynamics of granulation and its effect on transport, in the presence of zonal flow coupling. The dynamics is described by a

statistical theory based on the 2 point correlation:

$$\left(\frac{\partial}{\partial t} + T(1,2)\right)\langle \delta f(1)\delta f(2)\rangle = P(1,2) \tag{4.3a}$$

Here $\langle \delta f(1)\delta f(2)\rangle$ is phase space density correlation function, called 'phasetrophy' [30], since it is analogous to enstrophy in QG turbulence. $T(1,2)$ determines the life time of correlation due to relative streaming, $\tilde{v}_{E\times B}$ scattering, and collisions. $P(1,2) \sim -\langle \tilde{v}_r \delta f\rangle \langle f\rangle'$ is the production of phasetrophy due to the relaxation process. In the following analysis, we show that production due to polarization charge introduces zonal flow coupling to the statistical granulation dynamics. The granulation evolution with zonal flow is compared to the C-D theorem for the QG system. We argue that the granulation evolution equation with zonal flow takes the form of the prey equation in the general predator-prey system. Thus, as other DW-ZF turbulence systems, granulations and zonal flows also form a self-regulating system in phase space. We also derive the transport flux associated with the granulation induced relaxation process. The mean field evolution is extracted from $P(1,2)$ by noting that $df/dt = 0$ and $d/dt\langle \delta f^2\rangle = -\partial_t \langle f\rangle^2$. For drift turbulence,

$$\partial_t \langle f\rangle = -\partial_r \langle \tilde{v}_r \delta f\rangle = -\partial_r[-D\partial_r\langle f\rangle + F\langle f\rangle] \tag{4.3b}$$

Here D is analogous to the familiar quasilinear diffusion term, and F is the dynamical friction term, which arises from granulation. We show that dynamical friction due to zonal flow is non-zero. Specifically, dynamical friction accounts for the contribution to $P(1,2)$ from the fluctuation Reynolds work on the zonal flow.

The remainder of the paper is organized as follows. In section II, single structure growth is formulated with zonal flow and linked to the C-D momentum theorem. Section III treats the case of multiple structures, using statistical theory. Phase space density granulation evolution is formulated in the presence of zonal flow. The connection of the result to C-D momentum theorems, as well as the implications for transport, are discussed. Section IV presents conclusions and discussion.

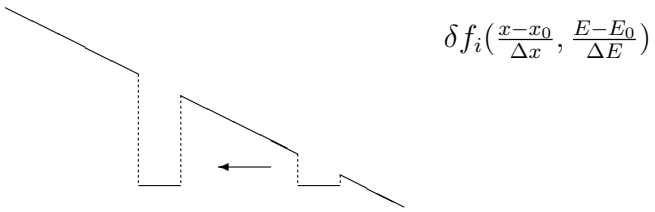

Figure 4.4: The growth of hole. Since $df/dt = 0$, a hole can grow by moving against background gradient. Here we consider a localized hole around (x_0, E_0), with the extent Δx and ΔE.

4.2 Single phase space structure and zonal flow

In this section, we discuss the interaction between a single phase space structure and zonal flows, a situation which corresponds to the limit $K \gg 1$. In this limit, particle trapping becomes important and a coherent structure, such as a hole or a blob, emerges. Such a structure can grow when the background distribution has a gradient due to inhomogeneity, since total f must be conserved along a trajectory; for example, a hole in phase space can grow when propagating up a background mean gradient(Fig.4.4). In the following, we consider the structure growth dynamics[20, 34] and show that a structure is dynamically coupled to zonal flow since radial transport and thus growth of a structure necessitates a flux of polarization charge, so as to maintain charge balance.

Here, we consider the structure dynamics in the model[100] described above:

$$(\partial_t + v_D\partial_y)f + \{\frac{c}{B}\phi, f\} = C(f) \tag{4.4a}$$

$$\frac{\delta n_i}{n_0} + \rho_s^2\nabla_\perp^2\frac{q\phi}{T_e} = \frac{\delta n_e}{n_0} \tag{4.4b}$$

The first equation is a bounce kinetic equation for the guiding center ion distribution, with an energy dependent drift velocity[101] $v_D = \bar{v}_D\bar{E}$ where $\bar{E} \equiv E/T_i$

and the Poisson bracket $\{\phi, f\} \equiv \partial_x\phi\partial_y f - \partial_y\phi\partial_x f$. Note that magnetic trapping does not allow correlated particles to disperse in the parallel direction. The second equation is the Gyrokinetic Poisson equation[39, 40], which includes polarization charge. Given the weakly dispersive character of long wave length drift waves in the model, the correlation time $\tau_{ac} \sim (|d\omega/dk_\theta - \omega/k_\theta|\Delta k_\theta)^{-1}$ can become long. For example if $\omega = \sqrt{\epsilon}\omega_*/(1+\rho_s^2k_\perp^2)$, we have:

$$\tau_{ac} \sim \left(\frac{2\sqrt{\epsilon}k_\theta^2\rho_s^2}{(1+k_\perp^2\rho_s^2)^2}v_*\Delta k_\theta\right)^{-1} \tag{4.5}$$

Then we easily see that τ_{ac} can be long for drift waves with $k_\theta\rho < 1$, even if the k spectrum is broad, i.e. $\Delta k_\theta\rho \sim 1$. Hence, the Kubo number can be large $K = \tau_{ac}\tilde{v}/\Delta_c \gg 1$ for this model. In this limit with strongly coherent resonances, it seems likely that a coherent structure, such as hole, blob or clump, can form[96, 97](Fig.4.1).

Given the possibility of structure formation, we consider the dynamics of a fluctuation $\delta f((x-x_0)/\Delta x, (E-E_0)/\Delta E)$, which is localized in a phase space point (x_0, E_0) with an extent Δx and ΔE, Fig.4.4. Here x_0 is the location of a structure we are considering and E_0 is the energy at resonance, i.e. $\omega - \bar{\omega}_d\bar{E}_0 = 0$. $\Delta x \sim \Delta_c$ is size of a structure in radial direction and the width in velocity space ΔE is estimated from $\bar{\omega}_d\Delta\bar{E} \sim \tau_{circ}^{-1} \sim \tilde{v}_E/\Delta_c$, so $\Delta\bar{E} \sim \tilde{v}_E/(\bar{\omega}_d\Delta_c)$.

A structure in phase space can grow as depicted in Fig.4.4, whose dynamics is described by δf^2 evolution[20, 34]. Since Eq.(4.4a) can be written as $df/dt = C(f)$, it implies $df^2/dt = 2fC(f)$. Writing $f = f_0 + \delta f$ and assuming $\partial_t\delta f/\delta f \gg \partial_t f_0/f_0$, the δf^2 evolution is obtained as

$$\partial_t \int d^3v\langle\delta f_i^2\rangle = -2\frac{d}{dt}\int d^3v\langle\delta f_i f_{i,0}\rangle + 2\langle fC(f)\rangle \tag{4.6a}$$

Here, f_0 includes the background mean distribution $\langle f\rangle$ as well as the depletion due to the structure. δf is a perturbation. $\langle ...\rangle$ denotes an ensemble average, which corresponds to the zonal average in y direction here. As in Fig.4.4, the distortion $\delta f((x-x_0)/\Delta x, (E-E_0)/\Delta E)$ is localized around a phase space point. Then we

expand f_0 about that point as

$$f_{i,0} = f_{i,0}(x_0, E_0) + (x - x_0) \left. \frac{\partial \langle f_i \rangle}{\partial x} \right|_{(x_0, E_0)} + ... \tag{4.6b}$$

Note that the expansion is only carried out in x here. This reflects the fact that in Eq.(4.4a) energy is not scattered by turbulence, since the bounce averaged $v_\parallel \tilde{E}_\parallel$ vanishes, i.e. $dE/dt = (e/m_i)\langle v_\parallel \tilde{E}_\parallel \rangle_b = 0$ where $\langle ... \rangle_b = \int dl/v_\parallel (...) / \int dl/v_\parallel$ is a bounce average. Using the expansion, the structure evolution equation now becomes

$$\partial_t \int d^3v \frac{\langle \delta f_i^2 \rangle}{2} = -\langle \tilde{v}_r \tilde{n}_i \rangle \left. \frac{\partial \langle f \rangle}{\partial x} \right|_0 + \langle f C(f) \rangle \tag{4.6c}$$

where the subscript 0 denotes a location of the structure in phase space (x_0, E_0), $d(x - x_0)/dt = \tilde{v}_r$ and $\int d^3v \delta f_i = \tilde{n}_i$. Eq.(4.6c) relates the distortion of the mean dstribution to the growth of the perturbation. Note that the structure growth, Eq.(4.6c), differs from the drift hole growth derived in an earlier study[34] in that; i) structure growth here is decoupled from velocity space scattering; and ii) structure growth here *is* coupled to zonal flow generation. The first difference is trivial, since we are dealing with a bounce kinetic equation here, so there is no parallel acceleration. The second, more physically relevant difference arises since the net dipole moment of the structure, including polarization charge, is conserved[20], $\int dx \sum_\alpha q_\alpha n_\alpha(x) x$. In other word, since quasi-neutrality including polarization charge is maintained $\langle \tilde{v}_r \tilde{n}_i \rangle = \langle \tilde{v}_r \tilde{n}_e \rangle - \langle \tilde{v}_r \tilde{n}_{pol} \rangle$ and $\langle \tilde{v}_r \tilde{n}_{pol} \rangle \sim \langle \tilde{v}_r \nabla_\perp^2 \tilde{\phi} \rangle \sim \partial_r \langle \tilde{v}_r \tilde{v}_\theta \rangle$ via the Taylor identity[35], ion structure growth is intrinsically coupled to zonal flow growth via flux of polarization charge. This gives

$$\partial_t \int d^3v \frac{\langle \delta f_i^2 \rangle}{2 \partial \langle f_i \rangle / \partial x|_0} = -\langle \tilde{v}_r \tilde{n}_e \rangle + \frac{n_0}{\omega_{c,i}} \partial_r \langle \tilde{v}_r \tilde{v}_\theta \rangle + \frac{\langle f C(f) \rangle}{\partial \langle f_i \rangle / \partial x|_0} \tag{4.6d}$$

which clearly states that the single structure growth cannot decouple from zonal flow evolution. Note that zonal flow coupling here appears through polarization charge flux, for the same reason as zonal flow coupling in QG turbulence appears through vorticity flux[35].

In Eq.(4.6d), the particle flux appears in the right hand side. Then, one may ask how we reconcile Eq.(4.6d) with heat flux drive. This may be resolved by going back to Eq.(4.6a) and by taking E moment of δf^2. This leads to

$$\partial_t \int d^3v E\langle \delta f_i^2 \rangle = -2\langle \tilde{v}_r \tilde{T}_i \rangle \left. \frac{\partial \langle f \rangle}{\partial x} \right|_0 + 2\int d^3v E\langle fC(f) \rangle \tag{4.7}$$

where $\langle \tilde{v}_r \tilde{T}_i \rangle \equiv \int d^3v E\langle \tilde{v}_r \delta f_i \rangle$. Eq.(4.7), together with heat balance equation $Q_0 = -\chi_{neo}\langle T_i \rangle' + \int d^3v E\langle \tilde{v}_r \delta f_i \rangle$, describes energetics of the system.

The structure evolution, Eq.(4.6d), reveals a momentum constraint for the interaction between a single phase space structure and zonal flow. Using the momentum balance $\partial_t \langle v_\theta \rangle + \partial_r \langle \tilde{v}_r \tilde{v}_\theta \rangle = -\nu \langle v_\theta \rangle$ gives

$$\frac{\partial}{\partial t}\left(\frac{n_0}{\omega_{c,i}} \langle v_\theta \rangle + \int d^3v \frac{\langle \delta f_i^2 \rangle}{2\langle f_i \rangle'|_0} \right) = -\langle \tilde{v}_r \tilde{n}_e \rangle - n_0 \frac{\nu}{\omega_c} \langle v_\theta \rangle + \frac{\langle fC(f) \rangle}{\partial \langle f_i \rangle / \partial x|_0} \tag{4.8}$$

Hence, we see that up to constant factors $\int d^3v \langle \delta f_i^2 \rangle / (\partial \langle f_i \rangle / \partial x)|_0$ can be thought of as a generalized momentum associated with fluctuation, namely the pseudomomentum of a single phase space structure which accounts for the zonal momentum of the structure. Eq.(4.8) states that a structure growth in phase space is dynamically coupled to zonal flow to conserve zonal momentum. At stationary state, electron flux can sustain a flow against collisional drag, $\langle v_\theta \rangle = -(\omega_c/\nu)\langle \tilde{v}_r \tilde{n}_e \rangle / n_0$; localized ion structure scatters electrons and can pump zonal flow growth. The statement that *a single localized structure in phase space can drive zonal flow* should be regarded as interesting, in light of the total absence of the familiar wave interaction-based mechanisms of zonal flow generation, such as inverse cascade[102], the Rhines mechanism[78], modulational instability[17], etc. Indeed, Eq.(4.8) supports the notion that PV transport or mixing and one direction of symmetry are all that is required for zonal flow generation[103].

At this point, it is interesting to compare Eq.(4.8) to the Charney-Drazin momentum theorem for a potential vorticity conserving, quasigeostrophic turbu-

Table 4.2: Comparison of quasi-geostrophic system and gyrokinetic system

	QG system	GK system
'Potential Vorticity'	PV, $q = \nabla_\perp^2\phi + F(\phi, n)$	GK Poisson, Pol Charge $\int d^3v f + \rho_s^2\nabla_\perp^2\phi = g(\phi, n_e, ...)$
Conservation of PV	$dq/dt = \partial_t q + \{q, \phi\} = 0$	$df/dt = \partial_t f + \{f, H\} = 0$
Circulation	$\Gamma = \oint (V + 2\Omega a \sin\theta) dl$	$\Gamma = \oint \mathbf{v} \cdot d\mathbf{x}$
Kelvin's Thm.	Yes	Yes (Lynden-Bell, '67)
C-D Theorem	Yes	Yes for non-resonant limit Yes for resonant limit

lence. The theorem[71] is proved for the Hasegawa-Wakatani system[73]

$$\frac{\partial}{\partial t}\left\{\frac{\langle\delta q^2\rangle}{2\langle q\rangle'} + \langle v_\theta\rangle\right\} = -\langle\tilde{v}_r\tilde{n}_e\rangle - \nu\langle v_\theta\rangle - \frac{1}{\langle q\rangle'}\left(\frac{\partial}{\partial r}\left\langle\tilde{v}_r\frac{\delta q^2}{2}\right\rangle + D_0\langle(\nabla\delta q)^2\rangle\right) \tag{4.9}$$

Here $q = n - \rho_s^2\nabla_\perp^2(e\phi/T_e)$, $\langle\delta q^2\rangle/\langle q\rangle'$ is the wave activity density or the negative of pseudomomentum[83], D_0 is a diffusivity of potential vorticity, and ν is a collisional drag on flow. $Pr = 1$ was assumed. As $\langle\delta q^2\rangle/\langle q\rangle' \sim -|v_*|^{-1}\sum_k(1+\rho_s^2k_\perp^2)^2|\hat{\phi}|_k^2 \sim -\sum_k k_\theta(\mathcal{E}_k/\omega_k)$, which is recognizable as the negative of the wave momentum density, the theorem states a momentum constraint for self-regulating DW-ZF turbulence system. Now each term in Eq.(4.8) has its counterpart in Eq.(4.9). The kinetic analogue of wave activity density, $\langle\delta f_i^2\rangle/\langle f\rangle'|_0$, can be contrasted to wave activity density $\langle\delta q^2\rangle/\langle q\rangle'$. The both terms are related to the momentum of fluctuations, although $-\langle\delta f_i^2\rangle/\langle f_i\rangle'|_0$ is the momentum of a phase space structure in the presence of strong wave-particle interaction. Particle flux and zonal flow drag appear in both equations. The underlying physics which unifies the two different systems is the conservation of 'potential vorticity', which consists of generalized or extended fluid vorticityt; for QG system PV consists of fluid vorticity plus the 'planetary' part related to β or v_*; for GK system it consists of polarization charge plus electron density. This ultimately follows from the Kelvin's theorem[104] for the conservation of total circulation, which underpins the Charney-Drazin theorem for flow momentum and a generalized pseudomomentum. See Table 4.2 for the comparison.

We note, though, Eq.(4.8) defines the pseudomomentum of phase space structure and is not a mere mathematical transcription of the Charney-Drazin theorem for QG system to another structurally similar system, i.e. the GK system. The extension of the theorem to the kinetic system is subtle, since kinetic system has a singularity from wave-particle resonance, with no counterpart in the QG system. The subtlety becomes apparent when we try to physically interpret the kinetic wave activity density, $\langle \delta f^2 \rangle / \langle f \rangle'$. Of course, in the non-resonant limit, the kinetic wave activity density corresponds to the negative of pseudomomentum associated with waves, as $\delta f_k \simeq (-\tilde{v}_{r,k}\langle f \rangle')/(-i\omega_k)$ and $\int \sqrt{E} dE \langle \delta f^2 \rangle / \langle f \rangle' \sim \int \sqrt{E} dE \sum_k \langle f \rangle' (k_\theta^2 |\tilde{\phi}|_k^2)/\omega_k^2 \sim -\sum_k (\mathcal{E}_k/\omega_k) k_\theta$ where $\mathcal{E}_k$ is the wave energy density. In the resonant limit, however, we cannot physically interpret the kinetic wave activity density based on the comparison between GK and QG turbulence. The above discussion of the ion structure growth reveals $-\int \sqrt{E} dE \langle \delta f_i^2 \rangle / \langle f_i \rangle'|_0$ as the pseudomomentum associated with phase space structure, and extends the interpretation of the kinetic wave activity density $\int \sqrt{E} dE \langle \delta f^2 \rangle / \langle f \rangle'$ to the case of resonant particles. This also suggests the robustness of the C-D momentum theorem: the momentum theorem holds, in both QG and GK systems, in the both non-resonant and resonant limit.

4.3 Multi-structures in phase space and zonal flow

In this section, we move from the problem of a single structure to the problem of multi-structures and discuss aspects of relaxation and transport in phase space turbulence for $K \sim 1$, where structures can form but also break, leading to formation of incoherent granular fluctuations in phase space. To formulate transport with such fluctuation, we first consider a model to characterize granularity of phase space density, which leads us to the calculation of phase space density correlation[21, 33] $\langle \delta f(1) \delta f(2) \rangle$. Note that $\langle ... \rangle$ is defined as the average over $\mathbf{x}_+ = (\mathbf{x_1} + \mathbf{x}_2)/2$ in this section. As discussed in the last section, a single structure in phase space interacts with zonal flow; hence it is plausible to expect

multi-structure or granulation to also interacts with the zonal flow. In the following, we derive the time evolution of phase space density granulation and show that granulation is dynamically coupled to zonal flow via production. This coupling is due to zonal momentum exchange in the δf^2 production process and is *not* simply due to usual effects of shear suppression, cross phase modification, etc. Then we turn to transport calculation due to phase space density granulation. Since phase space density granulation interacts with zonal flow, the zonal flow leaves a footprint in granulation driven transport. In the following, we argue that zonal flow introduces a novel effect in transport via dynamical friction.

4.3.1 Model and its dielectric function

The model we utilize here[33] consists of bounce averaged kinetic equations for ions and electrons ($\sigma = i, e$)

$$\left(\frac{\partial}{\partial t} + v_D(E)\frac{\partial}{\partial y} + \mathbf{v}_E \cdot \nabla + \nu_{eff}^{\sigma}\right)\delta h_\sigma = \frac{\partial}{\partial t}\frac{q_\sigma \tilde{\phi}}{T_\sigma}\langle f_\sigma\rangle - \tilde{\mathbf{v}}_{ExB}\cdot\nabla\langle f_\sigma\rangle \tag{4.10a}$$

and the Gyrokinetic Poisson equation[39, 40]

$$\frac{\delta n_e}{n_0} = \frac{\delta n_i}{n_0} + \rho_i^2\nabla_\perp^2\frac{q\tilde{\phi}}{T_i} \tag{4.10b}$$

Here δh is the non-adiabatic part of distribution function fluctuation, $\delta f_\sigma = -(q_\sigma\tilde{\phi}/T_\sigma)\langle f_\sigma\rangle + \delta h_\sigma$, $v_D(E) = \bar{v}_D\bar{E}$ where $\bar{E} = E/T_i$ is the drift due to magnetic field curvature and inhomogeneity, and a Krook operator was used, $C(\delta f_\sigma) = -\nu_{eff}^{\sigma}\delta h_\sigma$. Electrons are assumed to be dissipative with the energy dependent collision frequency[101] $\nu_{eff}(E) = (\nu_e/\epsilon_0)\bar{E_e}^{-3/2}$ where $\bar{E}_e \equiv E/T_e$. ϵ_0 is the inverse aspect ratio. We note that a singularity associated with the electron collision frequency at $\bar{E} = 0$ does not cause any problem in the calculation performed in the manuscript, as its *inverse* i.e. $\bar{E}^{3/2}(\nu_e/\epsilon_0)^{-1}$ appears as the relevant quantity, and is manifestly non-singular. Specifically, the electron frequency appears in $\mathrm{Im}\epsilon_e \propto \int\sqrt{\bar{E}}d\bar{E}\bar{E}^{3/2}e^{-\bar{E}}(\nu_e/\epsilon_0)^{-1}(...)$ which can be integrated analytically. See appendix A for the calculation. We also note that the strong electron collisions

($\nu_e/\epsilon_0 \gg \omega_{*e}, 1/\tau_c$) smears out electron granulation formation, as the propagator for trapped electron becomes $g_{k\omega} = i(\omega - \omega_{D,e}\bar{E}_e + i/\tau_c + i\nu_e/\epsilon_0 \bar{E}_e^{-3/2})^{-1} \simeq (\nu_e/\epsilon_0)\bar{E}_e^{3/2}$. Thus the electrons are *laminar* in this model and we focus on the ion granulation dynamics. The model we use here is quite general - 2D ion guiding center advection, polarization charge in GK Poisson equation, and precession drift resonance. It is arguably the simplest model of GK drift wave turbulence with wave-particle resonance effects.

In the later calculation, we need the plasma response function, or plasma dielectric for the model. This is given by (See Appendix A for the derivation.)

$$\begin{aligned}\hat{\epsilon}(k,\omega) =& \frac{T_i}{T_e} + \rho_i^2 k_\perp^2 + 1 - P\int d^3v \frac{\omega - \omega_*^i(E)}{\omega - \bar{\omega}_D\bar{E} - k_\theta\langle v_E\rangle(r)}\langle f_i\rangle \\ &+ i\mathrm{Im}\epsilon_i + i\mathrm{Im}\epsilon_e + i\mathrm{Im}\epsilon_{pol} \end{aligned} \tag{4.11a}$$

where $\omega_*^\sigma(E) \equiv (k_\theta c T_\sigma \langle f_\sigma(E)\rangle')/(q_\sigma B\langle f_\sigma(E)\rangle) = k_\theta v_*^\sigma(1 + \eta_\sigma(\bar{E} - 3/2))$, $v_*^i \equiv -(\rho_i/|L_n|)v_{thi}$, $v_*^e = (\rho_s/|L_n|)c_s$, and P denotes the principle part of the integral. The first term is from adiabatic electrons. The second term is from polarization charge. The second line includes ion contribution from adiabatic passing and trapped populations. The imaginary part of the dielectric is

$$\mathrm{Im}\epsilon_i = \sqrt{2\epsilon_0}\frac{2}{\sqrt{\pi}}\sqrt{\bar{E}_{res}}\pi\frac{\omega - \omega_*^i(\bar{E}_{res})}{|\bar{\omega}_D|}e^{-\bar{E}_{res}} \tag{4.11b}$$

$$\mathrm{Im}\epsilon_e = \frac{4}{\sqrt{\pi}}\frac{\sqrt{2\epsilon_0}}{\nu_e/\epsilon_0}\frac{T_i}{T_e}(\omega - \omega_*^e(1 + \frac{3}{2}\eta_e)) \tag{4.11c}$$

$$\mathrm{Im}\epsilon_{pol} = -2\rho_i^2 k_r \partial_r \tag{4.11d}$$

where $\bar{E}_{res} \equiv (\omega - k_\theta\langle v_\theta\rangle'(r - r_0))/\bar{\omega}_D$. $\mathrm{Im}\epsilon_i$ arises from the resonance between waves and toroidal ion precession. Note that shear flow alters the resonant frequency $\bar{\omega}_D\bar{E} \to \bar{\omega}_D\bar{E} + k_\theta\langle v_\theta\rangle'(r - r_0)$. $\mathrm{Im}\epsilon_e$ comes from collisional dissipation in electrons. $\mathrm{Im}\epsilon_{pol}$ originates from an envelope coupling via modulation, i.e. $k_r \to k_r - i\partial_r$, where ∂_r captures the envelope variation of the fluctuation spectrum, which is slow compared to k_r (Fig.4.3). As in Fig.4.2, granulations produce a wake with a spatial extent, which contributes to the slow envelope variation. This

envelope introduces two different scales in the fluctuation; a micro-scale which is characterized by mode wave number k_r and an envelope variation which is captured by the derivative acting on the slow scale envelope, ∂_r. The confluence of the two different radial scales leads to $k_r \to k_r - i\partial_r$ and $\epsilon_{pol} \sim k_\perp^2 \sim k_r^2 - 2ik_r\partial_r$, so $\mathrm{Im}\epsilon_{pol} \sim -2k_r\partial_r$. Noting the role of polarization charge in single structure dynamics and the dynamical friction $F \propto \mathrm{Im}\epsilon$, we will see that the envelope coupling term $\mathrm{Im}\epsilon_{pol}$ introduces zonal flow coupling to the mean field evolution via $F \sim \mathrm{Im}\epsilon_{pol}$. Note also that the plasma dielectric is now an operator, since $\mathrm{Im}\epsilon_{pol} \propto \partial_r$. Also, hereafter it is understood that $r - r_0 = x$.

4.3.2 Derivation of phasetrophy evolution

In this section, we derive the time evolution equation for phase space density correlation[21] $\langle \delta h(1)\delta h(2)\rangle$. Phase space density correlation can be compared to several physical quantities, Fig.4.5. Phase space density correlation $\langle \delta h^2\rangle$ can be thought of as 'potential enstrophy' in phase space or 'phasetrophy'[30], since phase space density f in the GK system is similar to the potential vorticity q in the QG system (Table4.2). Following the analogue between the QG and the GK system, the phasetrophy gives the kinetic wave activity density, which is closely related to the fluctuation pseudomomentum. Alternatively, phase space density correlation evolution $\langle \delta f(1)\delta f(2)\rangle$ is also related to the fluctuation entropy in kinetics, i.e. $s = \int \sqrt{E}dE\langle \delta f^2\rangle/\langle f\rangle$.

$\langle \delta h(1)\delta h(2)\rangle$ evolution is derived as follows[21, 30, 33]. Upon multiplying $\delta h(2)$, adding the equation with 1 and 2 exchanged, introducing the relative coordinate $y_- \equiv y_1 - y_2$, and averaging over $\mathbf{x}_+ = (\mathbf{x}_1 + \mathbf{x}_2)/2$, Eq.(4.10$a$) for ions gives

$$\frac{\partial}{\partial t}\langle \delta h(1)\delta h(2)\rangle + v_{rel}\frac{\partial}{\partial y_-}\langle \delta h(1)\delta h(2)\rangle + T(1,2) + C(1,2) = P(1,2) \qquad (4.12)$$

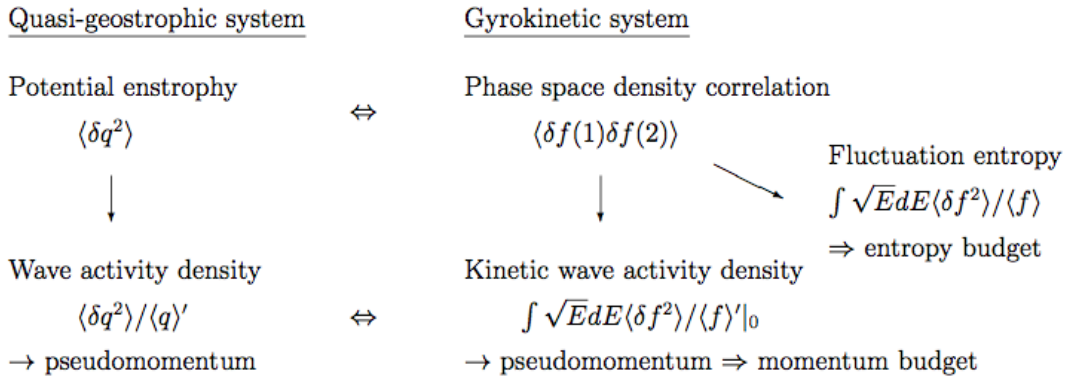

Figure 4.5: Relation of 'phasetrophy' $\langle \delta f(1) \delta f(2) \rangle$ to other physical quantities

Here the terms in the lefthand side are

$$v_{rel} \equiv \bar{v}_D(\bar{E}_1 - \bar{E}_2) + \langle v_E \rangle'(x_1 - x_2) \tag{4.13a}$$

$$T(1,2) \equiv \langle \delta h(2) \tilde{\mathbf{v}}_{E\times B}(1) \cdot \nabla \delta h(1) \rangle + (1 \leftrightarrow 2) \tag{4.13b}$$

$$C(1,2) \equiv \langle \delta h(2) \nu_{eff}(1) \delta h(1) \rangle + (1 \leftrightarrow 2) \tag{4.13c}$$

$(1 \leftrightarrow 2)$ denotes the term with the arguments 1 and 2 exchanged. v_{rel} is the relative velocity of particles at two different points in phase space. $T(1,2)$ is the triplet term which describes the decorrelation process due to nonlinear $\tilde{v}_{E\times B}$ scattering. $C(1,2)$ is the collisional cut-off. After a closure calculation[33] of the triplet term, the lefthand side of Eq.(4.12) reduces to

$$\left(\frac{\partial}{\partial t} + \bar{v}_D E_- \frac{\partial}{\partial y_-} + \langle v_E \rangle' x_- \frac{\partial}{\partial y_-} - \frac{\partial}{\partial \mathbf{x}_-} \cdot \mathbf{D}_{rel} \cdot \frac{\partial}{\partial \mathbf{x}_-} \right) \langle \delta h(1) \delta h(2) \rangle + C(1,2) \tag{4.14}$$

where $\mathbf{D}_{rel}$ is the relative diffusion matrix

$$\mathbf{D}_{rel} = \sum_{k\omega} \{1 - \cos(\mathbf{k} \cdot \mathbf{x}_-)\} \langle \tilde{\mathbf{v}}_{E\times B} \tilde{\mathbf{v}}_{E\times B} \rangle_{k\omega} \mathrm{Re} \frac{i}{\omega - k_\theta \bar{v}_D \bar{E} - k_\theta \langle v_E \rangle' x + i/\tau_c} \tag{4.15}$$

The relative streaming of the magnetic drift, zonal flow shear, the relative diffusion, and $C(1,2)$ together determine an effective life time of correlation. In the limit of $1 \to 2$, since $v_{rel} \to 0$ and $\mathbf{D}_{rel} \propto k_\perp^2 x_-^2 \to 0$, the lifetime is determined by the collisional cut-off.

The righthand side of Eq.(4.12) is

$$P(1,2) \equiv -\left\langle \tilde{v}^r_{E\times B}(1)\delta h(2)\right\rangle \langle f_i(1)\rangle' + \left\langle \delta h(2)\partial_t \frac{q\tilde{\phi}(1)}{T_i}\right\rangle \langle f_i(1)\rangle + (1 \leftrightarrow 2) \tag{4.16a}$$

$P(1,2)$ is the production of phasetrophy due to transport and relaxation. Note that the first term in the production $P(1,2)$ has a generic form expected for production, namely flux $\langle \tilde{v}_r \delta f\rangle$ times gradient $\langle f\rangle'$. In terms of Fourier components, we have

$$P(1,2) = \mathrm{Re}\sum_{k\omega}(-i\omega + i\omega^i_*(1))\left\langle \frac{q\tilde{\phi}(1)}{T_i}\delta h^*(2)\right\rangle_{k\omega} e^{i\mathbf{k}\cdot\mathbf{x}_-}\langle f_i(1)\rangle + (1 \leftrightarrow 2) \tag{4.16b}$$

where $\mathbf{x}_- \equiv \mathbf{x}_1 - \mathbf{x}_2$, $\omega^i_*(1) \equiv (k_\theta c T_i \langle f_i(1)\rangle')/(qB\langle f_i(1)\rangle) = k_\theta v^i_*(1+\eta_i(\bar{E}-3/2))$, $v^i_* \equiv -(\rho_i/|L_n|)v_{thi}$ and $\langle ...\rangle_{k\omega}$ is the Fourier spectrum of a correlation function, i.e. $\langle f(\mathbf{x}_1,t_1)g(\mathbf{x}_2,t_2)\rangle = \sum_{k\omega}\langle fg\rangle_{k\omega}e^{i\mathbf{k}\cdot\mathbf{x}_- - i\omega t_-}$. As $\delta h = \delta h^c + \widetilde{\delta h}$, the production term consists of two parts, namely coherent and incoherent production[22, 98, 30](Fig.(4.6)). The coherent part originates from a response of phase space density fluctuation to potential fluctuation $\tilde{\phi}$, namely $\delta h^c_{k\omega} \sim R(k,\omega)\tilde{\phi}_{k\omega}$. The incoherent part originates from granulation $\widetilde{\delta h}$. While moving through plasmas, granulations or macro-particles in phase space can emit wave wakes via Cerenkov processes (Fig.4.2). These wakes are in turn absorbed by plasma. This process effectively produces a macro-particle wake and induces dynamical friction on ion phase space density granulations. This in turn produces incoherent production, $\tilde{P} \propto \mathrm{Im}\epsilon$. We calculate both coherent and incoherent production in the following(Fig.(4.6)).

To calculate the production term due to the coherent response, we need $\delta h^c_{k\omega}$, the part of δh phase-coherent with fluctuation potential. $\delta h^c_{k\omega}$ can be calcu-

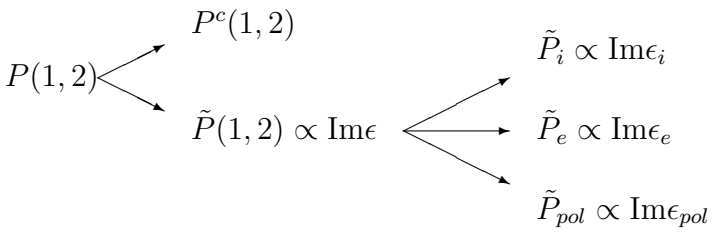

Figure 4.6: List of terms to be calculated

lated as a response to $\tilde{\phi}_{k\omega}$ from Eq.(4.10a) as

$$\delta h^c_{k\omega} = g_{k\omega}(-i\omega + i\omega^i_*)\left(\frac{q\tilde{\phi}}{T_i}\right)_{k\omega}\langle f_i\rangle \tag{4.17}$$

where $g_{k\omega} \equiv (-i\omega + i\bar{\omega}_D\bar{E} + ik_\theta\langle v_E\rangle' x + 1/\tau_c)^{-1}$ is a propagator, and $1/\tau_c$ comes from resonance broadening[105] due to the nonlinear $\mathbf{E}\times\mathbf{B}$ scattering, so $\tau_c^{-1} \sim k_\perp^2 D_\perp$ and $D_\perp = \sum_{k\omega} \mathrm{Re}g_{k\omega}(c/B)^2\langle\tilde{\phi}^2\rangle_{k\omega}$. Note that in the weak turbulence limit of $1/\tau_c < \omega$, $\mathrm{Re}g_{k\omega} \to \pi\delta(\omega - \bar{\omega}_D\bar{E} - k_\theta\langle v_E\rangle' x)$, which is the expression we use later to obtain the net ion phasetrophy production, Eq. (4.28). This is essentially the linear response. Then using the expression for $\delta h^c_{k\omega}$ gives

$$P^c(1,2) \equiv \mathrm{Re}\sum_{k\omega}(-i\omega + i\omega^i_*(1))\left\langle \frac{q\tilde{\phi}(1)}{T_i}\delta h^{c*}(2)\right\rangle_{k\omega}\langle f_i(1)\rangle e^{i\mathbf{k}\cdot\mathbf{x}_-} + (1\leftrightarrow 2) \tag{4.18a}$$

$$= \sum_{k\omega}(\omega - \omega^i_*(1))(\omega - \omega^i_*(2))\mathrm{Re}g_{k\omega}(2)\left\langle \frac{q\tilde{\phi}(1)}{T_i}\frac{q\tilde{\phi}^*(2)}{T_i}\right\rangle_{k\omega} \times \langle f_i(1)\rangle\langle f_i(2)\rangle e^{i\mathbf{k}\cdot\mathbf{x}_-} + (1\leftrightarrow 2) \tag{4.18b}$$

$$\to 2\sum_{k\omega}(\omega - \omega^i_*(E))^2\langle f_i\rangle^2\mathrm{Re}g_{k\omega}\lim_{1\to 2}\left\langle \frac{q\tilde{\phi}(1)}{T_i}\frac{q\tilde{\phi}^*(2)}{T_i}\right\rangle_{k\omega} \tag{4.18c}$$

where in the last line we took the limit of $1 \to 2$. This term corresponds to the production due to diffusive flux of phase space density by $\tilde{v}_{E\times B}$ scattering. This

can be checked, for $\omega - \omega_*^i \sim k_\theta \rho_i v_{thi} \langle f \rangle' / \langle f \rangle$,

$$P^c \sim 2 \sum_{k\omega} v_{thi}^2 \mathrm{Re} g_{k\omega} k_\theta^2 \rho_i^2 \left\langle \left(\frac{q\tilde{\phi}}{T_i} \right)^2 \right\rangle_{k\omega} \langle f_i \rangle'^2 = 2D \langle f_i \rangle'^2 \tag{4.18d}$$

Here $D \equiv \sum_{k\omega} v_{thi}^2 \mathrm{Re} g_{k\omega} k_\theta^2 \rho_i^2 \left\langle (q\tilde{\phi}/T_i)^2 \right\rangle_{k\omega}$ is the diffusion coefficient due to $E \times B$ scattering. Eq.(4.18d) is the familiar quasi-linear result.

Note that the spectrum $\langle \tilde{\phi}^2 \rangle_{k\omega}$ is not arbitrary here; $\langle \tilde{\phi}^2 \rangle_{k\omega}$ is produced by granulation $\langle \widetilde{\delta h}^2 \rangle_{k\omega}$ via Cerenkov emission. The potential fluctuation is self-consistently calculated[21] by solving the quasi-neutrality condition via the GK Poisson equation

$$\hat{\epsilon}(k, \omega) \frac{q\tilde{\phi}_{k\omega}}{T_i} = \left(\frac{\widetilde{\delta n_i}}{n_0} \right)_{k\omega} \tag{4.19}$$

where $(\widetilde{\delta n_i}/n_0)_{k\omega} = \int d^3 v \widetilde{\delta h}_{k\omega}$ may be thought of as the emission by incoherent granulation. The quasi-neutrality condition can be solved with the help of Green's function defined by

$$\hat{\epsilon}(x) G(x, x') = \delta(x - x'), \tag{4.20}$$

which yields

$$\frac{q\tilde{\phi}_{k\omega}(x)}{T_i} = \int dx' G(x, x') \frac{\widetilde{\delta n}_{k\omega}(x')}{n_0} = \int dx' d^3 v G(x, x') \widetilde{\delta h}_{k\omega}(\mathbf{v}, x') \tag{4.21a}$$

Note that Eq.(4.21a) is only valid for nearly steady state with saturated waves, since in that case the homogeneous or eigenvalue solution of the quasi-neutrality condition, i.e. $\epsilon(k, \omega_k) = 0$ with $\tilde{\phi}_k \sim e^{-i\omega_k t}$, is damped so only the inhomogeneous solution due to the incoherent emission remains in Eq.(4.21a). Given that caveat, the self-consistent spectrum is obtained as

$$\begin{aligned} &\left\langle \frac{q\tilde{\phi}(1)}{T_i} \frac{q\tilde{\phi}^*(2)}{T_i} \right\rangle_{k\omega} \\ &= \int dx_1' dx_2' d^3 v_1 d^3 v_2 G(x_1, x_1') G^*(x_2, x_2') \langle \widetilde{\delta h}(x_1', \mathbf{v}_1) \widetilde{\delta h}^*(x_2', \mathbf{v}_2) \rangle_{k\omega} \end{aligned}$$

Eq.(4.22) suggests that the self-consistent spectrum at x depends on the gran-

ulation fluctuations at different locations x_1', x_2'. Note that in the local limit $G(x,x') = \epsilon^{-1}(k,\omega)\delta(x-x')$ and Eq.(4.22) reduces to a familiar form $\langle\tilde{\phi}^2\rangle_{k\omega} \sim \langle\widetilde{\delta n}^2\rangle_{k\omega}/|\epsilon(k,\omega)|^2$.

With the self-consistent spectrum, the coherent production can be rewritten as

$$\lim_{1\to 2} P^c(1,2) = 2\sum_{k\omega}(\omega-\omega_*^i(E))^2\langle f_i\rangle^2 \mathrm{Re} g_{k\omega} \times \int dx_1' dx_2' d^3v_1 d^3v_2 G(x_1,x_1')G^*(x_2,x_2')\langle\widetilde{\delta h}(x_1',\mathbf{v}_1)\widetilde{\delta h}^*(x_2',\mathbf{v}_2)\rangle_{k\omega} \tag{4.22}$$

A form which is more useful for the later calculation is obtained by relating k,ω spectrum to k spectrum via the orbit propagator[21, 33, 30]

$$\langle\widetilde{\delta h}(1)\widetilde{\delta h}^*(2)\rangle_{k\omega} \cong 2\pi\delta(\omega-\bar{\omega}_D\bar{E}_2 - k_\theta\langle v_E\rangle x_2)\langle\widetilde{\delta h}(1)\widetilde{\delta h}^*(2)\rangle_k \tag{4.23}$$

Upon integrating over energy, we obtain

$$\lim_{1\to 2} P^c(1,2) = 2\sum_{k\omega}(\omega-\omega_*^i(E))^2\langle f_i\rangle \mathrm{Re} g_{k\omega} \times \sqrt{2\epsilon_0}\frac{2}{\sqrt{\pi}}\frac{2\pi}{|\bar{\omega}_D|}e^{-\bar{E}}\int dx_1' dx_2' G(x,x_1')G^*(x,x_2') \times \sqrt{\bar{E}_{res}(x_2')}\left\langle \frac{\widetilde{\delta n}(x_1')}{n_0}\widetilde{\delta h}^*(x_2',\bar{E}_{res}(x_2'))\right\rangle_k \tag{4.24}$$

Note that Eq.(4.24) is not as simple as its local limit

$$\lim_{1\to 2} P^c(1,2) = 2\sum_{k\omega}(\omega-\omega_*^i(E))^2\langle f_i\rangle \mathrm{Re} g_{k\omega} \times \sqrt{2\epsilon_0}\frac{2}{\sqrt{\pi}}\frac{2\pi}{|\bar{\omega}_D|}e^{-\bar{E}}\frac{\sqrt{\bar{E}_{res}}}{|\epsilon(k,\omega)|^2}\left\langle \frac{\widetilde{\delta n}}{n_0}\widetilde{\delta h}^*(\bar{E}_{res})\right\rangle_k \tag{4.25}$$

The difference arises from zonal flow coupling. In the presence of zonal flows, the plasma dielectric becomes an operator via envelope coupling $\mathrm{Im}\epsilon_{pol} \propto \partial_r$ and the resonance is altered from $\delta(\omega-\bar{\omega}_D\bar{E})$ to $\delta(\omega-\bar{\omega}_D\bar{E}-k_\theta\langle v_E\rangle' x)$. The modified resonance functions introduce a spatial integral (via inversion of the operator using

a Green's function) and space dependent velocity integral Jacobian $\sqrt{\bar{E}_{res}(x)}$. These, then, form an 'non-local' influence kernel.

Now we turn to the calculation of the production term due to incoherent, granular fluctuations;

$$\tilde{P}(1,2) \equiv \mathrm{Re}\sum_{k\omega}(-i\omega + i\omega_*^i(1))\left\langle \frac{q\tilde{\phi}(1)}{T_i}\widetilde{\delta h}^*(2)\right\rangle_{k\omega}\langle f_i(1)\rangle e^{i\mathbf{k}\cdot\mathbf{x}_-} + (1\leftrightarrow 2) \quad (4.26a)$$

Expressing the potential fluctuation in terms of the incoherent fluctuation and inserting a unit operator $\hat{\epsilon}^*(x)\int dx' G^*(x,x') = 1$ gives

$$\begin{aligned}\tilde{P}(1,2) =& \mathrm{Re}\sum_{k\omega}(-i\omega + i\omega_*^i(1))\langle f_i(1)\rangle e^{i\mathbf{k}\cdot\mathbf{x}_-}\int dx_1' dx_2' G(x_1,x_1')\hat{\epsilon}^*(x_2)G^*(x_2,x_2')\\ &\times\left\langle \frac{\widetilde{\delta n}(x_1')}{n_0}\widetilde{\delta h}^*(x_2)\right\rangle_{k\omega} + (1\leftrightarrow 2)\\ \to& -2\sum_{k\omega}(\omega-\omega_*^i(E))\langle f_i(E)\rangle\\ &\times\int dx_1' dx_2' G(x,x_1')\mathrm{Im}\hat{\epsilon}(x)G^*(x,x_2')\left\langle \frac{\widetilde{\delta n}(x_1')}{n_0}\widetilde{\delta h}^*(x)\right\rangle_{k\omega} \end{aligned} \quad (4.26b)$$

As noted above, $\tilde{P}(1,2)$ is directly proportional to $\mathrm{Im}\epsilon$. As $\mathrm{Im}\epsilon = \mathrm{Im}\epsilon_i + \mathrm{Im}\epsilon_e + \mathrm{Im}\epsilon_{pol}$, $\tilde{P}(1,2)$ consists of pieces from ions, electrons, and polarization charges. We calculate each piece in the following(Fig.4.6).

We start by calculating ion induced incoherent production. This term is related to drag on phase space density exerted by ions - i.e. granulations emit waves via Cerenkov emission, while waves are in turn absorbed by ions, $\propto \mathrm{Im}\epsilon_i$. This leads to a drag on ion phase space density granulations, and incoherent production. Using the expression for $\mathrm{Im}\epsilon_i$ and noting[33]

$$\left\langle \frac{\widetilde{\delta n}(1)}{n_0}\widetilde{\delta h}^*(2)\right\rangle_{k\omega} = \left\langle \frac{\widetilde{\delta n}(1)}{n_0}\widetilde{\delta h}^*(2)\right\rangle_{k} 2\pi\delta(\omega - \bar{\omega}_D\bar{E}_2 - k_\theta\langle v_E\rangle' x_2) \quad (4.27a)$$

gives

$$\tilde{P}_i = -2\sum_{k\omega}(\omega-\omega_*^i(E))^2\langle f_i(E)\rangle\sqrt{2\epsilon_0}\frac{2}{\sqrt{\pi}}\sqrt{\bar{E}_{res}}\frac{\pi}{|\omega_D|}$$
$$\times e^{-\bar{E}_{res}}2\pi\delta(\omega-\bar{\omega}_D\bar{E}-k_\theta\langle v_E\rangle' x)$$
$$\times\int dx_1' dx_2' G(x,x_1')G^*(x,x_2')\left\langle\frac{\widetilde{\delta n}(x_1')}{n_0}\widetilde{\delta h}^*(x)\right\rangle_k \tag{4.27b}$$

In the local limit we have:

$$\tilde{P}_i = -2\sum_{k\omega}(\omega-\omega_*^i(E))^2\langle f_i(E)\rangle\sqrt{2\epsilon_0}\frac{2}{\sqrt{\pi}}\sqrt{\bar{E}_{res}}\frac{\pi}{|\omega_D|}$$
$$\times e^{-\bar{E}_{res}}2\pi\delta(\omega-\bar{\omega}_D\bar{E})\frac{1}{|\epsilon(k,\omega)|^2}\left\langle\frac{\widetilde{\delta n}}{n_0}\widetilde{\delta h}^*\right\rangle_k \tag{4.27c}$$

The incoherent production by ions Eq.(4.27b) and the coherent production Eq.(4.24) adds to give an effective coherent production $P_{i,i}\equiv P^c+\tilde{P}_i$:

$$P_{i,i} = 2\sum_{k\omega}(\omega-\omega_*^i(E))^2\langle f_i(E)\rangle^2\mathrm{Re}g_{k\omega}S_{k\omega} \tag{4.28}$$

where

$$S_{k\omega}\equiv\sqrt{2\epsilon_0}\frac{2}{\sqrt{\pi}}\frac{2\pi}{|\bar{\omega}_D|}\left(\frac{2\pi T_i}{m_i}\right)^{3/2}\int dx_1' dx_2' G(x,x_1')G^*(x,x_2')$$
$$\times\left\{\sqrt{\bar{E}_{res}(x_2')}\left\langle\frac{\widetilde{\delta n}(x_1')}{n_0}\widetilde{\delta h}^*(x_2',\bar{E}_{res}(x_2'))\right\rangle_k\right.$$
$$\left.-\sqrt{\bar{E}_{res}(x)}\left\langle\frac{\widetilde{\delta n}(x_1')}{n_0}\widetilde{\delta h}^*(x)\right\rangle_k\right\} \tag{4.29}$$

Here $S_{k\omega}$ is the effective fluctuation spectrum, shifted by the incoherent production contribution, as can be seen in the subtraction in the curly bracket. In the absence of the incoherent production contribution, $S_{k\omega}\to\langle(q\tilde{\phi}/T_i)^2\rangle_{k\omega}$. The net production Eq.(4.28) takes the form of coherent production - the incoherent contribution is rescaled into the coherent part. This may be viewed as a renormalization of

coherent production due to self-feedback from *ion* incoherent production(Fig.4.7) - i.e. 'bare' coherent production P^c produces $\widetilde{\delta h}^2$ which acts back through the incoherent ion production term $\tilde{P}_i$. Physically speaking, we may understand this as a self-field due to phase space density; while a test ion phase space density is scattered by $\tilde{v}_{E\times B}$, it also produces a self-field $\tilde{\phi}_{self} \sim \epsilon^{-1}(k,\omega)\int d^3v\widetilde{\delta h}_{test}$. The self-field, in turn, is coupled to other ions, which leads to absorption $\propto \mathrm{Im}\epsilon_i$. Through the coupling, the test ion phase space density feels the effect of the other ions as dynamical friction due to Cerenkov emission, thus leading to the renormalization of the $\tilde{v}_{E\times B}$ scattering of test phase space density. This can be expressed as a net 'renormalized' production $P_{i,i} \sim 2\bar{D}\langle f\rangle'^2$ where

$$\bar{D} \equiv \sum_{k\omega} v_{thi}^2 \mathrm{Re} g_{k\omega} k_\theta^2 \rho_i^2 S_{k\omega} \tag{4.30}$$

is a 'renormalized' diffusion coefficient. Of course, if we turn off the self-feedback from the incoherent production, $\bar{D}$ reduces to a 'bare' diffusion coefficient $\bar{D} \to \sum_{k\omega} v_{thi}^2 \mathrm{Re} g_{k\omega} k_\theta^2 \rho_i^2 \left\langle (q\tilde{\phi}/T_i)^2 \right\rangle_{k\omega}$.

Note that we do *not* have the cancelation between the coherent and incoherent parts as found in analyses with effectively 1D resonance dynamics[33], $\delta(\omega - \bar{\omega}_D \bar{E})$. Here, the resonance function is $\delta(\omega - \bar{\omega}_D\bar{E} - k_\theta\langle v_E\rangle' x)$ and thus 2D with (E,x). In 2D, E and x can change their value while $\bar{\omega}_D\bar{E} + k_\theta\langle v_E\rangle' x$ unchanged, as in a $(E,x) \to (E',x')$ scattering event. In contrast, in 1D, $\bar{E}$ cannot change its value while $\bar{\omega}_D\bar{E}$ is unchanged. This leaves initial state = final state, so relaxation is impossible and thus the like-species production must vanish. Indeed, by turning off zonal flow in the resonance dynamics in Eq.(4.28), we can recover the 1D result:

$$\begin{aligned} P^c + \tilde{P}_i &\propto \delta(\omega - \bar{\omega}_D\bar{E} - k_\theta\langle v_E\rangle' x) S_{k\omega} \\ &\to \delta(\bar{E}_{res} - \bar{E}) \left\{ e^{-\bar{E}} \left\langle \frac{\widetilde{\delta n}}{n_0} \widetilde{\delta h}^*(\bar{E}_{res}) \right\rangle_k - e^{-\bar{E}_{res}} \left\langle \frac{\widetilde{\delta n}}{n_0} \widetilde{\delta h}^*(E) \right\rangle_k \right\} \to 0 \end{aligned} \tag{4.31}$$

Thus the cancellation is a special case and an artifact of the 1D resonance dynamics.

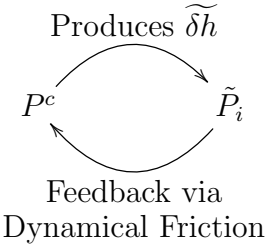

Figure 4.7: Renormalization of coherent production

Now we consider the calculation of other components in the incoherent production term(Fig.4.6). The incoherent production due to electrons arises from the coupling of ion phase space density to electrons via $\mathrm{Im}\epsilon_e$ (i.e. drag). Here, ion phase space granulation emits waves via Cerenkov emission, while waves are, in turn, collisionally dissipated by electrons, $\mathrm{Im}\epsilon_e \propto \nu_e^{-1}$. This leads to drag on phase space density and incoherent production by electrons:

$$\tilde{P}_e = -2\sum_{k\omega}(\omega - \omega_*^i(E))\langle f_i(E)\rangle \mathrm{Im}\epsilon_e$$
$$\times \int dx_1' dx_2' G(x,x_1')G^*(x,x_2')\left\langle \frac{\widetilde{\delta n}(x_1')}{n_0}\widetilde{\delta h}^*(x)\right\rangle_{k\omega} \tag{4.32a}$$

This term reduces to the result which was derived earlier[33] by going to the local limit $G(x-x') = \epsilon^{-1}(k,\omega)\delta(x-x')$, relating the k,ω spectrum to the k spectrum via the orbit propagator, and utilizing the frequency ordering $\omega_*^i > \omega$:

$$\tilde{P}_e = 4\pi\sum_k \omega_*^i\left(\frac{\eta_i}{\eta_{i,cr}(\bar{E})} - 1\right)\langle f_i(E)\rangle \frac{\mathrm{Im}\epsilon_e}{|\epsilon(k,\bar{\omega}_D\bar{E})|^2}\left\langle \frac{\widetilde{\delta n}}{n_0}\widetilde{\delta h}^*\right\rangle_k \tag{4.32b}$$

where $\eta_{i,cr} \equiv (3/2 - \bar{E})^{-1}$ is an energy dependent threshold for the onset of the ion transport driven by granulations. This term was utilized to calculate anomalous transport of ion heat and particles[33].

Incoherent production also arises from polarization charge. While moving through phase space, an ion granulation leaves a wake with a spatial extent (Fig.4.2). The resulting spatial envelope of the fluctuation spectrum necessarily is coupled to the polarization charge via $\mathrm{Im}\epsilon_{pol} \propto \partial_r$. This leads to a wake drag on

the phase space macro-particle and thus incoherent production by the polarization charge coupling:

$$\tilde{P}_{pol} = -2\sum_{k\omega}(\omega - \omega_*^i(E))\langle f_i(E)\rangle \int dx_1' dx_2' G(x, x_1') \times (-2\rho_i^2 k_r \partial_r) G^*(x, x_2') \left\langle \frac{\widetilde{\delta n}(x_1')}{n_0} \widetilde{\delta h}^*(x) \right\rangle_{k\omega} \tag{4.33a}$$

Noting that polarization charges correspond to fluid vorticity and introduces zonal flow coupling in the *single* structure growth, we expect that $\tilde{P}_{pol}$ induces zonal flow coupling in the *multi*-structure case. To see the connection to zonal flow, we go to the local limit

$$\tilde{P}_{pol} \simeq -2\sum_{k\omega}(\omega - \omega_*^i(E))\langle f_i(E)\rangle(-2\rho_i^2 k_r)\frac{1}{|\epsilon(k,\omega)|^2}\left\langle \frac{\widetilde{\delta n}}{n_0}\partial_r \widetilde{\delta h}^* \right\rangle_{k\omega} \tag{4.33b}$$

Since it contains $k_\theta k_r$ weighed by spectrum via $\omega_*^i \simeq k_\theta v_*^i$, Eq.(4.33b) resembles the Reynolds stress. To show the Reynolds stress connection explicitly, and for the sake of simplicity, we take $\omega - \omega_*^i(E) \simeq -k_\theta v_*^i$, divide $\tilde{P}_{pol}$ by $\langle f\rangle$, and integrate $\tilde{P}_{pol}$ over velocity space, which yields

$$\begin{aligned}\int d^3v \frac{\tilde{P}_{pol}}{2\langle f_i\rangle} &\simeq -\sum_{k\omega}\frac{v_*^i k_\theta \rho_i^2 k_r}{|\epsilon(k,\omega)|^2}\partial_r \left\langle \frac{\widetilde{\delta n}}{n_0}\int d^3v \widetilde{\delta h}^* \right\rangle_{k\omega} \\ &= -\sum_{k\omega} v_*^i k_\theta \rho_i^2 k_r \partial_r \left\langle \frac{\tilde{q\phi}}{T_i}\frac{\tilde{q\phi}^*}{T_i} \right\rangle_{k\omega} = \frac{v_*^i}{v_{thi}^2}\partial_r \langle \tilde{v}_r \tilde{v}_\theta\rangle \end{aligned} \tag{4.33c}$$

Hence, we see that the incoherent production via polarization charge induces zonal flow coupling to the granulation dynamics, and clearly links production to the Reynolds force.

Relative magnitude of $\tilde{P}_{pol}$, for example to $\tilde{P}_e$ (the latter leads to anomalous ion heat and particle transport[33]), can be evaluated as

$$\frac{\tilde{P}_{pol}}{\tilde{P}_e} \sim \frac{\overline{k_r k_\theta}}{\overline{k_\theta^2}}\frac{\eta_e}{1+3\eta_e/2}\frac{\nu_e}{\epsilon_0^{3/2}\omega_{c,i}}\frac{L_{T_e}}{L_{env}} \tag{4.34}$$

Here the bar denotes spectral average, i.e. $\overline{(...)} \equiv \sum_{k\omega}(...)\langle\tilde{\phi}^2\rangle_{k\omega}/\sum_{k\omega}\langle\tilde{\phi}^2\rangle_{k\omega}$, L_{env} is the scale length of envelope variation. Setting $L_{env} \sim \sqrt{\rho_i L_{T_e}}$, typical of mesoscales, we have

$$\frac{\tilde{P}_{pol}}{\tilde{P}_e} \sim \frac{\overline{k_r k_\theta}}{\overline{k_\theta^2}} \frac{\eta_e}{1+3\eta_e/2} \frac{\nu_e/\epsilon_0}{v_{thi}/L_{T_e}} \frac{1}{\epsilon_0^{1/2}} \sqrt{\frac{\rho_i}{L_{T_e}}} \tag{4.35}$$

Here typically $\overline{k_r k_\theta}/\overline{k_\theta^2} \sim \eta_e/(1+3\eta_e/2) \sim O(1)$. While $\sqrt{(\rho_i/L_{T_e})}$ is small, it is multiplied by $\epsilon_0^{-1/2} > 1$ and $(\nu_e/\epsilon_0)/(v_{thi}/L_{T_e}) > 1$ (by the frequency ordering for electron collisions). Then we can see that $\tilde{P}_{pol}/\tilde{P}_e$ can easily be order unity and thus $\tilde{P}_{pol}$ should be included in the analysis. This is especially true around a ion barrier region where the gradients are steep.

In summary, we obtained the evolution equation for phasetrophy as

$$\left(\frac{\partial}{\partial t} + \tau_L^{-1}\right) \lim_{1\to 2} \langle \delta h(1) \delta h(2) \rangle = \lim_{1\to 2} P(1,2) \tag{4.36}$$

where τ_L^{-1} is

$$\tau_L^{-1} \lim_{1\to 2} \langle \delta h(1) \delta h(2) \rangle = \lim_{1\to 2} \left(v_{rel} \frac{\partial}{\partial y_-} \langle \delta h(1) \delta h(2) \rangle + T(1,2) + C(1,2) \right) \tag{4.37}$$

where $v_{rel} = \bar{v}_D \bar{E}_- + \langle v_E \rangle' x_-$, $T(1,2)$ is the triplet term defined by Eq.(4.13b) and $C(1,2)$ is the collision term defined by Eq.(4.13c). The key difference between τ_L^{-1} and $P(1,2)$ is their small scale behavior. As $1 \to 2$, τ_L^{-1} approaches to a small value which is determined by collisions, $\tau_L^{-1} \to 2\nu_{eff}\langle \delta h^2 \rangle$ where a Krook operator $C(1,2) = \nu_{eff}\langle \delta h(1) \delta h(2) \rangle$ is used for the purposes of estimation. As $1 \to 2$,

$P(1,2)$ remains finite and the total production is

$$\lim_{1\to 2} P(1,2) \equiv P_{i,i} + P_{i,e} + P_{i,pol} \tag{4.38a}$$

$$P_{i,i} = 2\sum_{k\omega}(\omega - \omega_*^i(E))^2\langle f_i\rangle^2 \mathrm{Re} g_{k\omega} S_{k\omega} \tag{4.38b}$$

$$P_{i,e} = -2\sum_{k\omega}(\omega - \omega_*^i(E))\langle f_i\rangle \frac{\mathrm{Im}\epsilon_e}{|\epsilon(k,\omega)|^2}\left\langle \widetilde{\frac{\delta n}{n_0}}\widetilde{\delta h}^*\right\rangle_{k\omega} \tag{4.38c}$$

$$P_{i,pol} = -2\sum_{k\omega}\langle f_i\rangle \frac{2v_*^i\rho_i^2 k_r k_\theta}{|\epsilon(k,\omega)|^2}\left\langle \widetilde{\frac{\delta n}{n_0}}\partial_r\widetilde{\delta h}^*\right\rangle_{k\omega} \tag{4.38d}$$

where $S_{k\omega}$ is the spectrum defined by Eq.(4.29). $P_{i,i}$ is renormalized coherent production. $P_{i,e}$ is due to the coupling of the ion wake to electron dissipation. $P_{i,pol}$ is from the coupling of the ion wake to polarization charge. This term introduces a novel zonal flow effect into granulation dynamics. This new effect is different from the conventional zonal flow effects such as shearing suppression of turbulence or cross-phase modification[106]. Indeed, this effect is akin to a reduction of the production term by scattering of momentum (and energy) to the zonal flow.

4.3.3 Phase space density granulation and zonal flows: Connection to the momentum theorem in quasigeostrophic system and its consequences

The phasetrophy evolution derived in the above can be put in a form where zonal flow coupling is more apparent. In doing so, we divide phasetrophy evolution by $\langle f\rangle$ and integrate over velocity space to obtain

$$\left(\frac{\partial}{\partial t} + \tau_L^{-1}\right)\int d^3v \frac{\langle \delta h^2\rangle}{2\langle f\rangle} = \int d^3v \frac{P_{i,i} + P_{i,e} + P_{i,pol}}{2\langle f\rangle} \tag{4.39}$$

where $\langle \delta h^2\rangle \equiv \lim_{1\to 2}\langle \delta h(1)\delta h(2)\rangle$. $P_{i,pol}$ term introduces zonal flow coupling as discussed above. Utilizing the expression for $P_{i,pol}$ gives

$$\frac{\partial}{\partial t}\int d^3v \frac{\langle \delta h^2\rangle}{2\langle f\rangle} = \int d^3v \frac{P_{i,i} + P_{i,e}}{2\langle f\rangle} + \frac{v_*^i}{v_{thi}^2}\partial_r\langle \tilde{v}_r\tilde{v}_\theta\rangle - \tau_L^{-1}\int d^3v \frac{\langle \delta h^2\rangle}{2\langle f\rangle} \tag{4.40}$$

Thus, as in the single structure limit, phase space density granulation evolution is also dynamically coupled to zonal flows.

Eq.(4.40) has the same structure as the fundamental momentum constraint in QG system, namely the C-D momentum theorem. For comparison, below we re-write the C-D theorem for the Hasegawa-Wakatani system in a similar form:

$$\frac{\partial}{\partial t}\frac{\langle \delta q^2\rangle}{2\langle q\rangle'} = -\langle \tilde{v}_r \tilde{n}_e\rangle + \partial_r \langle \tilde{v}_r \tilde{v}_\theta\rangle - \frac{1}{\langle q\rangle'}\left(\frac{\partial}{\partial r}\left\langle \tilde{v}_r \frac{\delta q^2}{2}\right\rangle + D_0\langle(\nabla \delta q)^2\rangle\right) \tag{4.41}$$

$$\frac{\partial}{\partial t}\int d^3v \frac{\langle \delta h^2\rangle}{2\langle f\rangle} = \int d^3v \frac{P_{i,i}+P_{i,e}}{2\langle f\rangle} + \frac{v_*^i}{v_{thi}^2}\partial_r\langle \tilde{v}_r\tilde{v}_\theta\rangle - \tau_L^{-1}\int d^3v \frac{\langle \delta h^2\rangle}{2\langle f\rangle} \tag{4.42}$$

Each term in Eq.(4.41) has a clear counterpart in Eq.(4.42). The phasetrophy $\langle \delta h^2\rangle$ is the counterpart of potential enstrophy $\langle \delta q^2\rangle$. $P_{i,i}$ and $P_{i,e}$ represent the effect of relaxation, thus leading to flux of both particles and heat. This clearly corresponds to the particle flux in the momentum theorem for the Hasegawa-Wakatani system. The lifetime of phasetrophy τ_L is analogous to the lifetime of enstrophy via turbulence spreading[107] and viscous dissipation of $\langle \delta q^2\rangle$.

As a consequence, a similar statement as the non-acceleration theorem[74] by Charney and Drazin follows; in the absence of production and dissipation of phase space density granulation, stationary granulation cannot accelerate flow against frictional drag. This in turn implies that if we have any production or dissipation of phase space density granulation, we must have a corresponding adjustment of the flow, and vice versa.

The coupled system of phase space density granulation and zonal flow shows a self-regulating behavior, as Eq.(4.40) and the momentum balance equation for zonal flow form a type of predator-prey system:

$$\frac{\partial}{\partial t}\int d^3v \frac{\langle \delta h^2\rangle}{2\langle f\rangle} = \int d^3v \frac{P_{i,i}+P_{i,e}}{2\langle f\rangle} + \frac{v_*^i}{v_{thi}^2}\partial_r\langle \tilde{v}_r\tilde{v}_\theta\rangle - \tau_L^{-1}\int d^3v \frac{\langle \delta h^2\rangle}{2\langle f\rangle} \tag{4.43a}$$

$$\frac{\partial}{\partial t}\langle v_\theta\rangle = -\partial_r\langle \tilde{v}_r\tilde{v}_\theta\rangle - \nu\langle v_\theta\rangle \tag{4.43b}$$

which clearly has the same structure as the familiar predator-prey model[17, 55]:

$$\partial_t \varepsilon = \gamma_L \varepsilon - \alpha V'^2 \varepsilon - \Delta\omega(\varepsilon)\varepsilon \tag{4.44a}$$

$$\partial_t V'^2 = \alpha V'^2 \varepsilon - \nu_{col} V'^2 \tag{4.44b}$$

where ε is the turbulence intensity, V'^2 is flow shear, γ_L is linear growth rate of a mode, α represents a coupling between flow and fluctuations, $\Delta\omega$ is a decorrelation rate, ν_{col} is the collisional drag on the flow. Then, by comparison, Eq.(4.43a) can be viewed as the equation for prey, which here is the phasetrophy. The prey are produced by mean field relaxation due to $P_{i,i}$ and $P_{i,e}$. Death of prey occurs due to the granulation dispersion τ_L^{-1} and due to coupling to the predator, namely the zonal flow $\partial_r \langle \tilde{v}_r \tilde{v}_\theta \rangle$. Eq.(4.43b) is the equation for the predator. The predator is pumped by consuming the prey, such as phase space density granulations which drive the Reynolds stress. *The predator-prey system here may be compared to the kinetic predator-prey system derived based on entropy balance[36]. Ultimately, the both systems are derived from the dynamics of the same quantity, namely phase space density correlation δf^2, which is the fundamental quantity.*

The coupled system of granulations and zonal flows can lead to non-trivial, finite intensity state with zonal flow coupling, namely the zero production state. In a weakly collisional system, zonal flows allow a stationary state with zero total production:

$$0 \cong \int d^3v \frac{P_{i,i} + P_{i,e}}{2\langle f \rangle} + \frac{v_*^i}{v_{thi}^2} \partial_r \langle \tilde{v}_r \tilde{v}_\theta \rangle \tag{4.45}$$

The zero production state is of practical interest, since mean field evolution is also vanishes, $\partial_t \langle f \rangle \sim P_{tot} \simeq 0$. Access to the zero production state requires the balance of the relaxation drive $P_{i,i} + P_{i,e}$ with the zonal flow drive $P_{i,pol} \sim \partial_r \langle \tilde{v}_r \tilde{v}_\theta \rangle$. In turn, in the zero net production state a stationary zonal flow can be sustained against collisional drag:

$$\begin{aligned} \langle v_\theta \rangle &= \frac{1}{\nu} \frac{v_{thi}^2}{v_*^i} \int d^3v \frac{P_{i,i} + P_{i,e}}{2\langle f \rangle} \\ &\simeq -\frac{\omega_{c,i}}{\nu} \frac{\langle \tilde{v}_r \tilde{n}_e \rangle}{n_0} + \frac{1}{\nu} \frac{v_{thi}^2}{v_*^i} \int d^3v \frac{P_{i,i}}{2\langle f \rangle} \end{aligned} \tag{4.46}$$

where we used

$$\int d^3v \frac{P_{i,e}}{2\langle f\rangle} \simeq \int d^3v \sum_{k\omega} k_\theta v_*^i \frac{\mathrm{Im}\epsilon_e}{|\epsilon(k,\omega)|^2} \left\langle \frac{\widetilde{\delta n}}{n_0} \widetilde{\delta h}^* \right\rangle_{k\omega}$$
$$= -\frac{v_*^i}{v_{thi}} \frac{1}{\rho_i} \frac{\langle \tilde{v}_r \tilde{n}_e \rangle}{n_0} \tag{4.47}$$

Eq.(4.46) can be compared to the stationary zonal flows in the Hasegawa-Wakatani system and GK system in the single structure limit. The close correspondence is evident. In each system, electron flux can support stationary zonal flow against collisional drag.

4.3.4 Transport

Since $2P = \partial_t \langle \delta f^2 \rangle \simeq -\partial_t \langle f \rangle^2$, the production term is related to the mean field evolution and transport. The transport flux can be extracted from the phasetrophy production term, $\lim_{1\to 2} P(1,2) \sim -\langle \tilde{v}_r \delta f \rangle \langle f \rangle'$, as:

$$J(r) \equiv \langle \tilde{v}_r \delta f \rangle = J_{i,i} + J_{i,e} + J_{i,pol} \tag{4.48a}$$
$$J_{i,i} = \sum_{k\omega} (\omega - \omega_*^i(E)) \langle f_i(E) \rangle k_\theta \rho_i v_{thi} \mathrm{Re} g_{k\omega} S_{k\omega} \tag{4.48b}$$
$$J_{i,e} = -\sum_{k\omega} k_\theta \rho_i v_{thi} \frac{\mathrm{Im}\epsilon_e}{|\epsilon(k,\omega)|^2} \left\langle \frac{\widetilde{\delta n}}{n_0} \widetilde{\delta h}^* \right\rangle_{k\omega} \tag{4.48c}$$
$$J_{i,pol} = -\sum_{k\omega} k_\theta \rho_i v_{thi} \frac{(-2\rho_i^2 k_r)}{|\epsilon(k,\omega)|^2} \left\langle \frac{\widetilde{\delta n}}{n_0} \partial_r \widetilde{\delta h}^* \right\rangle_{k\omega} \tag{4.48d}$$

where $S_{k\omega}$ is the spectrum defined by Eq.(4.29). $J_{i,i}$ is the flux which arises from the net ion production $P_{i,i}$. $J_{i,i}$ is the diffusive part of the total flux, as $J_{i,i} \simeq -\bar{D}\langle f_i \rangle'$ for $\omega < \omega_*$. Here $\bar{D} = \sum_{k\omega} v_{thi}^2 \mathrm{Re} g_{k\omega} k_\theta^2 \rho_i^2 S_{k\omega}$ is the renormalized diffusivity. $J_{i,i}$ simplifies in certain limits. If we neglect the effect of incoherent fluctuations and retain the spectrum only due to eigenmodes, $J_{i,i}$ reduces to the quasilinear flux:

$$J_{i,i} \simeq -\sum_k \rho_s^2 k_\theta^2 c_s^2 \mathrm{Re} g_k \left| \frac{q\tilde{\phi}}{T_e} \right|_k^2 \langle f \rangle' \tag{4.49}$$

If we go to the local limit, we have $J_{i,i} \to 0$ corresponding to $P_{i,i} \to 0$. The net $J_{i,i} \propto \bar{D} \propto P_{i,i}$ arises from the non-cancelation between the coherent and the ion incoherent productions.

$J_{i,e}$ is the dynamical friction which originates from the ion wake drag on the electrons. Here dissipative non-adiabatic electrons are assumed, $\mathrm{Im}\epsilon_e \propto \nu_e^{-1}$. $J_{i,e}$ is utilized to explain the anomalous transport of ion heat and particles due to ion clumps[33].

$J_{i,pol}$ is the novel piece here, which originates from polarization charge and describes zonal flow coupling. $J_{i,pol}$ may be understood as a zonal flow induced collisionless friction[37] exerted on the ion phase space density. Note that $J_{i,pol}$ algebraically competes against other fluxes. The competition can lead to a saturated state with the zero total flux $J(r) = \langle \tilde{v}_r \delta f \rangle = J_{i,i} + J_{i,e} + J_{i,pol} \simeq 0$, which corresponds to the zero net production state discussed above. Here, transport suppression is achieved by the competition between relaxation and Reynolds work, i.e. Eq.(4.45). This is different from the conventional view of transport suppression by zonal flow shearing. Moreover, retaining dynamical friction is *essential* to the recovery of this effect.

4.4 Conclusions

In this paper, we present a theory for relaxation and transport in collisionless GK turbulence with zonal flow. This theory treats the effects of both phase space structures and zonal flows. The principal results of the paper are:

1. In the strongly resonant limit for $K \gg 1$, the growth of even a single localized structure in phase space is seen to be strongly coupled to zonal flows. $-\int \sqrt{E} dE \langle \delta f^2 \rangle / \langle f \rangle|_0$ is identified as the zonal pseudomomentum carried by the phase space structure. The net invariance of total dipole moment was used to reveal the zonal flow coupling in the structure growth equation. The foundation of this is the conservation of zonal momentum between phase space fluid and zonal flow. The resultant expression, Eq.(4.8), is shown to be closely related and very similar to the Charney-Drazin theorem for the

Hasegawa-Wakatani system, a fundamental momentum constraint in quasi-geostrophic systems.

2. For $K \sim 1$, a statistical theory of granulation evolution and mean field ($\langle f \rangle$) evolution was formulated in the presence of zonal flows. In particular:

   (a) Zonal flow coupling in the granulation dynamics is introduced by the production due to polarization charge mixing. The production due to polarization charge arises due to envelope coupling, which can be introduced by the spatial variation intrinsic to the wake emitted by granulation. Other processes, such as mode propagation and absorption etc, can contribute to the envelope structure. The production due to the polarization charge, necessarily coupled via the GK Poisson equation, is explicitly related to Reynolds force, Eq.(4.33c).

   (b) The coupled system of granulations and zonal flow form a type of self-regulating, kinetic predator-prey system, Eq.(4.43a) and (4.43b). The coupling allows the system to achieve an finite amplitude state of vanishing production, by balancing granulation induced production due to ∇T relaxation with the Reynolds work which produces the zonal flow.

   (c) The mean field evolution is calculated and various contributions to the transport fluxes are given, including the diffusive flux as well as dynamical friction. Dynamical friction arises from the zonal flow, Eq.(4.48d). The dynamical friction competes against other fluxes algebraically. This is similar to the effect of zonal flow in the predator-prey system and is different from the conventionally invoked zonal flow effects on transport, namely cross phase modification and simple amplitude suppression.

Throughout the paper, the quantity which plays the central role is the phase space density correlation $\langle \delta f(1) \delta f(2) \rangle$. $\langle \delta f(1) \delta f(2) \rangle$ is the fundamental correlation, as we can easily translate or relate $\langle \delta f(1) \delta f(2) \rangle$ to other physical quantities, including the pseudomomentum of phase space turbulence, the fluctuation entropy, and the fluctuation phasetrophy $\langle \delta f^2 \rangle$ which is similar to potential enstrophy, Fig.4.8.

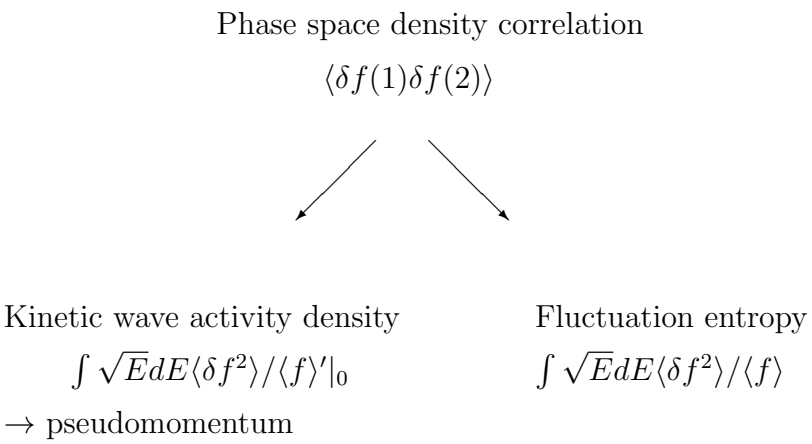

Figure 4.8: Relation of 'phasetrophy' $\langle \delta f(1) \delta f(2) \rangle$ to other relevant physical quantities

As $\langle \delta f^2 \rangle$ is closely related to different quantities, its time evolution can also be interpreted in several ways. The evolution of $\langle \delta f^2 \rangle$ can be related to the momentum conservation constraint for phase space turbulence, which is similar to the Charney-Drazin momentum theorem for QG turbulence. Alternatively, the evolution of $\langle \delta f^2 \rangle$ can be related to the entropy balance equation with production from relaxation drive, destruction from Reynolds work, and $\langle \delta f^2 \rangle$ coupling to small scale dissipation. See Table.4.3. In either case, GK turbulence and zonal flows are coupled via dynamical friction due to polarization charge and so form a self-regulating system.

The coupled system derived in this paper for describing GK turbulence and zonal flow conserves energy and zonal momentum. The momentum conservation is via dynamical friction due to zonal flow and sets a fundamental constraint on the modeling of GK turbulence and zonal flow generation. Thus, any GK model which includes zonal flow generation *must* also include dynamical friction, otherwise momentum and energy are not conserved between fluctuation and flows. Then, for example, we see that the usual quasilinear description of GK turbulence production and transport is not compatible with a proper description of zonal flow generation.

A similar behavior to the predator-prey type system described here is observed in the recent computational work[108] on the entropy transfer between

ITG/ETG and zonal flow. The *non-local* transfer of entropy between drift wave and zonal flow described in the work can be then understood as a simple variant of the well known zonal flow shearing feedback in the predator-prey system. Indeed, it has *long* been known that large scale shears produces non-local potential enstrophy transfer to small scales in QG systems[78]. Then, it is no surprise that large scale shear produces non-local entropy (closely related to phasetrophy, akin to potential enstrophy) transfer to small scales in GK systems.

In the related vein, nonlocality in *physical space* or *transport* is an important unresolved issue. The most clear physical process which underpins nonlocality is avalanching, process akin to coupled topplings of neighboring cites in a sandpile, which has also been observed in GK simulations. This paper does not treat avalanching. We note, however, that the response to phase space density granulations is intrinsically non-local, i.e. Eq.(4.22), and so can serve as a seed in granulation formation.

This paper sets forth the basic theory of relaxation in a system with granulations which also couple to zonal flows. The next step in this program is to solve the coupled phase space density correlation and zonal flow equations, i.e. Eqs (4.36) and (4.43b). This forthcoming work will examine possible wave and/or granulation driven relaxation processes, and the zonal flow effects on each of these. Special attention is focused on subcritical processes.

Finally, we point out that the paradigm considered here, namely relaxation and transport in the presence of phase space structures and zonal flows, is not only applicable to collisionless ITG turbulence but is also of interest in the context of energetic particle mode (EPM). Indeed, formation of structures in EPM is likely[69]. A key physical point here is that EPM excitation is due to precession resonance, which is rather coherent[109]. As a consequence, the mode localizes there the drive is strongest. Thus, a description in terms of screened macro-particles seems quite natural. Also, zonal flow generation in energetic particle induced Alfven turbulence has also been reported[110]. Thus, the framework presented here should be applicable to a self-consistent description of transport in EPM turbulence as well. This will be pursued in the near future.

4.A Appendix: derivation of plasma dielectric

Here we derive the plasma dielectric for the trapped ion mode model used in Section III. The derivation is standard; we linearize the kinetic equation and require a quasi-neutrality. The frequency ordering of interest here is

$$\omega_{ti},\ \omega_{bi} > \omega_*^i > \omega \sim \omega_{Di} > \nu_{eff}^i,$$
$$\omega_{te},\ \omega_{be} > \nu_{eff}^e > \omega_*^e > \omega.$$

where ω_t is the transit frequency, ω_b is the bounce frequency, ω_* is the diamagnetic frequency, ω_D is a frequency due to magnetic drift, $\nu_{eff} = \nu_c/\epsilon_0$ is effective collision frequency and ϵ_0 is the inverse aspect ratio. In the above frequency ordering, the linear calculation yields density perturbation as

$$\left(\frac{\delta n_i}{n_0}\right)_{k\omega} = -\frac{q\tilde{\phi}_{k\omega}}{T_i} + \int d^3v \frac{\omega - \omega_*^i(E)}{\omega - \bar{\omega}_D\bar{E} + k_\theta\langle v_E\rangle(r)}\frac{q\tilde{\phi}_{k\omega}}{T_i}\langle f_i\rangle + \left(\frac{\widetilde{\delta n_i}}{n_0}\right)_{k\omega} \tag{4.50}$$

$$\left(\frac{\delta n_e}{n_0}\right)_{k\omega} = \frac{q\tilde{\phi}_{k\omega}}{T_e} + i\int d^3v \frac{\omega - \omega_*^e(E)}{\nu_e/\epsilon_0}\bar{E}^{3/2}\frac{q\tilde{\phi}_{k\omega}}{T_e}\langle f_e\rangle \tag{4.51}$$

where $\omega_*^\sigma(E) \equiv (k_\theta c T_\sigma \langle f_\sigma(E)\rangle')/(q_\sigma B\langle f_\sigma(E)\rangle) = k_\theta v_*^\sigma(1 + \eta_\sigma(\bar{E} - 3/2))$, $v_*^i \equiv -(\rho_i/|L_n|)v_{thi}$, and $v_*^e = (\rho_s/|L_n|)c_s$. The ion density perturbation consists of two parts, as phase space density δh consists of two pieces, $\delta h = \delta h^c + \widetilde{\delta h}$. δh^c is a phase-coherent response to fluctuation potential, ϕ. This term, upon velocity integral, gives the ion density perturbation which is proportional to fluctuation potential. $\widetilde{\delta h}$ is an *in*coherent part which describes granulation effect. This leads to the last term in the ion density perturbation, $(\widetilde{\delta n_i}/n_0)_{k\omega} \equiv \int d^3v \widetilde{\delta h}_{k\omega}$. For electrons, the non-adiabatic response is retained from a phase shift due to collisions. On substituting the density perturbations into the Gyrokinetic Poisson equation, we have

$$\hat{\epsilon}(k,\omega)\frac{q\tilde{\phi}_{k\omega}}{T_i} = \left(\frac{\widetilde{\delta n_i}}{n_0}\right)_{k\omega} \tag{4.52}$$

where

$$\hat{\epsilon}(k,\omega) = \frac{T_i}{T_e} + \rho_i^2 k_\perp^2 + 1 - P\int d^3v \frac{\omega - \omega_*^i(E)}{\omega - \bar{\omega}_D\bar{E} - k_\theta\langle v_E\rangle(r)}\langle f_i\rangle + i\mathrm{Im}\epsilon_i + i\mathrm{Im}\epsilon_e + i\mathrm{Im}\epsilon_{pol} \tag{4.53}$$

P denotes the principle part of the integral. The imaginary part of the dielectric is defined as

$$\mathrm{Im}\epsilon_i \equiv \int d^3v(\omega - \omega_*^i(E))\pi\delta(\omega - \bar{\omega}_D\bar{E} - k_\theta\langle v_E\rangle(r))\langle f_i\rangle$$
$$= \sqrt{2\epsilon_0}\frac{2}{\sqrt{\pi}}\sqrt{\bar{E}_{res}}\pi\frac{\omega - \omega_*^i(\bar{E}_{res})}{|\bar{\omega}_D|}e^{-\bar{E}_{res}} \tag{4.54}$$

$$\mathrm{Im}\epsilon_e \equiv \int d^3v\frac{\omega - \omega_*^e(E)}{\nu_e/\epsilon_0}\bar{E}^{3/2}\frac{T_i}{T_e}\langle f_e\rangle$$
$$= \frac{4}{\sqrt{\pi}}\frac{\sqrt{2\epsilon_0}}{\nu_e/\epsilon_0}\frac{T_i}{T_e}(\omega - \omega_*^e(1 + \frac{3}{2}\eta_e)) \tag{4.55}$$

$$\mathrm{Im}\epsilon_{pol} \equiv -2\rho_i^2 k_r\partial_r \tag{4.56}$$

where $\bar{E}_{res} \equiv (\omega - k_\theta\langle v_E\rangle(x))/\bar{\omega}_D$.

The dispersion relation is obtained by setting $\mathrm{Re}\epsilon(k,\omega) = 0$:

$$\frac{T_i}{T_e} + \rho_i^2 k_\perp^2 + 1 - P\int d^3v\frac{\omega - \omega_*^i(E)}{\omega - \bar{\omega}_D\bar{E} - k_\theta\langle v_E\rangle(r)}\langle f_i\rangle = 0 \tag{4.57}$$

For $\omega > \bar{\omega}_D\bar{E}$, we have:

$$\frac{T_i}{T_e} + \rho_i^2 k_\perp^2 + 1 - \sqrt{2\epsilon_0}\left(1 - \frac{\omega_*^i}{\omega}\right) = 0 \tag{4.58}$$

and thus

$$\omega = \omega_k = -\frac{\sqrt{2\epsilon_0}\omega_*^i}{1 + \rho_i^2 k_\perp^2 + T_i/T_e - \sqrt{2\epsilon_0}} \tag{4.59}$$

4.B Appendix: derivation of zonal flow evolution equation

The mean vorticity evolution is obtained by taking time derivative of mean quasi-neutrality (Here $\langle ... \rangle$ is the zonal average):

$$\frac{\partial}{\partial t}\left(\left\langle \rho_s^2 \nabla_\perp^2 \frac{e\phi}{T_e} \right\rangle\right) = \frac{\partial}{\partial t}\left(\frac{\langle n_e \rangle}{n_0} - \frac{\langle n_i \rangle}{n_0}\right) \tag{4.60}$$

$$= \int d^3v (\partial_t \langle f_e \rangle - \partial_t \langle f_i \rangle) \tag{4.61}$$

The evolution of mean f_σ is

$$\partial_t \langle f_\sigma \rangle = -\partial_r \langle \tilde{v}_r \delta f_\sigma \rangle \tag{4.62}$$

Combining these, we obtain:

$$\frac{\partial}{\partial t}\left(\left\langle \rho_s^2 \partial_r^2 \frac{e\phi}{T_e} \right\rangle\right) = -\frac{\partial}{\partial r}\left\langle \tilde{v}_r \left(\frac{\delta n_e}{n_0} - \frac{\delta n_i}{n_0}\right) \right\rangle \tag{4.63}$$

Using quasi-neutrality, we have:

$$\frac{\partial}{\partial t}\left(\left\langle \rho_s^2 \partial_r^2 \frac{e\phi}{T_e} \right\rangle\right) = -\frac{\partial}{\partial r}\left\langle \tilde{v}_r \rho_s^2 \nabla_\perp^2 \frac{e\tilde{\phi}}{T_e} \right\rangle \tag{4.64}$$

The righthand side contains the flux of vorticity, which is Reynolds forcing via the identity[35, 71] $\langle \tilde{v}_r \phi \nabla_\perp^2 \tilde{\phi} \rangle = \partial_r \langle \tilde{v}_r \tilde{v}_\theta \rangle$. By integrating radially once, we obtain

$$\partial_t \langle v_\theta \rangle = -\partial_r \langle \tilde{v}_r \tilde{v}_\theta \rangle \tag{4.65}$$

As shown by F. L. Hinton and M.N. Rosenbluth[111], zonal flow is damped by collisions in the time scale $\tau \sim \epsilon_0 \tau_{ii}$ where $\tau_{ii} \sim 1/\nu_{ii}$. We model the effect by adding a collisional drag on the flow

$$\partial_t \langle v_\theta \rangle = -\partial_r \langle \tilde{v}_r \tilde{v}_\theta \rangle - \nu \langle v_\theta \rangle \tag{4.66}$$

where $\nu = \nu_{ii}/\epsilon_0$. We note that ν is different from the collisional damping of fluctuation used in the text, namely $C(\delta h_i) = -\nu_i \delta h_i$ and $C(\delta h_e) = -(\nu_e/\epsilon_0)\bar{E}^{-3/2}\delta h_e$.

We also note that here the collisional drag was added in an ad hoc manner in the zonal flow evolution Eq.(4.66). This effect may be recovered systematically by retaining a bounce averaged collision operator in Eq.(4.62). Explicitly, by retaining the collision term in Eq.(4.62), we see that the vorticity evolution equation (for zonal flow) becomes

$$\frac{\partial}{\partial t}\left(\left\langle \rho_s^2 \partial_r^2 \frac{e\phi}{T_e}\right\rangle\right) = -\frac{\partial}{\partial r}\left\langle \tilde{v}_r \rho_s^2 \nabla_\perp^2 \frac{e\tilde{\phi}}{T_e}\right\rangle + \int_{tr} d^3v \{\overline{C_e(\langle f_e\rangle)} - \overline{C_i(\langle f_i\rangle)}\} \qquad (4.67)$$

where $\overline{(...)}$ is the bounce average and the velocity integrals are limited to trapped electron and ions respectively. Following the argument by Hinton[111], we replace the ion collision integral by a collisional frictional damping $\nu = \nu_{ii}/\epsilon_0$ of the axisymmetric ($n = m = 0$) zonal potential,

$$\frac{\partial}{\partial t}\left(\left\langle \rho_s^2 \partial_r^2 \frac{e\phi}{T_e}\right\rangle\right) = -\frac{\partial}{\partial r}\left\langle \tilde{v}_r \rho_s^2 \nabla_\perp^2 \frac{e\tilde{\phi}}{T_e}\right\rangle - \nu\left\langle \rho_s^2 \partial_r^2 \frac{e\phi}{T_e}\right\rangle \qquad (4.68)$$

which leads to Eq.(4.66). Electron collisional effects are negligible, as that species is nearly Maxwellian for zonal modes.

Acknowledgement

Chapter 4 is a reprint of material appearing in Y. Kosuga and P. H. Diamond, Phys Plasmas, **18**, 122305 (2011). The dissertation author was the primary investigator and author of this article.

Table 4.3: Comparison of phase space density correlation evolution to other drift wave-zonal flow system

	Fluctuation intensity in Fluid DWT models, ε	Potential enstrophy in QG system, $\langle \delta q^2 \rangle$	Entropy $\int d^3v \langle \delta f^2 \rangle / \langle f \rangle$	Phase space density correlation $\langle \delta h(1) \delta h(2) \rangle$
Drive	Linear instability $\gamma_L \lvert\hat{\phi}\rvert^2$	Forcing, ...	Production by Heat transport $-\langle \tilde{v}_r \tilde{T}_i \rangle \langle T_i \rangle'$	Production by Relaxation $P_{i,i} + P_{i,e}$
Zonal flow coupling	Modulational Instability $-\alpha \lvert\hat{\phi}\rvert^2 V'^2$	Vorticity flux $\langle \tilde{v}_r \nabla^2 \phi \rangle = \partial_r \langle \tilde{v}_r \tilde{v}_\theta \rangle$	Entropy destruction by flow organization $-\langle \tilde{v}_r \tilde{v}_\theta \rangle \langle v_\theta \rangle' \to -\gamma_{ZF} \langle v_\theta \rangle'^2$	Dynamical Friction by polarization charge $P_{i,pol} \to v_* \partial_r \langle \tilde{v}_r \tilde{v}_\theta \rangle$
Coupled equation for turbulence and flow	Predator-prey system, ε & V'	Charney-Drazin or Predator-prey	Kinetic predator-prey $\int d^3v \langle \delta f^2 \rangle / \langle f \rangle$ & $\langle v_\theta \rangle$	Kinetic predator-prey or Kinetic Charney-Drazin

Chapter 5

Summary and discussion

In this thesis, phase space dynamics was studied and applied to understand problems in tokamak phenomenology. The model of phase space dynamics has a mathematical structure which is similar to that of potential vorticity dynamics in a quasi-2D system. Based on the comparison, mean squared fluctuation phase space density was interpreted as (potential) enstrophy in *phase space*, and was called as *phasetrophy*[30]. The phasetrophy was further related to fluctuation entropy, as well as the pseudomomentum of phase space structures.

Macroscopic consequences of the phase space dynamics were discussed as well. The evolution of fluctuation entropy was utilized to characterize flow generation by heat flux driven turbulence. In particular, fluctuation entropy was applied to describe tokamak as a heat engine system, where a heat is converted to a macroscopic flow. A figure of merit of the tokamak engine was introduced as efficiency of the flow generation process. The efficiency was defined as ratio of entropy production via heat input to entropy destruction via toroidal flow generation. The efficiency was proportional to the temperature gradient and inversely proportional to the safety factor q (and hence the plasma current). These parameter dependencies were similar to experimental scaling properties of tokamak intrinsic rotation.

Being collisionless, one characteristic of the phase space dynamics is that it involves wave-particle resonance. Once such resonance becomes strong enough, structures in phase space can form and impact macroscopic relaxation processes. It was shown that a *single* phase space structure (an electron drift hole) can extract

free energy and can relax plasma profiles. The free energy release by, and growth of, the electron drift hole was quite different from those of linear electron drift waves, in that the electron drift hole growth was nonlinear and triggered by ion dissipation. The difference allowed subcritical growth of the electron drift hole. This makes the electron drift hole more efficient in tapping free energy than electron drift waves, since growth can occur even when the electron drift waves are predicted to be stable or weakly unstable. It was also shown that the electron drift hole can drive zonal flows. The fact that a single phase space structure can drive zonal flows suggests that familiar concepts of zonal flow generation, such as inverse cascade, Rhine's mechanisms, modulational instability, etc. are useful but not fundamental. Rather, here it is phase space density mixing (related to potential vorticity mixing) that is responsible for the zonal flow generation in tokamaks.

The dynamics of multi-structures in phase space (granulation) was discussed as well. The granulation can drive transport, whose effect enters transport flux as dynamical friction. The granulation was also coupled to zonal flow, since the granulation has to scatter polarization charge to satisfy the quasi-neutrality condition. The coupled evolution of the granulation and zonal flow was formulated as a momentum theorem, where the kinetic pseudomomentum described the momentum of the structures. The implication of the coupled evolution in macroscopic relaxation and transport is that the zonal flow reduces transport by exerting dynamical friction. Transport reduction via dynamical friction by zonal flows is a fundamentally new effect.

The analysis presented here with phase space structures transcends the conventional quasilinear analysis of tokamak turbulence and transport. Such structure driven relaxation and transport can play a role in tokamak phenomenology, in particular when linear eigenmodes or waves are stable or weakly unstable. Such structure driven turbulence can possibly explain the transport level in a region that connects the tokamak core and edge (so-called 'No Man's Land'), where the quasi-linear analysis cannot explain the observed transport level.

Bibliography

[1] http://tempest.das.ucdavis.edu/pdg/ITER_Website/ITER.htm.

[2] http://en.wikipedia.org/wiki/Jupiter.

[3] J. E. Rice, A. Ince-Cushman, J. S. deGrassie, L. G. Eriksson, Y. Sakamoto, A. Scarabosio, A. Bortolon, K. H. Burrell, B. P. Duval, C. Fenzi-Bonizec, M. J. G. ans R. J. Groebner, G. T. Hoang, Y. Koide, E. S. Marmar, A. Pochelon, and Y. Podpaly, *Nucl. Fusion* **47**, 1618 (2007).

[4] J. E. Rice, J. W. Hughes, P. H. Diamond, Y. Kosuga, Y. A. Podpaly, M. L. Reinke, O. D. Gurcan, T. S. Hahm, A. E. Hubbard, E. S. Marmar, C. J. McDevitt, and D. G. Whyte, *Phys. Rev. Lett.* **106**, 215001 (2011).

[5] M. Lesur, P. H. Diamond, and Y. Kosuga, Nonlinear instabilities driven by coherent phase-space structures, US Transport Task Force Workshop, 2012.

[6] http://www.ducks.org/hunting/decoys/making-waves.

[7] B. B. Kadomtsev and E. W. Laing, *Tokamak Plasma: A Complex Physical System*, Institute of Physics Publishing, Bristol, 1993.

[8] K. Nishikawa and M. Wakatani, *Plasma Physics*, Springer-Verlag, Berlin, 1990.

[9] B. A. Carreras, *IEEE Transaction of Plasma Science* **25**, 1281 (1997).

[10] B. B. Kadomtsev, *Plasma Turbulence*, Academic Press, New York, 1965.

[11] E. J. Doyle, W. A. Houlberg, Y. Kamada, V. Mukhovatov, T. H. Osborne, A. Polevoi, G. Bateman, J. W. Connor, J. G. Cordey, T. Fujita, X. Garbet, T. Hahm, L. D. Horton, A. E. Hubbard, F. Imbeaux, F. Jenko, J. E. Kinsey, Y. Kishimoto, J. Li, T. C. Luce, Y. Martin, M. Ossipenko, V. Parail, A. Peeters, T. L. Rhodes,

J. E. Rice, C. M. Roach, V. Rozhansky, F. Ryter, G. Saibene, R. Sartori, A. C. C. Sips, J. A. Snipes, M. Sugihara, E. J. Synakowski, H. Takenaga, T. Takizuka, K. Thomsen, M. R. Wade, H. R. Wilson, I. T. P. T. Group, I. C. Database, M. T. Group, I. Pedestal, and E. T. Group, *Nucl. Fusion* **47**, S18 (2007).

[12] J. W. Connor and H. R. Wilson, *Plasma Phys. Control. Fusion* **36**, 719 (1993).

[13] K. Itoh, S. -I. Itoh, and A. Fukuyama, *Transport and Structural Formation in Plasmas*, Institute of Physics Publishing, Bristol, 1999.

[14] P. A. Davidson, *Turbulence: An Introduction for Scientists and Engineers*, Oxford University Press, Oxford, 2004.

[15] G. Rüdiger, *Differential rotation and stellar convection*, Gordon and Breach Science Publishers, 1989.

[16] G. K. Vallis, *Atmospheric and Oceanic Fluid Dynamics*, Cambridge University Press, 2006.

[17] P. H. Diamond, S.-I. Itoh, K. Itoh, and T. S. Hahm, *Plasma Phys. Control. Fusion* **47**, R35 (2005).

[18] K. H. Burrell, *Phys. Plasmas* **4**, 1499 (1997).

[19] I. B. Bernstein, J. M. Greene, and M. D. Kruskal, *Phys. Rev.* **108**, 546 (1957).

[20] T. H. Dupree, *Phys. Fluids* **25**, 277 (1982).

[21] T. H. Dupree, *Phys. Fluids* **15**, 334 (1972).

[22] T. H. Dupree, *Phys. Rev. Lett.* **25**, 789 (1970).

[23] J. E. Rice, W. D. Lee, E. S. Marmar, P. T. Bonoli, R. S. Granetz, M. J. Greenwald, A. E. Hubbard, I. H. Hutchinson, J. H. Irby, Y. Lin, D. Mossessian, J. A. Snipes, S. M. Wolfe, and S. J. Wukitch, *Nucl. Fusion* **44**, 379 (2004).

[24] F. Wagner, *Plasma Phys. Control. Fusion* **49**, B1 (2007).

[25] E. Mendoza, editor, *Reflections on the Motive Power of Fire - and other Papers on the Second Law of Thermodynamics*, Dover Publications, New York, 2005.

[26] H. Ozawa, A. Ohmura, R. D. Lorenz, and T. Pujol, *Rev. Geophys.* **41**, 1018 (2003).

[27] A. A. Vedenov, E. P. Velikov, and R. Z. Sagdeev, *Nucl. Fusion* **1**, 82 (1961).

[28] A. A. Galeev and R. Z. Sagdeev, *Reviews of Plasma Physics*, volume 7, Consultants Bureau, 1979.

[29] P. H. Diamond, C. J. McDevitt, Ö. D. Gürcan, T. S. Hahm, W. X. Wang, E. S. Yoon, I. Holod, Z. Lin, V. Naulin, and R. Singh, *Nucl. Fusion* **49**, 045002 (2009).

[30] P. H. Diamond, S.-I. Itoh, and K. Itoh, *Modern Plasma Physics Volume1: Physical Kinetics of Turbulent Plasmas*, Cambridge University Press, Cambridge, 2011.

[31] H. L. Berk, B. N. Breizman, and M. Pekker, *Phys. Plasmas* **2**, 3007 (1995).

[32] P. H. Diamond, P. L. Similon, P. W. Terry, C. W. Horton, S. M. Mahajan, J. D. Meiss, M. N. Rosenbluth, K. Swartz, T. Tajima, and R. D. Hazeltine, *Plasma Physics and Controlled Nuclear Fusion Research 1982*, volume 1, IAEA, Vienna, 1983.

[33] H. Biglari, P. H. Diamond, and P. W. Terry, *Phys. Fluids* **31**, 2644 (1988).

[34] P. W. Terry, P. H. Diamond, and T. S. Hahm, *Phys. Fluids B* **2**, 9 (1990).

[35] G. I. Taylor, *Phil. Trans. Roy. Soc. London.* **A215**, 1 (1915).

[36] Y. Kosuga, P. H. Diamond, and O. D. Gurcan, *Phys. Plasmas* **17**, 102313 (2010).

[37] Y. Kosuga and P. H. Diamond, *Plasma and Fusion Research* **5**, S2051 (2010).

[38] Y. Kosuga and P. H. Diamond, *Phys. Plasmas* **18**, 122305 (2011).

[39] T. S. Hahm, *Phys. Fluids* **31**, 1940 (1988).

[40] A. J. Brizard and T. S. Hahm, *Rev. Mod. Phys.* **79**, 421 (2007).

[41] K. Ida, Y. Miura, T. Matsuda, K. Itoh, S. Hidekuma, S. -I. Itoh, and JFT-2M Group, *Phys. Rev. Lett.* **74**, 1990 (1995).

[42] E. J. Strait, T. S. Taylor, A. D. Turnbull, J. R. Ferron, L. L. Lao, B. Rice, O. Sauter, S. J. Thomson, and D. Wroblewski, *Phys. Rev. Lett.* **34**, 535 (1995).

[43] W. M. Solomon, K. H. Burrell, J. S. deGrassie, R. Budny, R. J. Groebner, J. E. Kinsey, G. J. Kramer, T. C. Luce, M. A. Makowski, D. Mikkelsen, R. Nazikian, C. C. Petty, P. A. Politzer, S. D. Scott, M. A. V. Zeeland, and M. C. Zarnstorff, *Plasma Phys. Control. Fusion* **49**, B313 (2007).

[44] Z. Yan, M. Xu, P. H. Diamond, C. Holland, S. H. Muller, G. R. Tynan, and J. H. Yu, *Phys. Rev. Lett.* **104**, 065002 (2010).

[45] P. H. Diamond, C. J. McDevitt, Ö. D. Gürcan, T. S. Hahm, and V. Naulin, *Phys. Plasmas* **15**, 012303 (2008).

[46] Ö. D. Gürcan, P. H. Diamond, T. S. Hahm, and R. Singh, *Phys. Plasmas* **14**, 042306 (2007).

[47] T. S. Hahm, P. H. Diamond, Ö. D. Gürcan, and G. Rewoldt, *Phys. Plasmas* **14**, 072302 (2007).

[48] Ö. D. Gürcan, P. H. Diamond, and T. S. Hahm, *Phys. Rev. Lett.* **15**, 135001 (2008).

[49] T. S. Hahm, P. H. Diamond, Ö. D. Gürcan, and G. Rewoldt, *Phys. Plasmas* **15**, 055902 (2008).

[50] Z. Yoshida and S. M. Mahajan, *Phys. Plasmas* **15**, 032307 (2008).

[51] Ö. D. Gürcan, P. H. Diamond, C. J. McDevitt, and T. S. Hahm, *Phys. Plasmas* **17**, 032509 (2010).

[52] X. Garbet, N. Dubuit, E. Asp, Y. Sarazin, C. Bourdelle, P. Ghendrih, and G. T. Hoang, *Phys. Plasmas* **12**, 082511 (2005).

[53] P. H. Diamond and Y.-B. Kim, *Phys. Fluids B* **3**, 1626 (1991).

[54] T. H. Watanabe and H. Sugama, *Phys. Plasmas* **11**, 1476 (2004).

[55] P. H. Diamond, Y.-M. Liang, B. A. Carreras, and P. W. Terry, *Phys. Rev. Lett.* **72**, 2565 (1994).

[56] Z. Lin, T. S. Hahm, W. W. Lee, W. M. Tang, and P. H. Diamond, *Phys. Rev. Lett.* **83**, 3645 (1999).

[57] W. X. Wang, P. H. Diamond, T. S. Hahm, S. Ethier, G. Rewoldt, and W. M. Tang, *Phys. Plasmas* **17**, 072511 (2010).

[58] W.X. Wang, 2010, private communication.

[59] K. Ida, M. Yoshinuma, K. Nagaoka, M. Osakabe, S. Morita, M. Goto, M. Yokoyama, H. Funaba, S. Murakami, K. Ikeda, H. Nakano, K. Tsumori, Y. Takeiri, O. Kaneko, and LHD experiment group, *Nucl. Fusion* **50**, 064007 (2010).

[60] K. Ida, Y. Miura, K. Itoh, S. Hidekuma, S. -I. Itoh, and T. Matsuda, *J. Phys. Soc. Jpn.* **67**, 4089 (1998).

[61] Sanae-I. Itoh, *Phys. Fluids B* **4**, 796 (1992).

[62] J. M. Kwon, S. Yi, T. Rhee, P. H. Diamond, K. Miki, T. S. Hahm, O. D. Gurcan, and C. J. McDevitt, *Nucl. Fusion* **52**, 013004 (2012).

[63] A. Bortolon, B. P. Duval, A. Pochelon, and A. Scarabosio, *Phys. Rev. Lett.* **97**, 235003 (2006).

[64] J. A. Boedo, D. Rudakov, R. Moyer, S. Krasheninnikov, D. Whyte, G. McKee, G. Tynan, M. Schaffer, P. Stangeby, P. West, S. Allen, T. Evans, R. Fonck, E. Hollmann, A. Lenard, A. Mahdavi, G. Porter, M. Tillack, and G. Antar, *Phys. Plasmas* **8**, 4826 (2001).

[65] J. A. Boedo, D. L. Rudakov, R. A. Moyer, G. R. McKee, R. J. Colchin, M. J. Schaffer, P. G. Stangeby, W. P. West, S. L. Allen, T. E. Evans, R. J. Fonck, E. M. Hollmann, S. Krasheninnikov, A. W. Leonard, W. Nevins, M. A. Mahdavi, G. D. Porter, G. R. Tynan, D. G. White, and X. Xu, *Phys. Plasmas* **10**, 1670 (2003).

[66] T. H. Dupree, *Phys. Fluids* **26**, 2460 (1983).

[67] R. H. Berman, D. J. Tetreault, and T. H. Dupree, *Phys. Fluids* **28**, 155 (1985).

[68] R. H. Berman, T. H. Dupree, and D. J. Tetreault, *Phys. Fluids* **29**, 2860 (1986).

[69] M. Lesur, Y. Idomura, K. Shinohara, X. Garbet, and the JT-60 Team, *Phys. Plasmas* **17** (2010).

[70] M. Lesur and P. Diamond, Submitted., 2012.

[71] P. H. Diamond, O. D. Gurcan, T. S. Hahm, K. Miki, Y. Kosuga, and X. Garbet, *Plasma Phys. Control. Fusion* **50**, 124018 (2008).

[72] P. H. Diamond, A. Hasegawa, and K. Mima, *Plasma Phys. Control. Fusion* **53**, 124001 (2011).

[73] A. Hasegawa and M. Wakatani, *Phys. Rev. Lett.* **50**, 682 (1983).

[74] J. G. Charney and P. G. Drazin, *J. Geophys. Res.* **66**, 83 (1961).

[75] B. A. Carreras, K. Sidikman, P. H. Diamond, P. W. Terry, and L. Garcia, *Phys. Fluids B* **4**, 3115 (1992).

[76] L. D. Pearlstein and H. L. Berk, *Phys. Rev. Lett.* **23**, 220 (1969).

[77] A. Hasegawa, C. G. Maclennan, and Y. Kodama, *Phys. Fluids* **22**, 2122 (1979).

[78] P. B. Rhines and W. R. Holland, *Dynamics of Atmosphere and Oceans* **3**, 289 (1979).

[79] P. G. Drazin and W. H. Reid, *Hydrodynamic Stability*, Cambridge University Press, Cambridge, 2004.

[80] L. D. Landau and E. M. Lifshitz, *Quantum Mechanics (Non-relativistic Theory): Volume 3 (Course of Theoretical Physics)*, Butterworth-Heinemann, Oxford, 1977.

[81] C. J. McDevitt, P. H. Diamond, O. D. Gurcan, and T. S. Hahm, *Phys. Plasmas* **16**, 052302 (2009).

[82] C. J. McDevitt, P. H. Diamond, O. D. Gurcan, and T. S. Hahm, *Phys. Rev. Lett.* **103**, 205003 (2009).

[83] D. G. Andrew and M. E. McIntyre, *J. Fluid Mech.* **89**, 647 (1978).

[84] J. Binney and S. Tremaine, *Galactic Dynamics*, Princeton University Press, Princeton and Oxford, 2008.

[85] L. A. Charlton, B. A. Carreras, V. E. Lynch, K. L. Sidikman, and P. H. Diamond, *Phys. Plasmas* **1**, 2700 (1994).

[86] B. N. Rogers, W. Dorland, and M. Kotschenreuther, *Phys. Rev. Lett.* **85**, 5336 (2000).

[87] S. Champeaux and P. H. Diamond, *Phys. Lett. A* **288** (2001).

[88] Z. Guo, L. Chen, and F. Zonca, *Phys. Rev. Lett.* **103**, 055002 (2009).

[89] H. Biglari, P. H. Diamond, and P. W. Terry, *Phys. Rev. Lett.* **60**, 200 (1987).

[90] L. Lin, M. Porkolab, E. M. Edlund, J. C. Rost, M. Greenwald, N. Tsujii, J. Candy, R. E. Waltz, and D. R. Mikkelsen, *Plasma Phys. Control. Fusion* **51**, 065006 (2009).

[91] M. N. Rosenbluth and C. S. Liu, *Phys. Fluids* **15**, 1801 (1972).

[92] F. Zonca, S. Briguglio, L. Chen, G. Fogaccia, and G. Vlad, *Nucl. Fusion* **45**, 477 (2005).

[93] L. P. Pitaevskii and E. M. Lifshitz, *Physical Kinetics: Volume 10 (Course of Theoretical Physics)*, Pergamon, Oxford, 1981.

[94] M. B. Isichenko, *Rev. Mod. Phys.* **64**, 961 (1992).

[95] M. Vlad, F. Spineanu, J. H. Misguich, J. D. Reuss, R. Balescu, K. Itoh, and S.-I. Itoh, *Plasma Phys. Control. Fusion* **46**, 1051 (2004).

[96] H. L. Berk, B. N. Breizman, and N. V. Petviashvili, *Phys. Lett. A* **234**, 213 (1997).

[97] H. L. Berk, B. N. Breizman, J. Candy, M. Pekker, and N. V. Petviashvili, *Phys. Plasmas* **6**, 3102 (1999).

[98] B. B. Kadomtsev and O. P. Pogutse, *Phys. Rev. Lett.* **25**, 1155 (1970).

[99] G. Dif-Pradalier, P. H. Diamond, V. Grandgirard, Y. Sarazin, J. Abiteboul, X. Garbet, P. Ghendrih, A. Strugarek, S. Ku, and C. S. Chang, *Phys. Rev. E* **82**, 025401(R) (2010).

[100] G. Darmet, P. Ghendrih, Y. Sarazin, X. Garbet, and V. Grandgirard, *Communications in Nonlinear Science and Numerical Simulation* **13**, 53 (2008).

[101] B. B. Kadomtsev and O. P. Pogutse, *Reviews of Plasma Physics*, volume 5, Consultants Bureau, 1970.

[102] A. Hasegawa and K. Mima, *Phys. Fluids* **21**, 87 (1978).

[103] M. E. McIntyre, *Adv. Geosci.* **15**, 47 (2008).

[104] D. Lynden-Bell, *Mon. Not. R. Astr. Soc.* **136**, 101 (1967).

[105] T. H. Dupree and D. J. Tetreault, *Phys. Fluids* **21**, 425 (1978).

[106] H. Biglari, P. H. Diamond, and P. W. Terry, *Phys. Fluids B* **2** (1990).

[107] O. D. Gurcan, P. H. Diamond, and T. S. Hahm, *Phys. Plasmas* **13**, 052306 (2006).

[108] M. Nakata, T. Watanabe, H. Sugama, and Y. Idomura, Nonlinear entropy tranfer via zonal flows in gyrokinetic plasma turbulent transport, 1st Asia Pacific Transport Working Group International Conference, 2011.

[109] F. Zonca, S. Briguglio, L. Chen, G. Fogaccia, T. S. Hahm, A. V. Milovanov, and G. Vlad, *Plasma Phys. Control. Fusion* **48**, B15 (2006).

[110] D. A. Spong, B. A. Carreras, and C. L. Hedrick, *Phys. Plasmas* **1**, 1503 (1994).

[111] F. L. Hinton and M. N. Rosenbluth, *Plasma Phys. Control. Fusion* **41**, A653 (1999).